Synthesis and characterization of novel biodegradable thermoplastic elastomers

Widjaja, Leonardus Kresna

2011

Widjaja, L. K. (2011). Synthesis and characterization of novel biodegradable thermoplastic elastomers. Doctoral thesis, Nanyang Technological University, Singapore.

https://hdl.handle.net/10356/46298

https://doi.org/10.32657/10356/46298

Synthesis and Characterization of Novel Biodegradable Thermoplastic Elastomers

NANYANG TECHNOLOGICAL UNIVERSITY

SCHOOL OF MATERIALS SCIENCE AND ENGINEERING

Leonardus Kresna Widjaja

2011

A thesis submitted to the Nanyang Technological University in fulfillment of the requirement for the degree of Doctor of Philosophy

Acknowledgements

I would like to express my deepest gratitude to Prof. Marc Abadie, for his valuable guidance, encouragement and assistance throughout the whole project. His knowledge in polymer synthesis and characterization has enabled me to understand the basic principles of this project without much difficulty in the early years of my PhD.

I would also like to express my utmost thanks to Prof. Subbu S. Venkatraman, for his advice and help in completing this thesis. His vast experience in biomaterials research field has helped me a lot in the project. A big word of thanks shall be given to my research group members, Dr. Vitali Lipik and Liow Sing Shy for their opinions, ideas, and help. Huge credits for Dr. Wong Yee Shan, Dr. Sujay Chattopadhyay, Kong Jen Fong and Monica Suryana Tjin, whom all have been working with me and contributed a lot for this thesis.

My sincere thanks goes to Nelson Ng from previous Biomaterials Lab; Wilson Lim and Patrick Lai from Organic Materials Lab; Sharon Tan, Sandy Leong, and Tay Poh Tin from chemicals and consumables store; Tan Kek Koon and Poh Boon Sheng from computer facilities lab. I have received countless help from them, making the completion of this project much easier.

Last but not least, I would like to thank my family, my friends and all people whose names I could not possibly mention one by one, for their love, encouragement and support to me until the very end of this project.

Table of Contents

List of Figures

List of Schemes

List of Tables

Abstract

Biodegradable Thermoplastic Elastomer (BTPE) has the potential uses as implantable devices due to the possibility to change its chemistry and structure, thus controlling its elasticity. It also has potential applications in the biomedical area, especially in the area of controlled drug delivery and tissue engineering. Most of currently available biodegradable thermoplastic elastomers are polyurethanes, which contain urethane linkages. These versatile polymers have been used as implant materials for over 20 years but when they biodegrade in the body, the diamines produced are highly toxic. Synthesizing BTPE using a triblock copolymer made of biocompatible monomer will eliminate this problem.

This thesis presents the synthesis and characterization of novel biodegradable thermoplastic elastomers made of ε-caprolactone (CL), trimethylene carbonate (TMC), and L-lactide (LLA). Various A-B-A triblock copolymers (whereby B block is random copolymer of PCL and PTMC, and A block is PLLA) have been synthesized by varying their middle-block compositions as well as end-block amounts. Our study showed that the molar ratio of CL:TMC is the single most crucial parameter in determining the mechanical properties of the copolymers, along with the molar mass of the PLLA end-block.

Retaining the same basic middle-block of PCL/PTMC copolymer, the PLLA end-segment crystallinity was disrupted to examine its effect on elastomeric behavior. The addition of PCL into PLLA block enhances the elongation of the triblock considerably. With regards to the elasticity, however, creep test results show that

adding PCL to PLLA block seems to reduce the "equilibrium" recovery, while cyclic test results shows that the instantaneous recovery increased significantly with more PCL inside PLLA block.

The increase in elasticity for triblock copolymers with PCL inside PLLA hard block has led us to do a more thorough characterization of these copolymers. Interestingly, it was found during a cyclic test that although the recovery after the first elongation is low, the recovery increases during subsequent cycles (hence the name "Deformation-Induced Elasticity"). Using WAXD and orientation measurements, we were able to relate the DIE effect to the influence of the PCL crystallinity and orientation changes with addition of PCL to the end-block.

Another interesting copolymer system was also explored, a branched BTPE based on copolymers of PCL/PTMC as soft block and PLLA as hard block were synthesized by ring opening polymerization using $Sn(Oct)_2$ catalyst and pentaerythritol as initiator. Molar mass plays a significant role in determining the polymer's property. It was found that the molecular structures, thermal properties, as well as mechanical properties of the star-shaped copolymers changed considerably with composition.

Chapter 1 Introduction

1.1 Background and Current Challenges

Elastomers are crosslinked, amorphous polymers with application temperatures above their glass transition temperatures. Therefore, considerable amount of chain segment motions are possible when elastomers are in use [1]. The ability of the long polymer chains to reconfigure and align themselves in the direction of a stress applied gives rise to the material's high elasticity. The crosslinks ensure that the chains are able to return to their original configuration when the stress is removed, as irreversible chain slippage past one another is prevented. Depending on the specific material, elastomers are able to extend up to 1000% of their original lengths [2]. Such deformations will result in irreversible extensions without the crosslinks. However, elastomers generally have lower modulus values as compared to other flexible polymers. Figure 1.1 below compares the stress-strain behaviors of the various types of polymers.

As mentioned above, to attain high amounts of recovery after the applied deformation in elastomers, crosslinks are necessary. Although a crosslinked polymer generally refers to one having chemical bonds created between chains, an uncrosslinked polymer can also be made to behave like a chemically-crosslinked one by having clearly segregated "hard" and "soft" segments in its structure. This kind of elastomer is termed thermoplastic elastomer, since it has no permanent crosslinks in its structure to be thermosetting and can be made to flow at high temperatures.

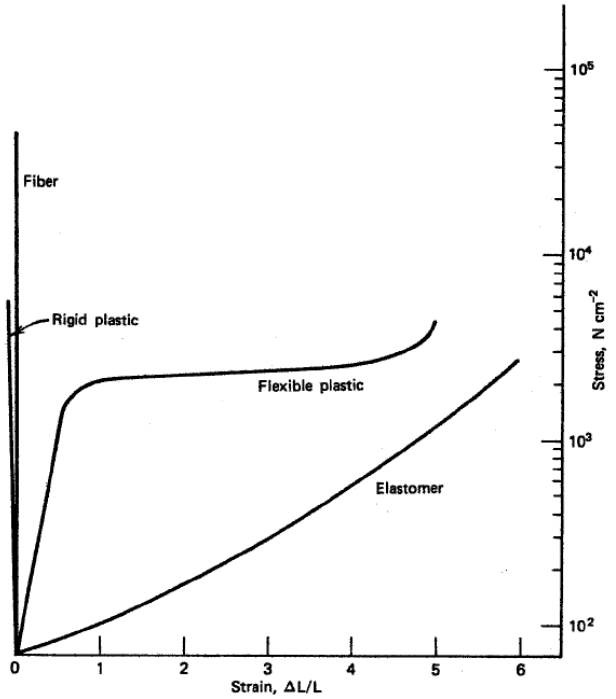

Figure 1.1 Stress-strain plots for a typical fiber, rigid plastic, flexible plastic and elastomer [2]

Thermoplastic elastomer (TPE) is a fast growing segment in the field of polymer manufacturing. Global demand for TPE has been predicted to rise 6.3 percent per year through 2011, with total of 3.7 million metric tons [3]. TPE will continue to be used primarily as a replacement for synthetic and natural rubber, and also for metals and rigid thermoplastics.

The main advantages of TPE over thermoset elastomer are the ease of processing (thus allowing it to be produced with lower cost), the wide variety of properties available, and the possibility of recycling and reuse. Besides the obvious environmental benefits of a recyclable raw material, TPE scrap material can be reprocessed. The disadvantages of these materials relative to the thermoset elastomer

are the poor chemical and temperature resistance, the general inability to mix TPE with fillers, and the relatively high cost of raw materials.

A large number of structures fall into the category of TPE. The first commercially available TPE was developed by Shell Development Company in the early 1960s, which became the KRATON family of materials. These materials are either poly (styrene-b-ethylenebutylene-b-styrene) (SEBS), poly(styrene-b-isoprene-b-styrene) (SIS), or poly(styrene-b-butadiene-b-styrene) (SBS) triblock copolymers. Approximately 50% of all TPE produced are SBS, SIS, or SEBS triblock copolymers. Fluorinated TPE is also another class of TPE which gains more popularity lately due to its ability to withstand very low temperatures, preserve elastomeric properties in space and to resist at high temperatures [4].

Although TPE have been around for quite some time, intensive research for biodegradable TPE (BTPE) just started recently and there are not many commercial elastomeric biodegradable/biocompatible materials in the market today. BTPE has the potential uses as implantable devices (plastic surgery, wound dressing, cardiovascular, maxillofacial, and orthopedic) due to the possibility to change their chemistry and structure, thus controlling their elasticity [5]. It also has potential applications in the biomedical area, especially in the area of controlled drug delivery and tissue engineering [6].

Porous scaffolds from biodegradable polyurethane, combined with bone marrow of the patient might potentially be used as bone substitutes [7]. The problem of rigid bone substitute such as shear forces at the interface between rigid and bone will be

prevented using elastomeric bone substitute. It creates a close contact with the original bone ends, promoting osteogenic cells proliferation and bone regeneration.

Elastomers have also found their use in osmotic pressure-driven drug delivery, which has been shown to provide a nearly constant release of drug for prolonged times effectively [8]. Early studies in osmotic delivery utilized non-degradable polymers, which were having a disadvantage of the need for surgical removal later on. Recent research in this area has demonstrated the possibility of constant release using this osmotic pressure mechanism with degradable elastomers [9].

Meanwhile in tissue engineering field, a three-dimensional polymer scaffold is created to support cell growth and orient growth towards the generation of replacement tissue. The purpose of mechanical stimulation in the field of elastic soft tissues such as smooth muscle, cartilage, and blood vessels has recently been well-established [10]. The mechanical properties of the biodegradable elastomers can be tailored to approximate those of these soft tissues [11], thereby providing a polymer scaffold that can provide an appropriate surface for cell attachment and growth, endure repeated dynamic loads, and ultimately degrade at a rate that permits the load to be transferred to the new tissue.

Most of currently available biodegradable thermoplastic elastomers are polyurethanes, which contain urethane (OCONH) linkages. The linkage is formed through the reaction of a diisocyanate and a diol, where the diol is usually a macroglycol soft segment; and the excellent secondary bonding between the urethane links gives rise to the hard segments. They usually have high elongation at break, high flexibility, and

low permanent deformation on static and dynamic loading. These versatile polymers have been used as implant materials for over 20 years but when they biodegrade in the body, the diamines produced are highly toxic [12].

So, there is the need to synthesize a biodegradable thermoplastic elastomer which does not contain any diisocyanate as the hard block or as a chain extender. To accomplish this, we propose to investigate an approach by using coordination-insertion ring opening polymerization to make "living polymers" that will in turn enable the construction of different polymer configurations having multi-functionalities without having diisocyanates incorporated inside the polymer structure.

1.2 Objectives and Scope of Study

The objectives of this thesis are:

- To synthesize BTPE by copolymerizing ε-caprolactone (CL), trimethylene carbonate (TMC) and L-lactide (LLA) with various compositions.
- To characterize the synthesized polymers structurally, thermally, and mechanically, with emphasis on the elastomeric properties. To estimate biodegradation of these polymers in vitro to predict their use in vivo.
- To correlate the compositions of the copolymers to the properties; this will allow us to understand, and then optimize the structures/compositions.

To achieve the objectives, several things need to be done, first is to find suitable polymers for the soft-block and hard-block of the BTPE. The hypothesis is that in order to have a good elongation and recovery, the soft-block has to be amorphous and the hard-block has to be semi-crystalline. The amorphous segment can be made of a random copolymer using two monomers over a certain composition range. For the hard-block, although it is possible to use just one monomer, in this work, the possibility of using a copolymer as the hard-block will be explored.

The next step is to synthesize the copolymers in various compositions of the hard-block and the soft-block. The molar mass of the copolymers will also be varied to give different properties. The hypothesis here is that having a long chain of soft-segment and just enough length of hard-segment will give elastomeric properties. If the hard-segment length is too short, there will not be enough physical crosslinks to hold the copolymer together during stretching. If the hard-segment is too long, the copolymer will become brittle with low elongation. The structures of the copolymers are going to be triblock or starblock copolymers. By using a triblock structure, there will be micro-phase segregation between the crystalline hard domains which are scattered inside amorphous soft matrix. This type of phase morphology creates a physical network made of flexible polymer chains which are cross-linked by the crystalline micro-domains. Theoretically, starblock structure will give the same kind of network as triblock copolymer, so it will be interesting to see the properties difference between the starblock and triblock copolymer given the same composition.

The synthesized copolymers will be characterized extensively in order to investigate its elastomeric properties. For structural properties, Size Exclusion Chromatography

(SEC) will be used for measuring molar mass, ^{1}H Nuclear Magnetic Resonance (NMR) and ^{13}C NMR for determining the structures and compositions of the copolymers. For thermal properties, Differential Scanning Calorimetry (DSC) will be used to observe the glass transition temperatures (T_g), melting temperatures (T_m), and change in enthalpy (ΔH) of the copolymers. For mechanical properties, Instron machine will be utilized to investigate the modulus, tensile strength, and elongation to break, as well as for cyclic loading test. Dynamic Mechanical Analysis (DMA) will be used for creep test which is one way to determine the copolymer's elastomeric property. Atomic Force Microscopy (AFM) and Wide Angle X-ray Diffraction (WAXD) are utilized to investigate the crystallinity of the copolymers. Lastly, degradation study using phosphate buffered saline (PBS) buffer will be done for some selected copolymers in order to simulate how fast these copolymers will degrade inside human body.

1.3 Structure and Organization of the Thesis

This thesis will be divided into five chapters. The first chapter consists of the background and current challenges that motivate this study, as well as the scope of this research work. *Chapter 2* starts with the discussion of the characteristic of thermoplastic elastomer, continued with a section for biodegradation mechanism. Then, the ring opening polymerization technique which was used for the copolymer synthesis will be reviewed, followed by a thorough literature study on existing biodegradable thermoplastic elastomers.

Chapter 3 outlines the materials used for the synthesis, the synthesis method, and the characterization method by different equipments. *Chapter 4-7* will be the essence of the thesis, containing the synthesis result and the copolymers characterization, accompanied by the necessary discussion of the results. *Chapter 4* talks about synthesis and characterization of triblock with P(CL-co-TMC) as soft-block and PLLA as hard-block. *Chapter 5* will be for triblock with P(CL-co-TMC) as soft-block and P(LLA-co-CL) as hard-block. *Chapter 6* will discuss about characterization on the enhanced elastomeric effect of triblocks from *Chapter 5*. *Chapter 7* will talk about starblock copolymer with P(CL-co-TMC) as soft-block and PLLA as hard-block. Finally, *Chapter 8* draws a conclusion of all works that have been done in the thesis, and also recommendations for future works.

Chapter 2 Literature Review

2.1 Thermoplastic Elastomer

A material should have several important criteria for it to qualify as a TPE. First it must be able to be stretched to considerable elongations and when the stress is removed, it has to return close to the original shape, second, it has to be able to be processed in a molten state at high temperature, and last, it should have no noticeable creep [13]. In order to achieve these characteristics, TPE are usually made of certain copolymer structure.

TPE are generally segmented copolymers consisting of soft and hard segments [14]. A matrix-domain type structure is formed during phase separation, identified by hard segment domains dispersed within the soft segment matrix. And also, at temperatures whereby the TPE is being used, the matrix will be in a melt state, whereby the domains are either glassy or crystalline. Because the molecules contain alternating soft and hard segments, each polymer chain runs alternately through the matrix and the domains. Therefore, the domains are linked together by the main valence chains. Ultimately, the soft segment matrix in the melt state is responsible for the high elongation-to-break while the rigid hard segment domains keep the polymer from having a viscous flow, thus resulting elasticity like a rubber. The chains which connect the domains together are being cross-linked by the secondary valence bonds

inside the domains. The cross-links break down when the temperatures go beyond the T_g or the T_m of the hard segment domains.

The crosslink distribution is related to the viscoelastic properties of the soft and hard segments, and also the degree of phase separation [14]. This can be seen on Figure 2.1 where we assume that the softening (T_g or T_m) of two homopolymers A and B happens respectively at T_A and T_B. The A-B random copolymer will start to soften at a temperature between T_A and T_B, and it will depend on the ratio of A to B in the copolymer whether it soften closer to T_A or T_B (Figure 2.1a). Figure 2.1b shows the wide temperature range from T_A to T_B upon which the softening of block copolymers having only short blocks without phase separation will happen. Meanwhile, segmented block copolymer having non-perfect phase segregation will have two different softening temperatures marked with $T_{A'}$ and $T_{B'}$ which might not be the same as T_A and T_B due to disordered segments and unclear domain boundaries (Figure 2.1c). Finally, segmented block copolymers having complete phase segregation will become soft partially right at T_A and T_B, and the modulus will be determined by the composition of A and B (Figure 2.1d).

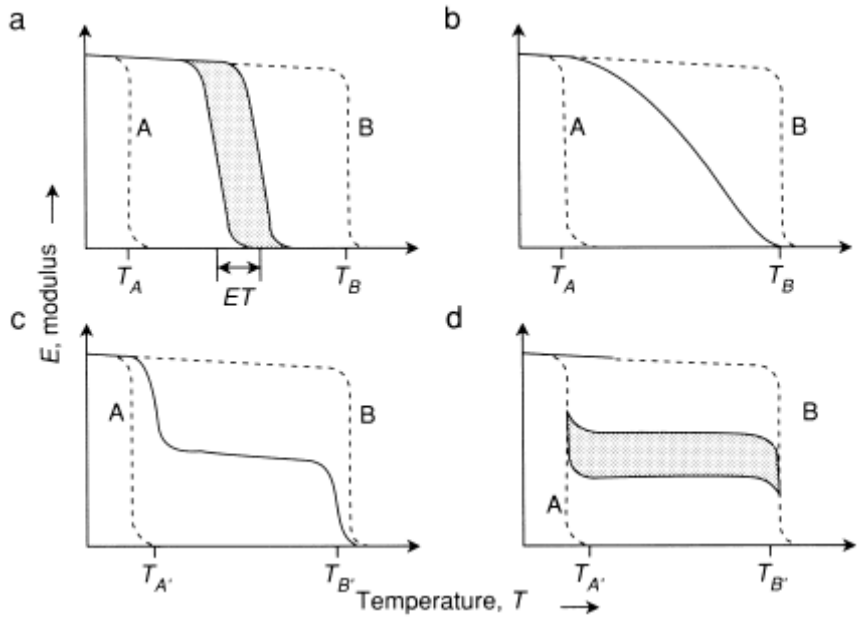

Figure 2.1 Dependence of modulus on temperature for various types of copolymers [14].

Thermoplastic elastomers commonly will have temperature versus modulus curve as seen in Figure 2.1c. The service temperature of the material has to be inside the plateau region. Typically through changes in the monomers type or composition, the plateau can be shifted upward or downward, giving the manufacturer a great deal of flexibility. Most TPE have certain similar structural characteristics. The monomers typically have long chain, making the material a block copolymer. The monomers are most of the times non-similar, which gives result to microphase separation on a nanometer length scale. The driving force for phase separation is always enthalpic and usually one to two orders of magnitude weaker than primary valence bonds. Hydrogen bonding, crystallinity, ionic, and van der Waals driving forces have been observed to cause microphase separation in these systems [15].

As it has been stated earlier, the two phases that make the matrix-domain system have different properties. The soft phase comprises a polymer that has T_g or T_m below the service temperature, resulting in highly mobile chains. The other phase, the hard phase, is made up of chains which are rigidly locked in place, because either the T_g or T_m is above the service temperature. The composition of the two phases determines the physical properties of the TPE by choosing which phase is isolated or continuous. The ability to easily vary these parameters through stoichiometry allows TPE to be used in the wide variety of applications.

2.2 Biodegradation Mechanism

Biodegradable polymers have many interesting applications and possibilities in the biomedical field. They have a main advantage which allows them to be left within the body without creating any negative effects to the surrounding tissue. The prerequisite to this advantage is that the materials used are carefully chosen to be non-toxic and biocompatible with the tissue in the particular application.

A polymer will be considered as biodegradable polymer if it experiences a decrease of its molar mass as well as a decline of its chemical and physical properties until the formation of CH_4, CO_2, H_2O, and also other low molar mass products under the influence of micro organisms in both anaerobic and aerobic environment [16]. Furthermore, the microbial biomass and residue would have to be non-toxic and finally be absorbed into natural geochemical cycle [17].

Several models describing biodegradation process have been proposed [18-19], most of which relate to hydrolysis as the prevalent and widely studied biodegradation pathway. There is increasing evidence, however, that oxidation chemistries also contribute to polymer biodegradation, particularly by action of the immune system [20-21]. Thus, the two main biodegradation mechanisms in biomedical polymers are hydrolysis and oxidation. These reactions may or may not be catalyzed by enzymes, depending on detailed characteristics of the polymer itself (e.g. chemical structure, M_w, morphology), and on device shape and its location in the body.

Hydrolysis is the scission of covalent bonds by water. Susceptibility of polymers to hydrolysis depends on chemical structure, morphology and dimensions, and also on their immediate environment. Hydrolysis may be catalyzed by acids, bases, salts and enzymes. Enzymes catalyzing hydrolysis, i.e. hydrolases, and generally highly specific to particular classes of polymers (or more precisely types of chemical bond), and include proteases, esterases, lipases and glycosidases [19].

There is increasing evidence that a number of polymers are subject to oxidative degradation *in vivo* brought about by the immune system. Implanted biomaterials typically evoke inflammatory responses in which polymorphonuclear leukocytes migrate into the site of inflammation, followed by monocytes which differentiate into macrophages [22]. When stimulated, macrophages produce large amounts of superoxide (O_2^-) and hydrogen peroxide via a process known as the "oxidative burst" [23]. Superoxide and peroxide by themselves are comparatively harmless, but in presence of metal centers such as iron or cobalt both are converted to hydroxyl

radicals (HO˙), which significantly accelerate degradation of various polymers *in vitro* [24].

2.2.1 Biodegradation Mechanism of Polycaprolactone

The proposed degradation mechanism of polycaprolactone starts with the hydrolysis of the polymer chain into 6-hydroxyhexanoic acid, which is an intermediate of ω-oxidation. Then it continues with β-oxidation to acetyl-CoA, which can undergo further degradation in the tricarboxylic acid (TCA) cycle as illustrated in Scheme 2.1 [25]. The molecular weight readily decreases during biodegradation, and is accompanied by a broadening of the molar mass distribution [26]. The degree of crystallinity of PCL will increase along with the degradation, a sign that the degradation happens in amorphous regions [27-28].

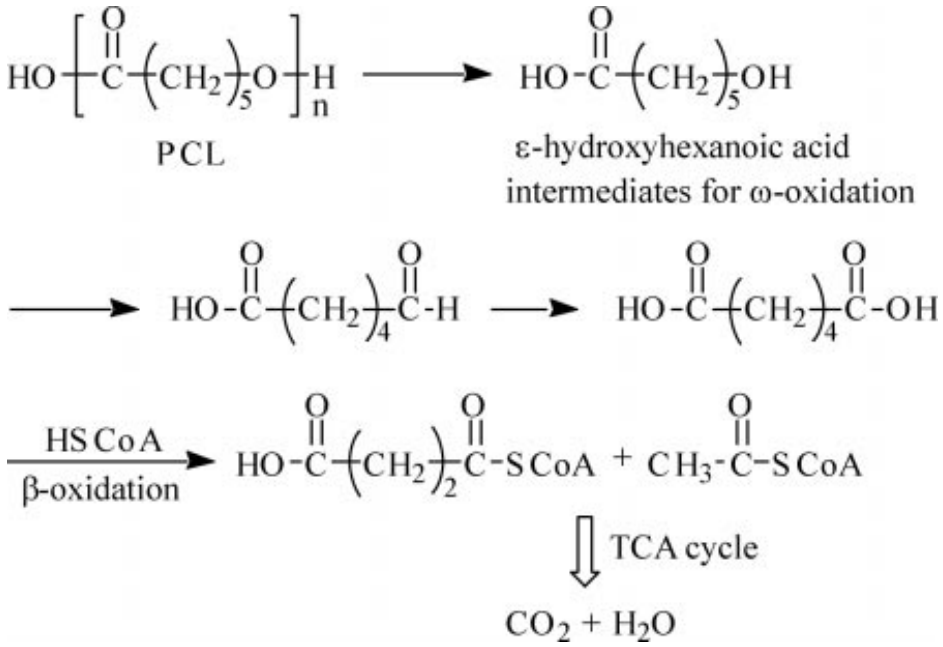

Scheme 2.1 PCL degradation mechanism.

2.2.2 Biodegradation Mechanism of Poly L-lactide

Inside an aqueous condition, PLLA degrades by hydrolysis of the ester bonds. The process is self-catalyzed by the protons on the carboxyl (COOH) end groups (Scheme 2.2) and the hydrolysis rate will increase exponentially along with the degradation time. The hydrolysis can be divided into three stages [29]. The molar mass of the polymers decreased rapidly during the first stage, most likely by random-chain scission, although no substantial weight loss was observed. During the second stage, the decrease in molar mass was then continued with increase in mass loss and monomer formation. When total weight loss is reached, around half of the copolymers would have been hydrolyzed into monomers. Finally on the last stage, hydrolysis of soluble oligomers kept occurring until the PLLA was completely hydrolyzed into its monomer, which is lactic acid.

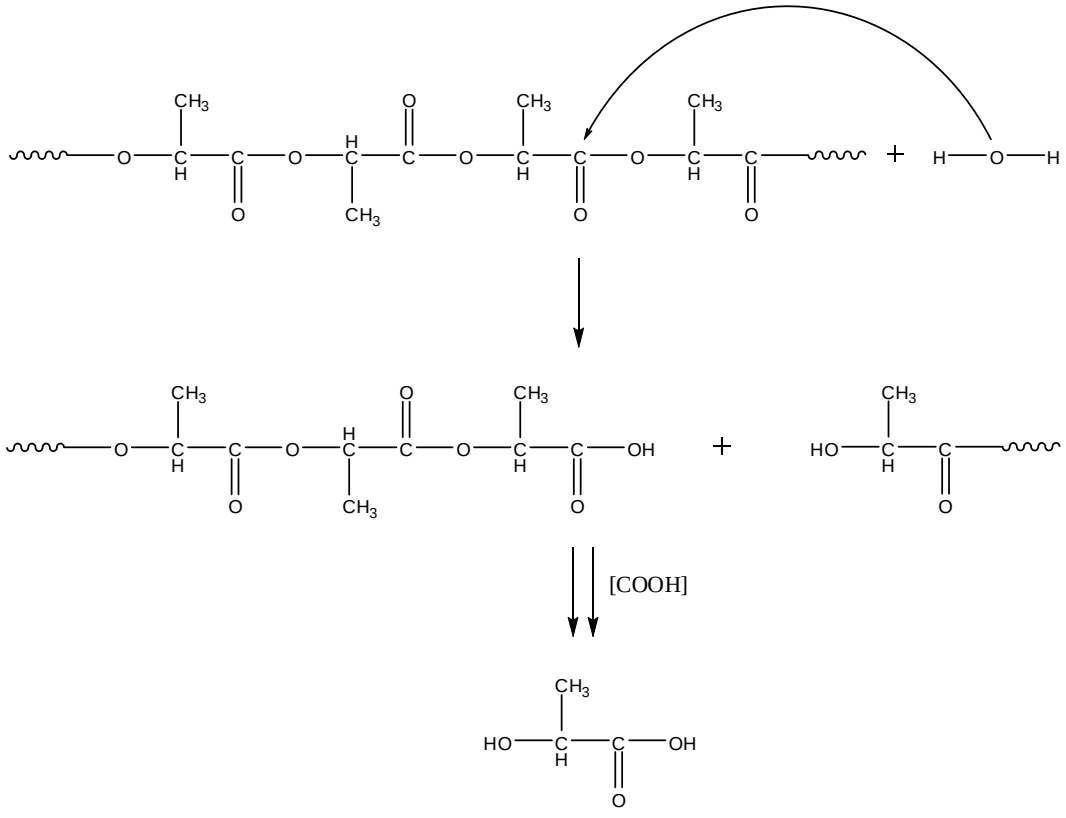

Scheme 2.2 PLLA degradation mechanism by hydrolysis.

2.2.3 Biodegradation Mechanism of Polytrimethylene carbonate

Like most polycarbonates, polytrimethylene carbonate (PTMC) undergoes degradation through hydrolysis and also enzymatic degradation. The carbonate bonds are basically more prone to hydrolysis compared to the ester linkage [30]. However, PTMC undergoes hydrolysis on a very slow rate; properties of high molar mass PTMC in vitro might not be affected for as long as a year and more [31]. In aqueous solution, PTMC molar mass is decreasing very slowly and furthermore, the nature of aqueous medium does not affect the rate. It may take years to have a total hydrolysis. PTMC's slow hydrolysis rate are caused by the lack of autocatalytic process [30] and its final product will be carbon dioxide and diols, as shown in Scheme 2.3. The degradation products from PTMC was investigated using gas chromatography-mass spectrometry analysis [31], and it has been identified that the major degradation product of PTMC was 1,3-propanediol, which correspond to the degradation mechanism of polycarbonates shown in Scheme 2.3.

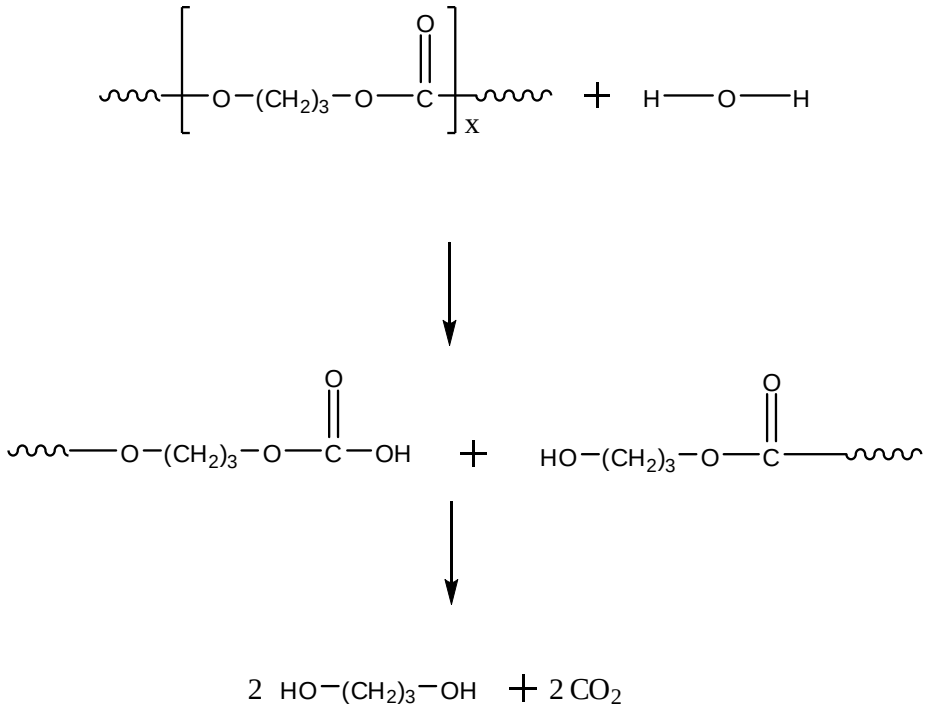

Scheme 2.3 Hydrolytic degradation scheme of PTMC

2.3 Ring Opening Polymerization (ROP)

There are two different ways to synthesize polyesters such as polylactides and polylactones, the first is by doing ROP on cyclic esters and secondly, by polycondensation of hydroxyl-carboxylic acids. Although it is cheaper compared to ROP, there are several disadvantages of polycondensation method. First, it is difficult to create specific end groups, to obtain high molar mass polymers, and to produce copolyesters which are well-defined. Because of the capability of generating many kinds of biodegradable polymers in a well-controlled system, the ROP using lactides and lactones monomers has been studied extensively for the last 50 years. Carothers et al. [32-34] were the first ones to thoroughly explore the ROP method for carbonates, lactones, and anhydrides. Subsequently, the technique has been used for a variety of monomers in order to synthesize many kinds of homopolymers as well as copolymers, and numerous types of catalyst plus initiator combinations have been studied. Most of the times, the synthesized polymers show promising properties as biocompatible or biodegradable materials.

By investigating the polymerization of cyclic esters we can get some benefits out of it. First, we will be able to explore the potential of polymer synthesis chemistry in order to produce many different types of polymers by fine-tuning the primary parameters determining the polymer properties. In order to get the most suitable polymer synthesis system for a specific industrial or technological process, optimization of experimental condition is important. The second benefit of investigating ROP is the possibility to create variety of advanced macromolecules, this range from homopolymers with specific end groups until copolymers with different structures, for

examples: graft, star, or block copolymers. Furthermore, the thermal, degradation, and mechanical properties of these various copolymers can be investigated to find the connection between the structure and the properties of the polymers. The last benefit for investigating ROP systems is because they will be important models for the purpose of examining the mechanisms [35] and kinetics [36] of basic reactions inside polymer synthesis.

2.3.1 Ring Opening Polymerization of Cyclic Monomers

By using ROP of the respective cyclic monomers, polylactides, polylactones, and polycarbonates of high molar mass are particularly synthesized. After cyclic esters monomers have been reacted together with an initiator or catalyst, polyester is formed. Scheme 2.4 shows the synthesis scheme of a cyclic ester undergoing ROP.

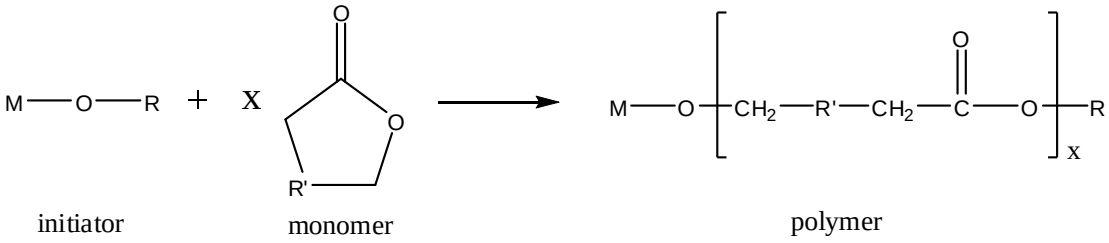

Scheme 2.4 Ring opening polymerization scheme of a cyclic ester.

Each polymer synthesized usually will have two different chain ends. One functional group which is the result of termination reaction will cap one end and the initiator's functional group will terminate the other end. Therefore, in order to suit the synthesized polymer's application, we can make a variation on the functional groups type by changing the initiator or catalyst and also the termination reaction. A major

factor in controlling both the hydrolytic and thermal stability of the synthesized polyester will be the types of end group and initiator [37-39]. Different functional groups that are useful for post-polymerization reactions may also be incorporated inside the structure of the polymer using this approach.

There are many ways to do ROP, it can be performed in dispersion, solution, emulsion or as a melt (bulk) polymerization [40-41]. An initiator or catalyst is needed to start the reaction [42]. High molar mass aliphatic polyesters with low polydispersity index are possible to be synthesized in short periods of time under reasonably mild conditions. Problems commonly encountered in condensation polymerization like the need to eliminate low molar mass by-products (such as water, and oligomers), high reaction temperatures, as well as exact stoichiometry are non-existence in ROP [43].

Determined by the type of initiator used, ROP is categorized into three different kinds of reaction mechanisms [44], which are: anionic, cationic, or coordination-insertion mechanisms [45-47]. Besides these three major mechanisms, there are several other initiation mechanism like active hydrogen [44], zwitterionic [48], or radical but those methods are not commonly practiced.

2.3.2 Ring-Opening Polymerization Using Coordination-Insertion Mechanism

Coordination-insertion ROP got its name from the fact that the propagation proceeds by monomers coordination into the active species, continued by monomer insertion

into the metal-oxygen bond by means of electrons rearrangement [46-47]. Scheme 2.5 illustrates a proposed scheme for the coordination-insertion mechanism. During propagation step, the alkoxide bond connects the polymer growing chain to the metal. Termination reaction by hydrolysis follows afterwards, creating a hydroxyl end group. By using alkoxy-substituted functional initiators, we can synthesize polymers having active end groups for post-polymerization reactions.

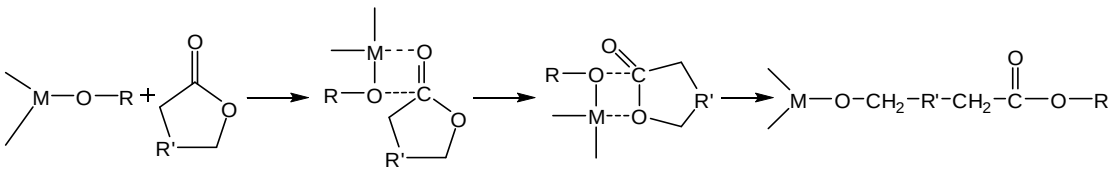

Scheme 2.5 The proposed reaction pathway of cyclic ester ROP using the coordination-insertion mechanism.

Being able to produce well-defined polyesters using living polymerization, coordination-insertion mechanism has been extensively studied [47]. Block copolymers are able to be synthesized by subsequent addition of monomer into the "living" system. However, careful monomers selection needs to be done so that the active center from the first block is nucleophilic enough to open the second monomer.

2.3.3 Transesterification Reactions in Ring Opening Polymerization

Duda et al. have shown that the initiator or catalyst in the ROP of lactides as well as lactones will cause transesterification reactions under two conditions: long reaction times [49], or high temperatures [50]. There are two types of transesterification

reactions (Scheme 2.6), intramolecular transesterification or back-biting will result in polymer chain degradation continued by formation of the cyclic oligomers while intermolecular transesterification will alter the order of copolymers therefore preventing block copolymers from forming [51]. Either way, both kinds of transesterification reaction will result in higher polydispersity.

As shown in Scheme 2.6, every intramolecular transesterification cuts the polymer chain in a randomly order. Consequently, a cut on the polymer chain will give rise to one new randomized, modified polymer as well as one free residual polymer. In this way, a copolymer previously having a block-like structure will transform into a random copolymer after experiencing a certain number of transesterifications [52-53].

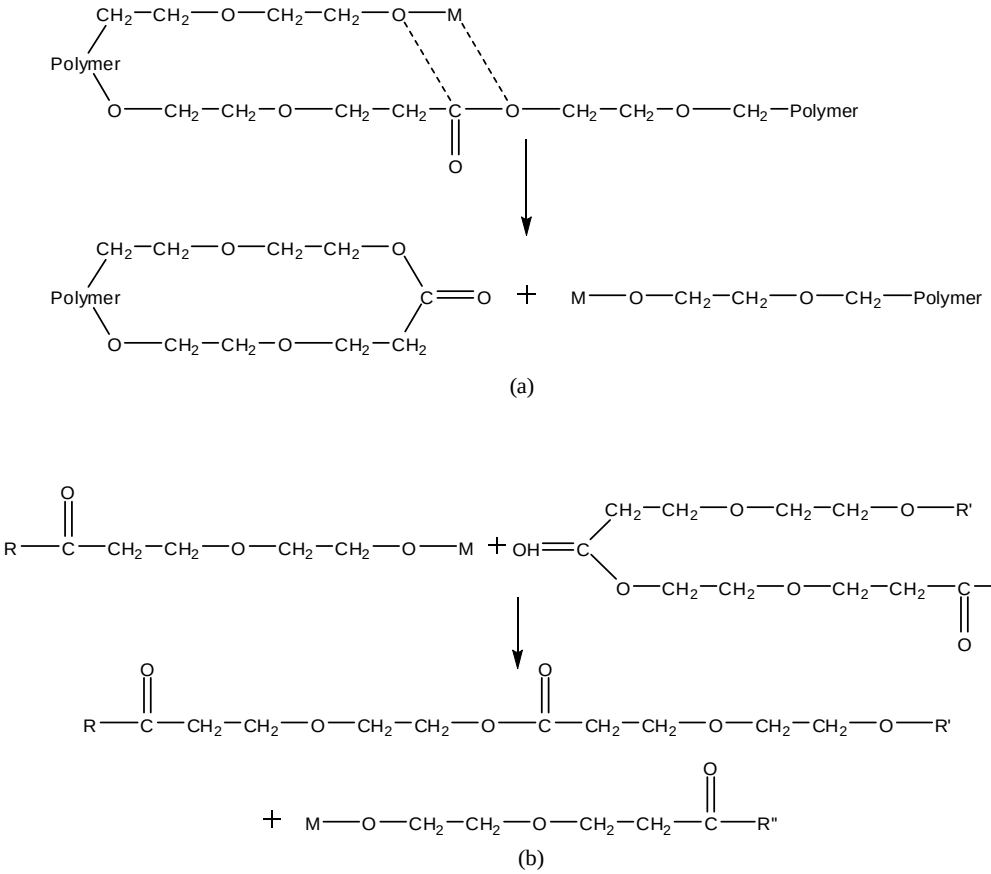

Scheme 2.6 Schematic presentation of intramolecular (a) and intermolecular (b) transesterification reactions.

Some of the variables that affect the amount of transesterifications include the time, temperature, and concentration of the reaction as well as type of initiator or catalyst [54]. The initiator will be somewhat active towards side-reactions like transesterification in accordance to the metal being used [54-55]. Dubois et al. have shown that the relative reactivity of various metal alkoxide initiators against the synthesized polymer chains will be: $Al(OR)_3$ < $Zn(OR)_2$ < $Ti(OR)_4$ < Bu_3SnOR < $Bu_2Sn(OR)_2$ [54].

For polylactide, the amount of the transesterification reactions occurring during polymerization is affected by the lactide configuration [56]. The extent of transesterification reactions for L-lactide (LLA) was observed to be significantly lower compared to when D-lactide (DLA) was synthesized. The variation in the amount of transesterification reactions was partially because of the different flexibility of the polymer chain. Because of the atactic lactide blocks, PLLA is more rigid than PDLA.

In the case for copolymerization of CL and LLA, the sequence of monomer addition is very crucial. Veld et al. reported that A-B block copolymers are able to be synthesized using ROP with ethanol as initiator and $SnOct_2$ as catalyst only if CL monomer is polymerized first [57]. When the LLA block is synthesized at the beginning and then the OH-terminated pre-polymer is used to start the polymerization of CL, the resulting copolymer will be completely randomized.

2.3.4 Catalysts and Initiators for the Ring Opening Polymerization

To be able to create copolymers with advanced structures, there are several promising and interesting ways, first is to synthesize new initiators, and second is to do ROP of either existing or new monomers as well as pre-polymers terminated with functional groups. Many types of organo-metallic compounds such as metal carboxylates and metal alkoxides have been used as catalysts or initiators in order to synthesize polymer effectively [58]. A lot of reactions which incorporate metal complexes as catalyst are very specific. Therefore, by choosing the ligands and metal carefully, a desired polymer structure can be achieved [59-60].

2.3.4.1 Tin 2-ethylhexanoate

Tin 2-ethylhexanoate, also known as $Sn(Oct)_2$ or stannous octoate, is used commonly as catalyst for the ROP of polylactones and polylactides [53, 61-65]. The usage of stannous octoate as food additive has been permitted by the U.S. Food and Drug Administration and furthermore, the polymerization mechanism has been well studied. Over quite some time, a few mechanisms have been suggested [35, 57, 66-67], however the ROP mechanism was confirmed only recently [68-71]. Since the monomer-to-$Sn(Oct)_2$ molar ratio does not influence the molar mass of the polymer, the $Sn(Oct)_2$ will not be considered as the actual initiator. The mechanism that is most possible is the coordination-insertion mechanism upon which an OH functional group is presumed to react with $Sn(Oct)_2$, generating the tin alkoxide complex initiator.

Two reaction schemes which differ slightly have been proposed from the studies on coordination-insertion mechanism. Kricheldorf et al. have suggested a mechanism [35, 70] whereby during propagation, the coinitiating OH-group and also the monomer are both attached to the $Sn(Oct)_2$ complex. Meanwhile, a mechanism whereby $Sn(Oct)_2$ complex is transformed to a tin alkoxide then continued with the complexation and finally ring-opening of the cyclic monomer, have been proposed by Penczek et al [66]. MALDI-TOF spectroscopy has been used to investigate the tin alkoxide complex for both CL [68] and lactide [69] polymerization for molar mass up to 1500 $g{\cdot}mol^{-1}$. Scheme 2.7 illustrates the two different schemes.

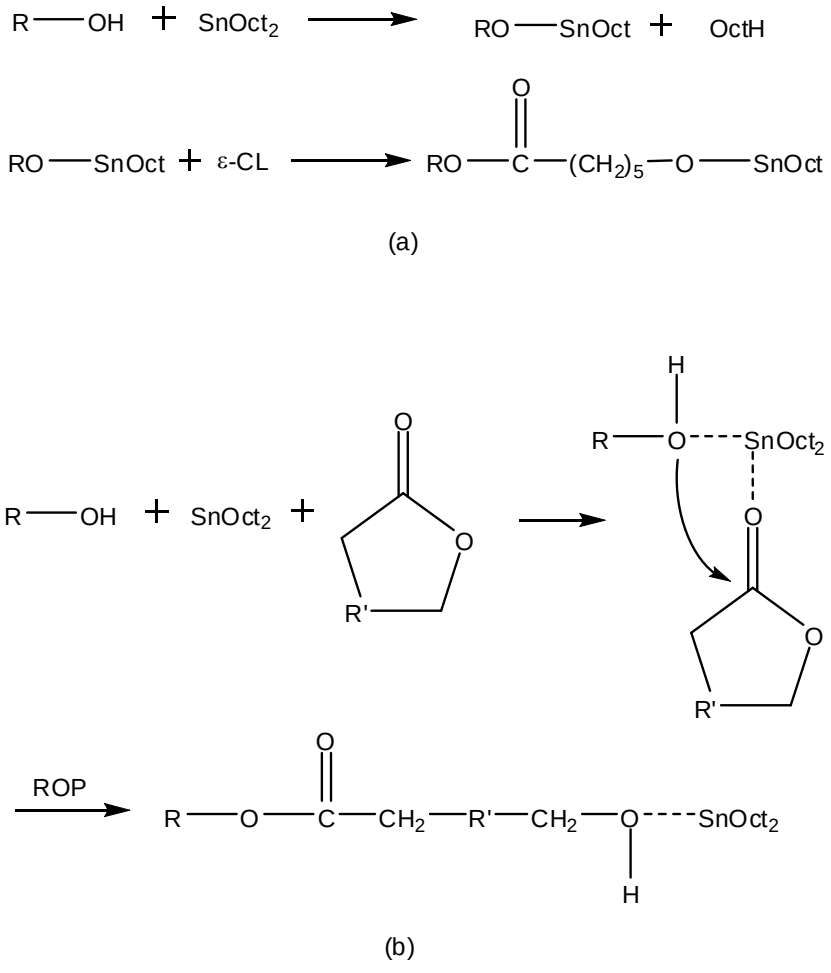

Scheme 2.7 The proposed major ROP mechanism using $Sn(Oct)_2$ as a catalyst, (a) formation of tin-alkoxide prior to ROP of CL and (b) complexation between an alcohol and monomer before the ROP

Unfortunately, $Sn(Oct)_2$ catalyst has been proved to be a powerful transesterification agent, therefore the synthesized copolymers generally will have a random structure [49]. The number of transesterification reactions will be higher if the reaction time or reaction temperature increase.

2.3.4.2. 2,2-Dimethyl-1,3-propanediol

2,2-Dimethyl-1,3-propanediol, which is also known as neopentyl glycol, is a dialcohol that acts as an difunctional initiator in ring opening polymerization, enabling us to synthesize triblock copolymer structure. 2,2-Dimethyl-1,3-propanediol has been used by several research groups for polymerization of CL, TMC, and L-lactide [72-75]. By using an alcohol initiator, we will be able to control the molar mass of the synthesized polymer.

2.3.4.3. 2,2-Bis(hydroxymethyl)1,3-propanediol

2,2-Bis(hydroxymethyl)1,3-propanediol, or more commonly known as pentaerythritol (Figure 2.2) is a white crystalline solid, which has four hydroxyl groups at its ends (four-armed). Thus, it serves as a useful initiator for producing star-shaped polymers with four targeted functional end groups. Moreover, pentaerythritol is halogen-free, it is therefore environmentally friendly, readily biodegradable and non-hazardous in water [76].

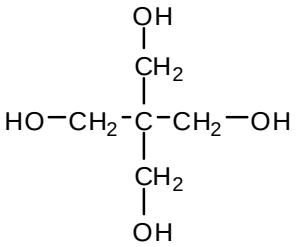

Figure 2.2 Structure of pentaerythritol.

2.3.4.2 Other initiators or catalysts

Besides $Sn(Oct)_2$, cyclic tin alkoxides, monotin alkoxides, and tin dialkoxides have been used as initiators in the ROP of cyclic esters. Cyclic tin alkoxides were studied in the first place due to their resistance towards hydrolysis [77]. The tin alkoxides are known to form cyclic species during synthesis and the dibutyltin alkoxides are known to exist as monomers and dimers [78]. The tin alkoxides have been observed to cause transesterification while initiating polymerization at moderate temperatures [79]. Ring ROP initiated by aluminum tri-isopropoxide has been thoroughly investigated by several research groups [80-84] because of the well-defined polymers it produced through living polymerization. ROP of lactones and lactides with initiators based on lanthanide alkoxide is a relatively recent discovery. The first case of lactone polymerization by lanthanide alkoxide complexes was reported in a DuPont patent written by McLain and Drysdale in 1991 [85]. Generally, the activity of these catalysts is much higher than that determined for aluminum alkoxides, especially in lactide polymerization [86-87].

2.3.5 Monomers for the Ring Opening Polymerization

2.3.5.1 ε - caprolactone

The ring-opening polymerization of ε–caprolactone (CL) produces polycaprolactone (PCL), a semi-crystalline, synthetic aliphatic polyester. It is soft, plastic and hydrophobic, with low T_g (between -65 to -60 ^oC) and also low melting temperature (between 59-64 ^oC) [88]. Figure 2.3 shows the chemical structure of CL during ROP.

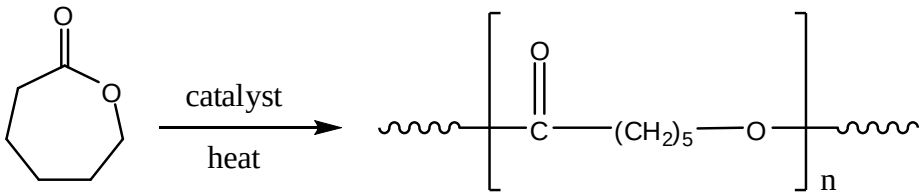

Figure 2.3 Chemical structure of ε-caprolactone undergoing ROP.

PCL has been used as a biodegradable suture as it is regarded as biocompatible, in other words, not only PCL is degradable but its degradation byproducts are also non-toxic [89-91]. However, PCL is highly hydrophobic, crystalline, and having a slow biodegradation rate, making it rather limited for its biomedical applications [92]. One way to reduce its crystallinity is to do random polymerization of PCL with PTMC or polylactide. Homopolymer of PCL degrades in a period of more than 24 months [93]. The degradation rate of PCL can be controlled by copolymerizing with other polymer such as PDLLA. It is also possible to improve the mechanical properties of PCL by copolymerizing it with a hard, brittle polymer like PLLA, producing a polymer which is tougher and thus more beneficial for various applications.

2.3.5.2 Trimethylene Carbonate

Poly (trimethylene carbonate) is synthesized by ROP of 1,3-dioxan-2-one using stannous chloride, stannous octoate, stannic bromide, or diethylzinc [30]. It is a biodegradable polymer that has a flexible feature. It is shown to be an elastomer due to its rubber like properties, which is amorphous in the relaxed state while crystalline in the stretched state [94-95]. PTMC has a T_g of about -20 ^oC [30]. Compared to PCL, PTMC has a lower mechanical property in term of modulus and tensile stress. However, the strain at break of PCL is much less than PTMC as PTMC is softer than PCL [96]. The chemical structure of PTMC during ROP is as follow.

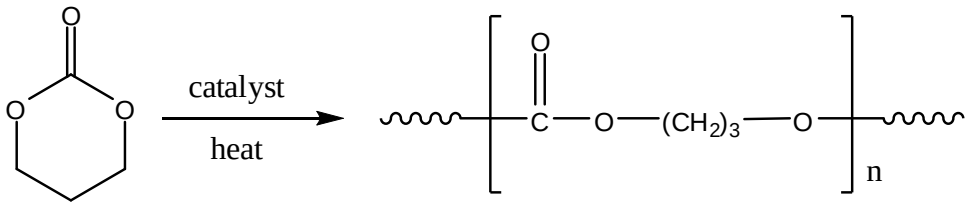

Figure 2.4 Chemical structure of trimethylene carbonate undergoing ROP.

2.3.5.3 L-Lactide

Polylactic acid is a produced by poly-condensation of lactic acid or by catalytic ROP of the lactide group. ROP by coordination initiators is the most efficient way of preparing polylactides as it allows a controlled synthesis and thus results in a narrow PDI [97]. Lactide is the cyclic di-ester of lactic acid which has two optical isomers, D-Lactide and L-Lactide. Polylactic acid (PLLA) is semicrystalline (37% crystallinity) [98]. It has a melting temperature between 175 to 178^oC and glass-transition temperature of 60 to 65^oC [89]. It also exhibits high tensile strength and low

elongation, thus has a high Young's modulus. The chemical structure of both PLLA is shown below.

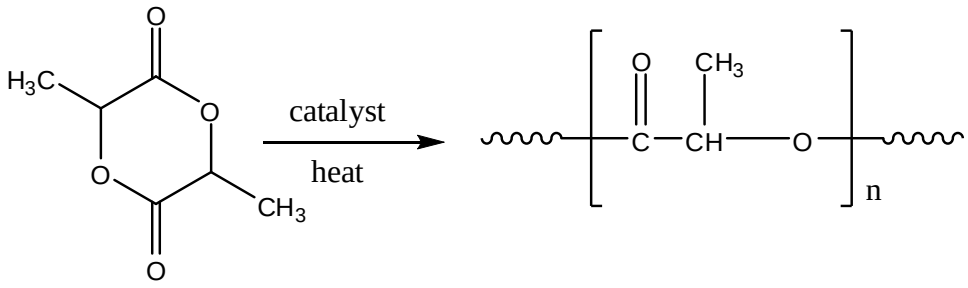

Figure 2.5 Chemical structure of L-lactide undergoing ROP.

When it is implanted in the body, PLLA is biocompatible. PLLA has a degradation time of 18 months order to be completely absorbed [99], compared to PDLLA which degrades between 12 to 16 months [100]. It degrades by hydrolytic scission to lactic acid which occurs naturally in carbohydrate metabolism [101]. The higher rates of PLLA degradation is due to higher water absorption in the amorphous domains.

2.4 Biodegradable Thermoplastic Elastomer

2.4.1 Polyurethanes

Biodegradable thermoplastic polyurethanes (BTPU) are a kind of thermoplastic elastomers (TPE) which have a wide variety of physical properties and chemical compositions [102]. Some research groups have studied BTPU which use degradable polyester as the soft block and various kinds of chain extender and diisocyanate as the hard block [103-106]. Changing the molar mass and composition of the polyester soft

block, or the ratio of diisocyanate to chain extender in the hard block will determine the physical properties of the polymer and affect the degradation rate [104-105, 107].

Numerous biomedical implants and devices have been fabricated from PU. However, the development of PU was slowing down in 1990s because cytocompatibility of PU was the main concern. A problem with degradation of PU is the potentially carcinogenic by-products from the hard segment. It is the corresponding diamine to the diisocyanate that can be toxic [108-111] and the formation of harmful isocyanates when cross-linking points degrade [112]. An oxidative mechanism for the PU hard segment degradation which leads to formation of diamines can be seen in scheme 2.8.

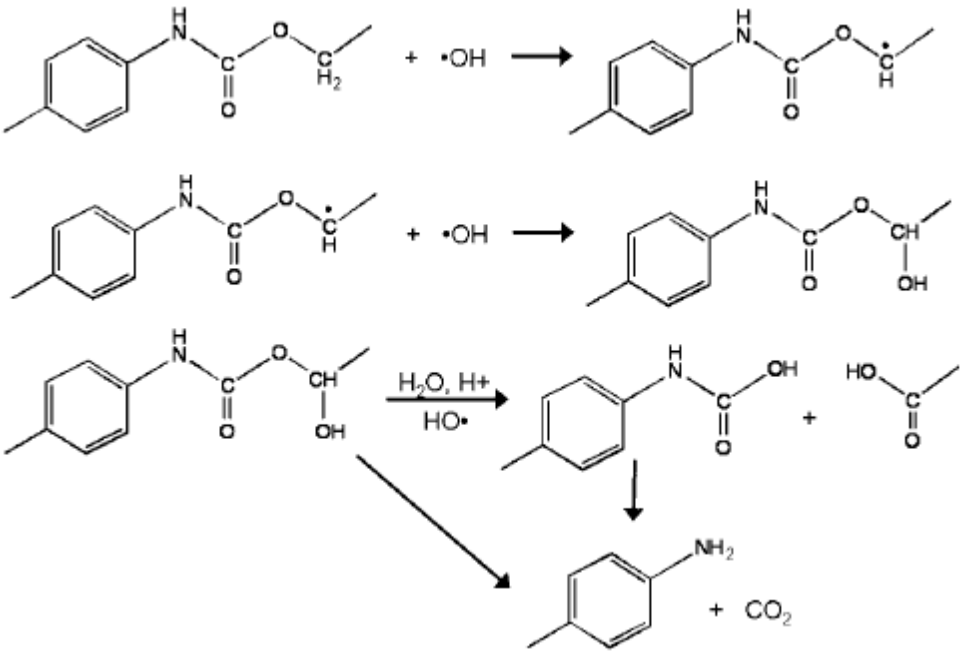

Scheme 2.8 Oxidative mechanism of PU hard segment biodegradation.

More recent studies suggested hard segment modification to produce more cytocompatible PU. In these studies, aliphatic diisocyanates such as lysine

diisocyanate (LDI), hexamethylene diisocyanate (HMDI) and 1,4-diisocyanato butane (BDI), are favored because it is believed to produce less or non-toxic linear diamine during degradation, but there are no data on the recovery properties of these PUs [113-114].

2.4.2 Triblock Copolymers

Biodegradable A-B-A triblock copolymers with ε-caprolactone (CL) as the B block and L-lactide as the A block have been reported by Qian et al [115]. It was observed that by increasing CL:LLA molar ratio from 10:90 to 70:30, higher elongation was achieved. But DSC results showed that in all compositions there were melting points from the CL block ranging from 45 to 53 °C. So, due to the crystallinity of CL, the triblock copolymers did not have elastomeric character. Meanwhile, similar triblock copolymers but using trimethylene carbonate (TMC) as the B block have also been studied [116-117]. With TMC being an amorphous middle block, the triblock copolymers were said to be elastomeric although no experimental data was provided regarding their recovery properties. It should be noted at this point that high elongation-to-break values are necessary but not sufficient to define elastomeric character: elastic recovery values of >70% is required.

Random copolymers of CL and TMC with interesting mechanical properties were synthesized by a few research groups [118-120], but without regard to synthesis of thermoplastic elastomers as the resulting copolymers were usually very soft. A-B-A triblock copolymers with CL and TMC as amorphous central blocks and L-lactide as crystalline blocks have also been investigated by Kricheldorf and Rost [121], but in order to get good mechanical properties, the triblock copolymers have to be converted

into multiblock copolymers through chain extension with 1,6-hexamethylenediisocyanate, whose toxicity under degradative conditions, is a concern. Even after transformation into multiblocks, these polymers are reported to have elongations-to-break (ε_b) of about 800%, with yielding or plastic deformation, which usually indicates poor recovery characteristics. In our opinion, there are no reports of triblock copolymers that are biodegradable and exhibit true elastomeric character in the literature.

2.4.3 Star-block Copolymers

In the search of new biodegradable elastomers with better mechanical and thermal properties, macromolecular structures such as star-copolymers are being explored. Figure 2.6 shows the schematic figure of four armed star-shaped polymers.

Figure 2.6 Illustration of four armed star-shaped polymers, (a) homopolymer of A and (b) block copolymer of A and B.

Star-shaped and branched polymers have been studied and they show promising rheological and mechanical properties. Compared to linear polymer with comparable

molecular weight, star-shaped polymer can be processed at lower temperatures [122], since they have a lower melt viscosity. For thermo-labile polymers like polylactides, having low melt viscosity is particularly beneficial [123]. Additionally, Puig et al. have observed enhanced phase separation on star-shaped structures [124]. This is very important for creating a thermoplastic elastomer, since a good phase separation is the key to have a better elastomeric property.

Star-shaped copolymers have been developed through many different methods. Basically, there are two different ways to synthesize star-shaped copolymers, the "arm-first" strategy and "core-first" approach. For polycarbonates and aliphatic polyester, the most common synthesis technique is to use a catalyst such as $Sn(Oct_2)$ and multi-functional alcohol as initiator which can start the ROP of selected monomer. Making use of the "core-first" approach, a few works have been done with regards to the synthesis of star-shaped polylactide with multi-functional initiator such as pentaerythritol [125-126] and glycerol [127] and SnOct2 as catalyst. In another paper, Dong et al. [128] investigated the synthesis of star-shaped PCL-PLGA50 copolymer with pentaerythritol or trimethylolpropane (TMP) initiator and $Sn(Oct_2)$ catalyst.

However, all the above works did not mention anything on the mechanical properties of the star copolymers. Joziasse et al. [129] synthesized star poly[(TMC)-co-(CL)] and its block copolymers with glycolide/lactide and did some mechanical characterization, but it was limited to tensile test only. As mentioned before, a good elongation alone is not enough to define characteristic of an elastomer. Thus there is a

need to investigate how starblock copolymer of CL, TMC, and L-lactide performs as an elastomeric material.

2.5 Summary

TPE is an uncrosslinked polymer that behaves like a chemically-crosslinked elastomer by having clearly segregated "hard" and "soft" segments in its structure. It has no permanent crosslinks in its structure to be thermosetting and can be made to flow at high temperatures thus making it easy to be processed using conventional methods (extrusion, injection molding). Furthermore, a wide range of structural, thermal, and mechanical properties are achievable by structure manipulation. If a TPE is made to be biodegradable then it has many potential uses in implantable medical devices.

For that reason the challenge is to synthesize a biodegradable TPE which has a good mechanical properties yet does not contain any diisocyanate as the hard block or as a chain extender as to avoid toxicity problem. To accomplish this, we propose to use an approach by using coordination-insertion ring opening polymerization to make "living polymers" that will in turn enable the construction of different polymer configurations having multi-functionalities. The copolymers will be characterized structurally, thermally, and mechanically, with emphasis on the elastomeric properties. And biodegradation study of these copolymers in vitro will be done to predict their use in vivo.

Chapter 3 Experimental Materials and Method

3.1 Materials

The monomers, ε-caprolactone (CL) (99%) was obtained from Fluka, dried over CaH_2 and distilled under nitrogen at reduced pressure. L-lactide (LLA) was obtained from Sigma Aldrich and purified by recrystallization from dry ethyl ether, and trimethylene carbonate (TMC) was purchased from Boehringer Ingelheim and purified by recrystallization from dry ethyl ether. The initiator for triblock copolymer, 2, 2-dimethyl 1, 3-propanediol (purumi, > 99.0 %) was from Fluka, initiator for starblock copolymer, Pentaerythritol, ≥99% was from Sigma Aldrich both were used without further purification. The catalyst, Tin (II) 2-ethylhexanoate ($SnOct_2$) from Sigma Aldrich was used as received. Toluene anhydrous (99.8%) was purchased from Sigma Aldrich and used as the polymerization solvent.

3.2 Synthesis Method

3.2.1 Random Copolymer of ε-Caprolactone and Trimethylene Carbonate

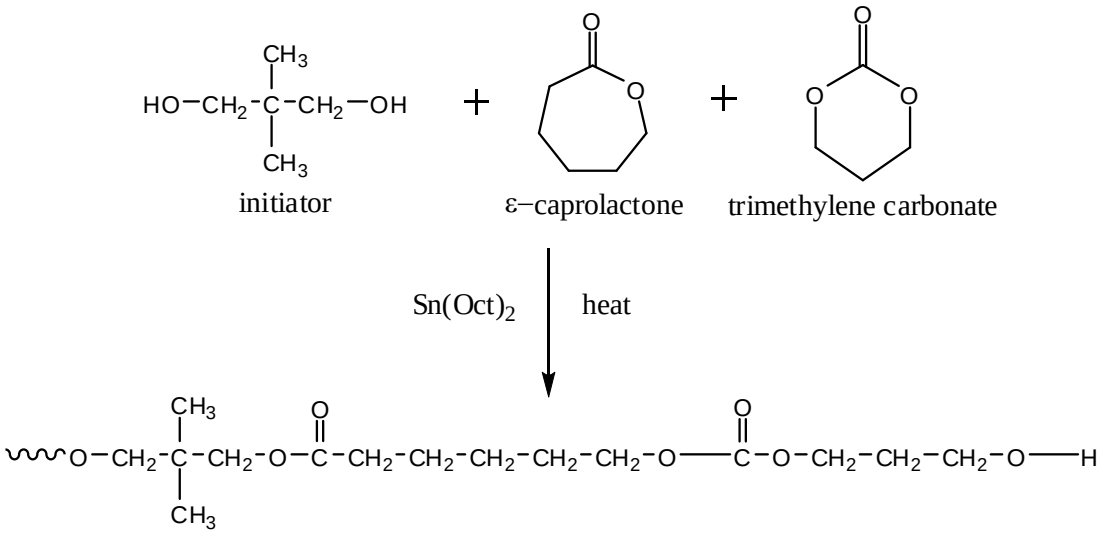

Scheme 3.1 Reaction schemes for synthesis of random copolymer of CL and TMC with 2,2-dimethyl-1,3-propanediol as initiator and $Sn(Oct)_2$ as catalyst.

Random copolymers of CL and TMC were synthesized as a preliminary study. The syntheses were done in a double-necked round bottom flask (100 ml) equipped with thermometer, condenser and magnetic stirrer. The flask was purged by argon, vacuumed twice and then kept under the argon atmosphere. The amount of monomers, initiator and catalyst used were varied for each copolymer. For the example of copolymer **CLTMC1** in Table 4.1, a mixture of CL (4 mL) and TMC (1.2 g) monomers were added to the 50 mL toluene and then 50.1 mg of 2,2-dimethyl-1,3-propanediol initiator was added. Finally, $Sn(Oct)_2$ as the catalyst (43 μL) was added to the mixture and the flask was immersed into silicone oil bath at a temperature of 140°C for 24 hours. The random copolymer was precipitated in 500 mL of methanol

and dried under vacuum (1 mbar) at room temperature for 3 days. The final states of the copolymers varied from wax (for CL:TMC 50:50) to powder (for CL:TMC 90:10)

3.2.2 Triblock Copolymer of ε-Caprolactone, Trimethylene Carbonate and L-Lactide

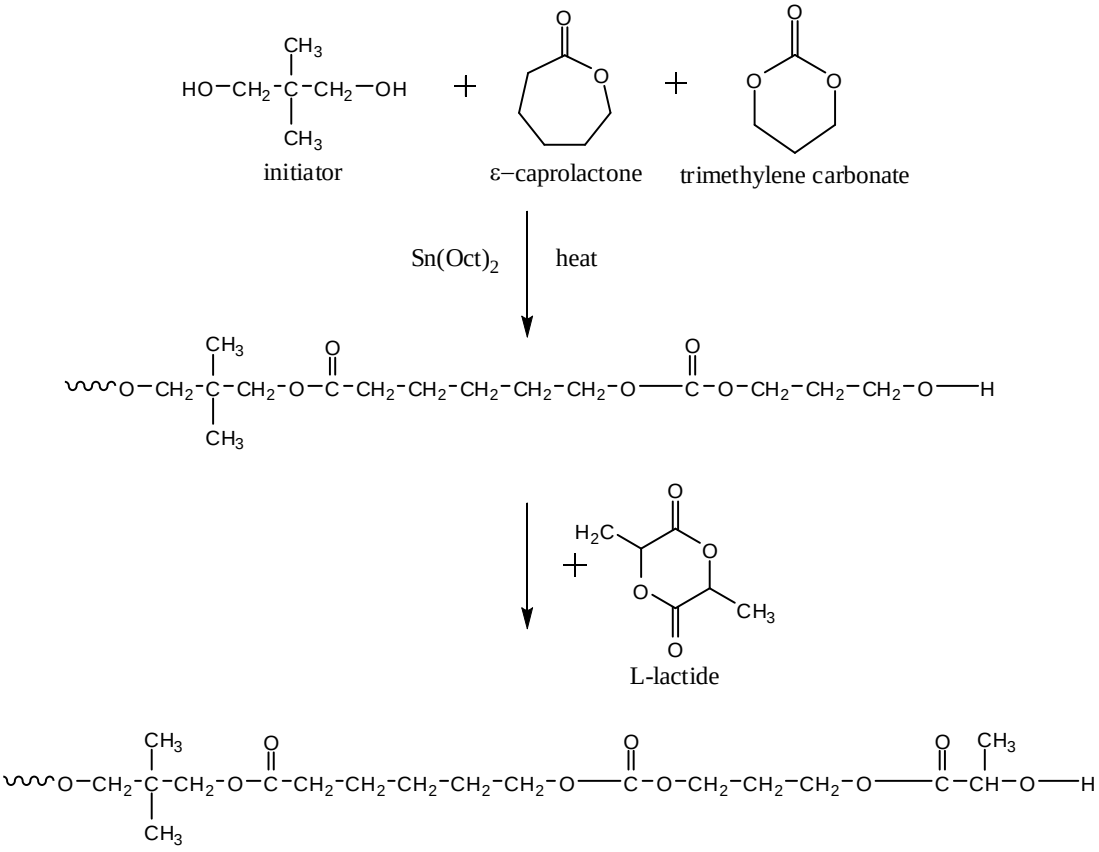

Scheme 3.2 Reaction schemes for synthesis of triblock copolymer made of CL and TMC as soft-block with L-LA as hardblock.

A-B-A triblock copolymers, where B is the soft segment made of a random copolymer of PCL + PTMC and A block is a PLLA (Scheme 3.2) or PLLA + PCL (Scheme 3.3) hard segment were prepared by one-step living coordination insertion ring-opening polymerization. The syntheses were done in a double necked round

bottom flask (100 ml) equipped with thermometer, condenser and magnetic stirrer. The flask was purged by argon, vacuumed twice and then kept under the argon atmosphere. The amount of monomers, initiator and catalyst used were varied for each copolymer. For the example of copolymer **A4** in Table 4.2, a mixture of CL (6 mL) and TMC (5.8 g) monomers were added to the 50 mL toluene and then 29.6 mg of 2,2-dimethyl-1,3-propanediol initiator was added. Finally, $Sn(Oct)_2$ as the catalyst (99 μL) was added to the mixture and the flask was immersed into silicone oil bath at a temperature of 140°C for 24 hours. A defined quantity of LLA (6.14 g) was then added to the flask and the mixture was reacted for another 24 hours. The block copolymer was precipitated in 500 mL of methanol and dried under vacuum for 3 days. The final states of the copolymers were white solid aggregates.

For other copolymers in this category, they were made by the same method using same $Sn(Oct)_2$ to monomer ratio and same monomer to solvent ratio, but varying the ratio of monomers and initiator to get different compositions and molar masses. The complete ratio of monomers, initiator, and catalyst used for all the copolymers are shown in Appendix A.

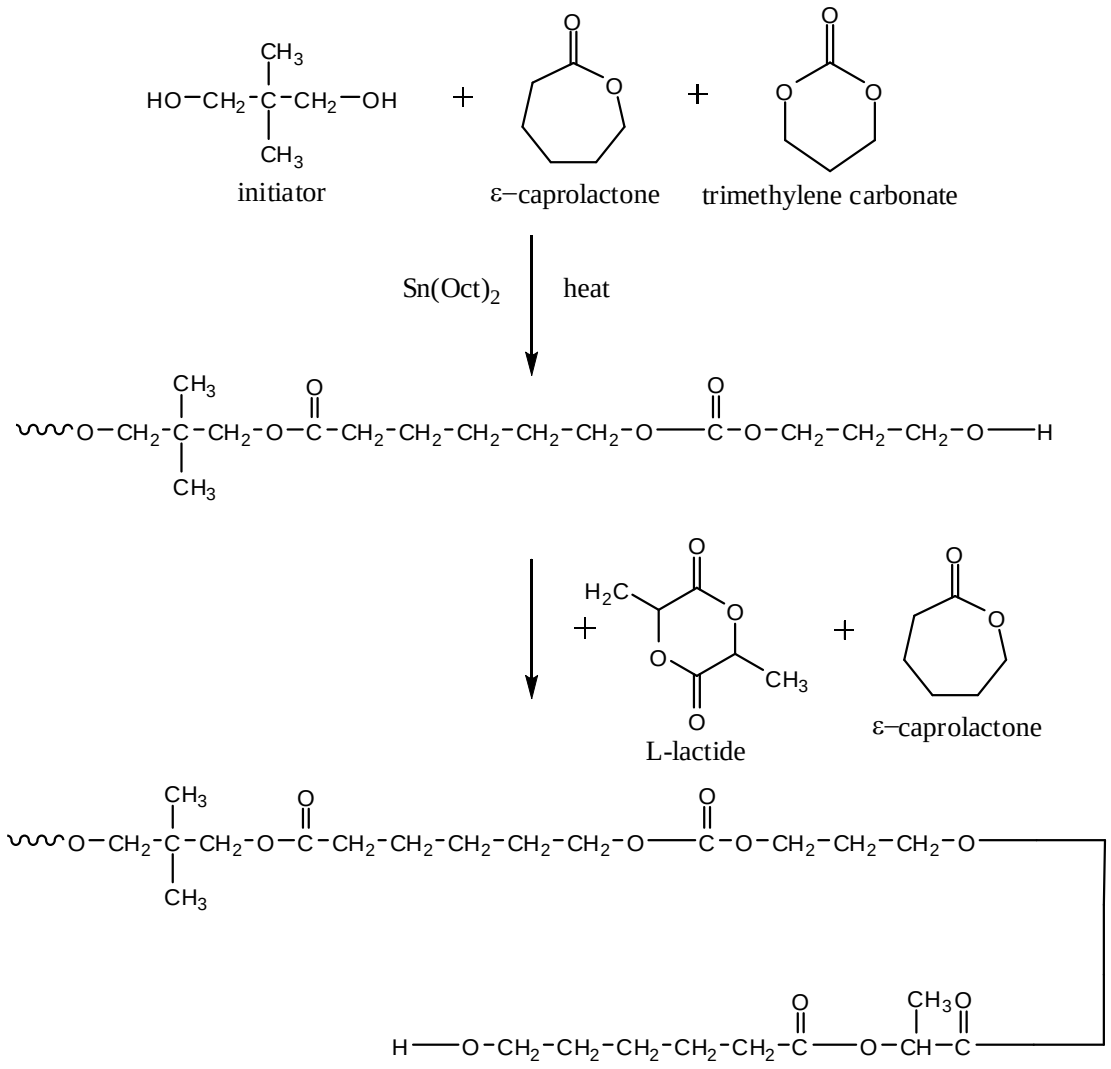

Scheme 3.3 Reaction schemes for synthesis of triblock copolymer made of PCL and PTMC as soft-block with PLLA and PCL as hardblock.

3.2.3 Starblock Copolymer of ε-Caprolactone, Trimethylene Carbonate and L-Lactide

Four armed star-shaped copolymerization was produced by pentaerythritol as the initiator. CL and TMC are the monomers for the soft block, while L-lactide is used for the hard block monomer. The synthesis was carried out at 140 °C in an inert

environment with $SnOct_2$ as the catalyst and toluene was used as solvent for the polymerization reaction.

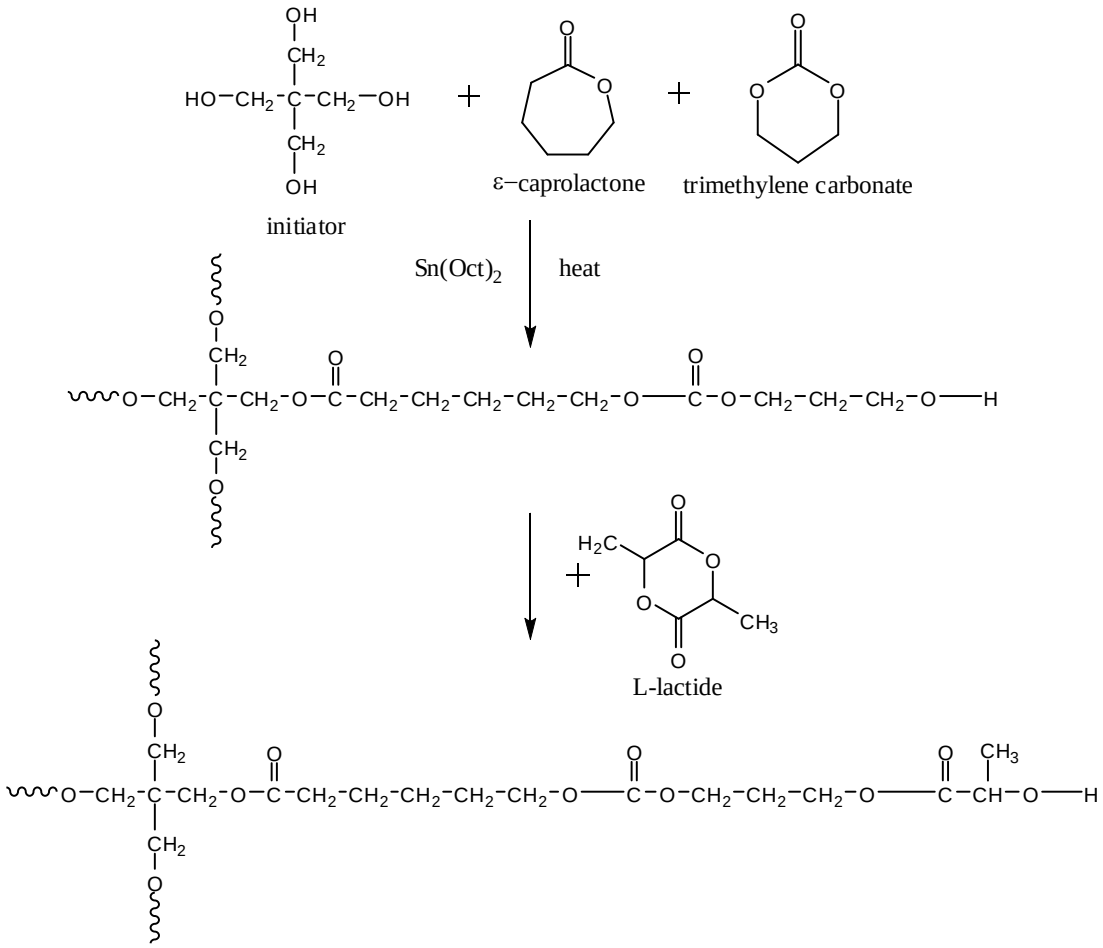

Scheme 3.4 Reaction schemes for synthesis of starblock copolymer made of PCL and PTMC as soft-block with PLLA as hardblock.

All syntheses were done in 100 mL double-necked round bottom flask equipped with thermometer, condenser, and magnetic stirrer. The flask was purged by argon gas, vacuumed twice and then it was kept under the argon atmosphere. The amount of monomers, initiator and catalyst used were varied for each copolymer. For the example of copolymer S**A3** in Table 7.1, a mixture of CL (6 mL) and TMC (5.8 g) monomers were added to the 50 mL toluene and then 77.3 mg of pentaerythritol

initiator was added. Finally, $Sn(Oct)_2$ as the catalyst (99 μL) was added to the mixture and the flask was immersed into silicone oil bath at a temperature of 140°C for 24 hours. A defined quantity of LLA (12.3 g) was then added to the flask and the mixture was reacted for another 24 hours. The star copolymer was precipitated in 500 mL of methanol and dried under vacuum (1 mbar) at room temperature for 3 days. The final state of the copolymers ranged between white powders to solid aggregates.

For other copolymers in this category, they were made by the same method using same $Sn(Oct)_2$ to monomer ratio and same monomer to solvent ratio, but varying the ratio of monomers and initiator to get different compositions and molar masses. The complete ratio of monomers, initiator, and catalyst used for all the copolymers are shown in Appendix A.

3.3 Characterization

3.3.1 Size Exclusion Chromatography (SEC)

Number average molar mass (M_n) of polymers was determined by size exclusion chromatography, SEC (Shimadzu LC-20AD with RI detector). Twelve polystyrene standards (Fluka) with narrow molar mass distribution in the range of 580-400,000 g/mol were used for calibration. All SEC measurements were carried out using three linear PLgel (5μm) mixed C columns (Polymer Laboratory) connected in series and maintained at 35±0.1 $^{\circ}$C and HPLC grade chloroform as mobile phase at 1.0 mL/min flow rate.

3.3.2 Nuclear Magnetic Resonance (NMR)

Compositions of CL, TMC, and LLA inside the polymer were determined by ^{1}H-NMR and chemical structure and the monomer sequence of the block copolymers were determined by ^{13}C-NMR. Both NMR spectra were recorded on a Bruker 400 MHz Spectrometer. A 25 mg sample (for ^{1}H-NMR) or 100 mg sample (for ^{13}C-NMR) was dissolved in 0.5 ml deuterated chloroform ($CDCl_3$) in a 5 mm diameter sample tube. The numbers of scans were 64 scans for ^{1}H-NMR and 1024 scans for ^{13}C-NMR.

3.3.3 Differential Scanning Calorimetry (DSC)

Glass transition temperatures (T_g) and melting temperatures (T_m) of the synthesized copolymers were analyzed by DSC. The T_g values were taken from the inflection point, and T_m values were taken from T_{max}. Using aluminum hermetic pan, samples weighing 5-10 mg were measured with heating rate of 10 $^{\circ}$C/min and cooling rate of 5 $^{\circ}$C/min in a temperature range of -90 to 225 $^{\circ}$C using TA Instruments Model Q10 DSC machine. All samples were scanned using two heating cycles and reported values were determined from the second scan.

3.3.4 Instron Machine

Polymer solutions in solvent (10% w/v) were cast using glass petri dishes. After being dried at ambient atmosphere for 4 days continued with drying in vacuum for 2 days, films with 0.2–0.3 mm thickness were acquired. Using these white translucent films, samples for mechanical properties test were cut into standard dog-bone shaped. Tensile test was carried out using the INSTRON 5848 microtester according to ASTM D882-91 standards. A cyclic loading test was also done on the INSTRON

machine. For recovery study, dog bone shape specimens were pulled in vertical direction at a rate of 10 mm/min at 25 °C up to elongation of 100%, 200%, and 300% consequently.

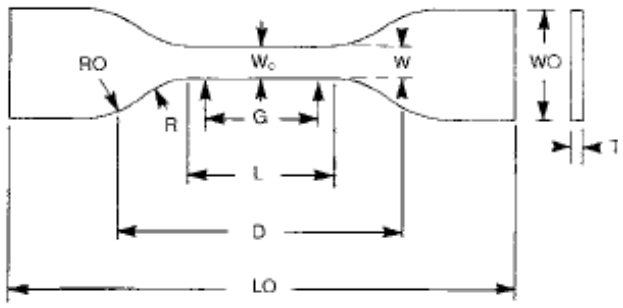

W – Width of narrow section	3.18 mm
L – Length of narrow section	9.53 mm
WO – Width overall, min	9.53 mm
LO – Length overall, min	63.5 mm
G – Gage length	7.62 mm
D – Distance between grips	25.4 mm
R – Radius of fillet	12.7 mm

Figure 3.1 Dog-bone specimen shape and dimensions.

3.3.5 Dynamic Mechanical Analyzer (DMA)

To fully characterize and quantify the elastomeric nature of the triblocks, the TA Instruments' Dynamic Mechanical Analyzer (DMA Q800) was utilized to measure creep and recovery under different stress levels. The experiment was conducted in film tension mode with sample thickness 0.2–0.3mm. The polymers were subjected to elongation up to 200% strain, at a rate of 10% strain per minute to determine their maximum tensile stress. For creep and recovery test, two level of stress were applied amounting to 30% and 80% of the maximum stress determined for each polymer. The films were subjected to displacement under the two stress levels for 30 min and then recovery was monitored for 30 minutes after stress removal. A minimum of 3 polymer specimens were studied for each experiment. All experiments are conducted at ambient temperature (25±1 °C).

3.3.5 Biodegradation

In vitro biodegradation of the copolymers was studied by monitoring the change in molar mass (M_n), mass of sample and ^{1}H NMR analysis (selected samples) of the copolymers over immersion time in 1.0 M Phosphate Buffered Saline (PBS) (pH=7.4). Film samples (5mm x 5mm x 0.2mm) cut from each copolymer sheet (prepared as mentioned before) were used for the degradation study followed by SEC measurement. Each piece of the film was immersed in 1.5 mL PBS buffer [1M, pH7.4] solution and incubated at 37 $^\circ$C. The PBS solutions were changed frequently to maintain the pH at around 7.4. Four representative samples were considered for each data point. After every time interval, samples were taken out, washed with fresh de-ionized water and dried in vacuum oven before measurement of molar mass (SEC) and dry weight (Sartorius). % change in M_n and mass loss (ML) was obtained by using the equation below comparing the starting molar mass (M_n^0) /mass of sample and the molar mass/mass of sample measured at various intervals (M_t).

$$ML = \frac{M_n{}^o - M_t}{M_n{}^0} \times 100\%$$

The ^{1}H NMR analysis was done to estimate the extent of hydrolysis in the mid- and end-blocks. The degraded samples after wash and vacuum drying were dissolved in $CDCl_3$ of 2.5% w/v concentration and 0.6mL of this solution was taken in NMR tube and capped. ^{1}H NMR spectra was obtained at room temperature using a Bruker 400 MHz Spectrometer.

3.3.6 Atomic Force Microscopy (AFM)

Atomic force microscopy was used to visualize the morphologies of the copolymers. A commercial AFM instrument (Dimension 3100 with Nanoscope IIIa controller, Veeco Instruments Inc., CA) equipped with a scanner (90 × 90 μm^2) was used to image the samples in tapping mode in air. Silicon cantilevers with the normal resonance frequency of 300 kHz and spring constants of 40 Nm^{-1} (Tap300Al, Budget Sensors, Bulgaria) were used. All images were captured with scan rate at 1~2 Hz and with 512 × 512 pixel resolution.

3.3.7 Wide-angle X-ray diffraction (WAXD)

Wide-angle X-ray diffraction (WAXD) measurements were carried out with a Bruker GADDS X-ray diffractometer, equipped with a two-dimensional (2D) area detector using monochromatic Cu Kα radiation. The beam size at the sample position was about 0.8mm in diameter. The sample-detector distance of 300mm was employed. The sample was mounted in such a manner that it is normal to the incident X-ray beam and the X-ray diffraction pattern was recorded on a 2D area detector.

For the evaluation of orientation of the crystal in both the soft and hard segments, the azimuthal intensity distribution $I(\phi)$ at 2θ = 16.5° and 21.5° were analyzed respectively. The peaks at 2θ = 16.5° and 21.5° represent the 110 reflection of the PLLA and PCL crystals respectively, which both appeared on the equator during stretching [130-131].

The Herman's orientation function, P_2 is used for quantifying the degree of crystal orientation and can be calculated using the following equations:

$$P_2 = \frac{3\langle cos^2\phi\rangle - 1}{2}$$

with

$$\langle cos^2\phi\rangle = \frac{\int_0^\pi I(\phi) sin\phi cos^2\phi d\phi}{\int_0^\pi I(\phi) sin\phi d\phi}$$

where ϕ is the azimuthal angle, being zero at the meridian and $\pi/2$ at the equator. The function takes a value of 1 for perfect orientation and zero for no orientation.

Chapter 4 Triblock Copolymers of ε-Caprolactone, Trimethylene Carbonate, and L-Lactide

Since the soft segment of thermoplastic elastomer is the segment which provides elastomeric character for the TPE, it must have a relatively low T_g and usually it must be an amorphous polymer. Among the various homopolymers that have been synthesized, PCL is the most suitable candidate for the soft segment of the TPE. It has a low T_g, and it has been proved to be biodegradable. Unfortunately, PCL is known to be highly crystalline, so we need to think of a way to control of the crystallinity of PCL in order to be able to drop it down to 0%, thus improving the elasticity of PCL.

One way to make amorphous PCL is by copolymerizing PCL with other polymer in order to disrupt the regularity of PCL packing in the chain, thus making it amorphous. Among the biodegradable polymers, PTMC is a good candidate for a few reasons. First, PTMC is an amorphous polymer by itself; second, it has a relatively low T_g about -20 °C [30]. Therefore, PTMC was chosen to be copolymerized with PCL in order to get an amorphous, low T_g soft-block.

4.1 Synthesis of Random Copolymer of PCL and PTMC

A few syntheses on this random copolymer were done, varying the molar mass and the composition of CL and TMC. Table 4.1 shows the properties of the synthesized copolymers. According to ^{1}H NMR analysis, the molar ratio of CL is always bigger

than the feed ratio. This can be explained using the reactivity ratio of CL and TMC. Albertsson et al. [132] has determined the reactivity ratio in a copolymer of CL and TMC synthesized using $Sn(Oct)_2$ catalyst at reaction temperature of 100 °C which is a similar condition to this work. Using the Fineman-Ross method, the reactivity ratio was found to be r_{CL} = 2.70 and r_{TMC} = 0.38, which resulted in r_{CL} x r_{TMC} = 1.03. This means the polymerization proceeded in a random fashion, and since $r_{CL} > r_{TMC}$, the copolymer will contain a larger proportion of CL.

Table 4.1 Properties of random copolymers of CL and TMC.

Polymer	feed ratio CL:TMC	molar ratio[a] CL:TMC	M_n[b] ($g \cdot mol^{-1}$)	PDI[b]	T_g (°C)	T_m (°C)	ΔH (J/g)
CLTMC1	75 : 25	77 : 23	19700	1.51	-58	42	37.2
CLTMC2	75 : 25	78 : 22	24200	1.30	-55	42	42.6
CLTMC3	75 : 25	77 : 23	36900	1.41	-54	44	40.3
CLTMC4	50 : 50	53 : 47	9600	1.47	-51	-	-
CLTMC5	50 : 50	52 : 48	14300	1.65	-51	-	-
CLTMC6	50 : 50	54 : 46	21300	1.54	-48	-	-
CLTMC7	50 : 50	53 : 47	32300	1.63	-48	-	-

[a] Determined by ^{1}H NMR analysis

[b] Obtained by SEC analysis

When the molar ratio of CL:TMC is 75:25, DSC result showed the presence of crystallinity via the observed T_m. When the molar ratio of CL:TMC was changed to 50:50, no T_m was observed at all regardless of the different molar masses, meaning the copolymers was totally amorphous. Based on this result, the triblock was synthesized using CL:TMC 50:50 as the soft-block and followed by other ratios, e.g. CL:TMC 75:25, and 90:10.

4.2 Triblock Copolymer of CL, TMC, and L-LA

All the synthesized triblock copolymers were categorized under three different groups. The grouping was based on the ratio of CL to TMC in the middle (soft) block. The CL:TMC in feed ratios were 50:50, 75:25 and 90:10 (Table 4.2, 4.3 and 4.4). Within each group, the ratio of CL to TMC of the middle block was kept constant and the molar mass of each block varied within that group. Thus, in the first group below, the CL:TMC molar ratio of the middle block was kept at 50:50 while the molar ratio between the mid-block and end-block as well as the molar mass of the triblocks were varied to study their effects on elastomeric character. Within each table, the second column designates the targeted molar ratio for each monomer sorted by increasing L-lactide content and for certain molar composition; within a fixed composition sub-group (e.g. **A2**, **A3**, **A4**), the polymers are presented in increasing order of molar mass.

4.2.1 Molar Mass and Structural Properties

4.2.1.1 PLLA-b-poly(CL-co-TMC)-b-PLLA with CL:TMC 50:50

Table 4.2 Molar ratio and molar mass of various PLLA-*b*-poly(CL-*co*-TMC)-*b*-PLLA with CL:TMC 50:50 (Group A).

Polymer	feed ratio CL:TMC:LLA	molar ratio[a] CL:TMC:LLA	M_n[b] ($g \cdot mol^{-1}$)	PDI[b]	M_n[c] P(CL-*co*-TMC) ($g \cdot mol^{-1}$)	M_n[c] PLLA ($g \cdot mol^{-1}$)
A1	1 : 1 : 0.38	1 : 0.92 : 0.21	32900	1.44	28700	4200
A2	1 : 1 : 0.75	1 : 0.92 : 0.53	23700	1.51	17300	6400
A3	1 : 1 : 0.75	1 : 0.91 : 0.58	37800	1.48	27000	10800
A4	1 : 1 : 0.75	1 : 0.85 : 0.66	43600	1.39	29600	14000

A5	1 : 1 : 1.50	1 : 0.94 : 1.26	16500	1.63	8900	7600
A6	1 : 1 : 1.50	1 : 0.94 : 1.27	31200	1.57	16700	14500
A7	1 : 1 : 1.50	1 : 0.96 : 1.24	40900	1.41	22200	18700
A8	1 : 1 : 1.50	1 : 0.83 : 1.35	49200	1.22	24900	24300
A9	1 : 1 : 3.00	1 : 0.95 : 2.77	25300	1.39	8800	16500

[a] Determined by ^{1}H NMR analysis

[b] Obtained by SEC analysis

[c] Block length calculated from the M_n by SEC and ^{1}H NMR result

Table 4.2 shows various A-B-A triblock copolymers with the B block made of a random copolymer of PCL and PTMC at a molar ratio of 50:50, and the A block made of PLLA. Nine triblocks with four different feed ratios ranging from CL:LLA equals 1:0.38 to 1:3 were successfully synthesized. The emphasis was put on feed ratio CL:LLA of 1:0.75 and 1:1.5 by further varying their molar mass. The number-average molar mass (M_n) obtained from the SEC analysis varied from 16500 to 49200 $g \cdot mol^{-1}$. From the calculation of the soft-block and hard-block length, it can be seen that for CL:LLA 1:0.75 the resulting hard-block will have a molar mass approximately half of that of the soft-block, while CL:LLA 1:1.5 and 1:3 will give hard-block molar masses equal to and double that of the soft-block respectively.

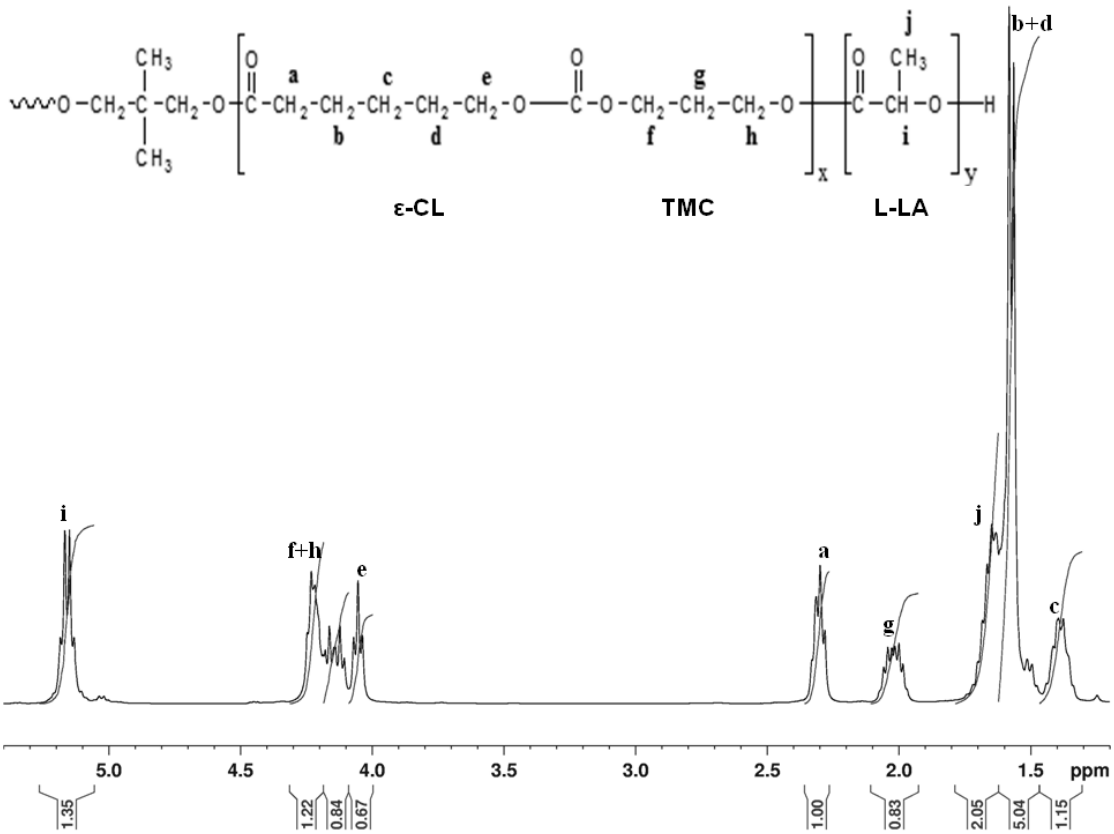

Figure 4.1 Structure of the triblock copolymer and its ^{1}H NMR spectrum for CL:TMC 50:50 (**A8**) in $CDCl_3$.

The typical ^{1}H NMR spectrum of the triblock copolymer is shown in Figure 4.1. The methylene protons from PCL: (**a**), (**b+d**), (**c**) and (**e**) are shown at 2.31, 1.66, 1.39, and 4.23 ppm respectively. Also, methylene protons from PTMC (**f+h**), and (**g**) are shown at 4.05 and 2.04 ppm, respectively. The methane (**i**) and methyl protons (**j**) of the PLLA block are shown at 5.16 and 1.64 ppm respectively. The peak splitting in the region of (**f+h**) and (**e**) peaks suggested randomization of PCL and PTMC. Monomer composition of the copolymer was determined from the integration ratio between proton signals (**a**), (**g**), and (**i**) (as the results are included in Table 4.2).

While the resulting CL to TMC molar ratios are close to the feed ratios, the L-lactide contents of the purified triblock copolymers were lower than expected from the target

composition as seen from the ^{1}H NMR result. This is due to the lower (90% to 95%) conversion of L-lactide [117] which might result from L-lactide transesterification during the polymerization [133]. Nevertheless, Table 4.2 shows that the composition of PLLA in the triblock copolymers can be reasonably well regulated.

4.2.1.2 PLLA-b-poly(CL-co-TMC)-b-PLLA with CL:TMC 75:25

Table 4.3 Molar ratio and molar mass of various PLLA-*b*-poly(CL-*co*-TMC)-*b*-PLLA with CL:TMC 75:25 (Group B).

Polymer	feed ratio CL:TMC:LLA	molar ratio[a] CL:TMC:LLA	M_n[b] ($g \cdot mol^{-1}$)	PDI[b]	M_n[c] P(CL-*co*-TMC) ($g \cdot mol^{-1}$)	M_n[c] PLLA ($g \cdot mol^{-1}$)
B1	1 : 0.33 : 0.5	1 : 0.31 : 0.38	31100	1.49	22600	8500
B2	1 : 0.33 : 0.5	1 : 0.29 : 0.38	35700	1.73	26000	9700
B3	1 : 0.33 : 1	1 : 0.25 : 1.03	41600	1.24	20200	21400
B4	1 : 0.33 : 1	1 : 0.28 : 0.85	56100	1.40	30200	25900

[a] Determined by ^{1}H NMR analysis

[b] Obtained by SEC analysis

[c] Block length calculated from the M_n by SEC and ^{1}H NMR result

Table 4.3 shows four triblock copolymers with a middle block of random copolymer with CL:TMC molar ratio of 75:25. Two different feed ratios were targeted, and each feed ratio has two copolymers with different molar mass, ranging from 31100 to 56100. Similar to group A, ^{1}H NMR data also showed good agreement for molar ratio of CL:TMC (targeted and achieved) and a slightly lower L-lactide content than targeted.

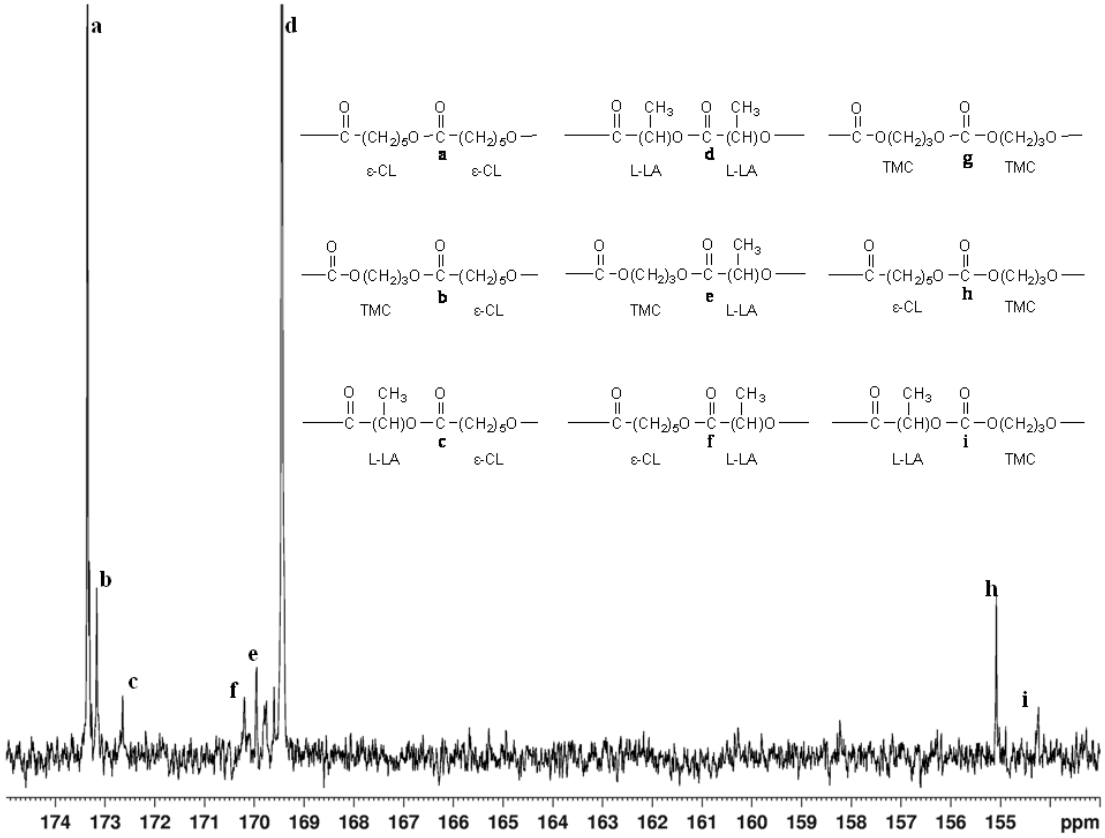

Figure 4.2 ^{13}C NMR spectrum from region of carbonyl carbon atoms of CL:TMC 75:25 (**B3**) in $CDCl_3$ and their peaks assignment.

Overall, the chemical shift of the triblock copolymers ^{13}C NMR spectrum were similar to the spectrum from terpolymer of CL, TMC, and PLLA reported by Jia et al [134]. It can be observed that the soft segment of the triblock copolymers with CL:TMC 75:25 was not as random as CL:TMC 50:50. For CL:TMC 50:50 the CO signal from either CL and TMC carbonyl atoms showed a dyad splitting of almost equal intensity, whereas for CL:TMC 75:25, although the CO signal from CL carbonyl atom still showed a dyad splitting into peak (**a**) (CL-CL dyad) and peak (**b**) (CL-TMC dyad) (Figure 4.2), the TMC carbonyl atom only showed TMC-CL dyad, peak (**h**) which is reasonable considering the CL:TMC 75:25 ratio.

From the L-lactide signals, it can be observed that there was indeed a certain amount of transesterification of the L-lactide block during the polymerization, as shown by a cluster of small peaks (**e**) and (**f**) located to the left of LLA-LLA dyad peak (**d**) which corresponds to TMC-LLA and CL-LLA sequence respectively. The occurrence of TMC-LLA and CL-LLA sequence showed that there was a randomization between the PLLA block and poly(CL-co-TMC) block. As mentioned in *Chapter 2*, transesterification, particularly the intermolecular transesterification reactions, modified the sequences of the copolymers and prevent the formation of block copolymers. Nevertheless, the low intensity of peaks (**e**) and (**f**) compared to peak **(d)** has shown that our copolymer is a triblock instead of a multiblock or random copolymer.

4.2.1.3 PLLA-b-poly(CL-co-TMC)-b-PLLA with CL:TMC 90:10

Table 4.4 Molar ratio and molar mass of various PLLA-*b*-poly(CL-*co*-TMC)-*b*-PLLA with CL:TMC 90:10 (Group C).

Polymer	feed ratio CL:TMC:LLA	molar ratio[a] CL:TMC:LLA	M_n [b] ($g \cdot mol^{-1}$)	PDI[b]	M_n [c] P(CL-*co*-TMC) ($g \cdot mol^{-1}$)	M_n [c] PLLA ($g \cdot mol^{-1}$)
C1	1 : 0.11 : 0.83	1 : 0.11 : 0.70	56500	1.11	31400	25100
C2	1 : 0.11 : 0.83	1 : 0.09 : 0.74	130300	1.29	70000	60300

[a] Determined by ^{1}H NMR analysis

[b] Obtained by SEC analysis

[c] Block length calculated from the M_n by SEC and ^{1}H NMR result

In Table 4.4 the middle block of the triblock copolymers were random copolymers of PCL and PTMC with CL:TMC molar ratio of 90:10. Only one molar ratio was synthesized, with two different molar mass, 56500 and 130300. Again, ^{1}H NMR data

showed good agreement for molar ratio of CL:TMC (targeted and achieved) and a slightly lower L-lactide content than targeted.

4.2.2 Thermal and Mechanical Properties

4.2.2.1 PLLA-b-poly(CL-co-TMC)-b-PLLA with CL:TMC 50:50

Table 4.5 Thermal and mechanical properties of various PLLA-*b*-poly(CL-*co*-TMC)-*b*-PLLA with CL:TMC 50:50 (Group A).

Polymer	T_g (°C)	T_m (°C)	ΔH (J/g)	Modulus (MPa)	Tensile Strength (MPa)	Max Strain, ε_b (%)
A1	-42	-	-	Too weak	Too weak	Too weak
A2	-40	127	5.5	Too weak	Too weak	Too weak
A3	-43	139	7.0	3.5 ± 0.5	1.5 ± 0.6	74 ± 17
A4	-47	140	8.4	2.3 ± 0.3	1.9 ± 0.1	421 ± 24
A5	-38	143	17.7	8.3 ± 0.6	2.6 ± 0.4	29 ± 6
A6	-41	152	20.3	10.8 ± 0.6	4.6 ± 0.8	60 ± 15
A7	-46	159	20.6	13.3 ± 0.7	4.5 ± 0.2	278 ± 37
A8	-44	149	19.1	12.5 ± 0.8	4.5 ± 0.6	520 ± 81
A9	-39	159	36.0	Too brittle	Too brittle	Too brittle

Clearly, at a ratio of 50:50 CL:TMC, all the synthesized middle blocks were amorphous, as no melting of the PCL could be measured, Figure 4.3(a). The L-lactide end-block was crystalline in all cases except for polymer **A1** which has a very low L-lactide content. Table 4.5 shows that the T_m of the end-block in the copolymers ranged between 126°C to 160°C. Since it is reported that the homopolymer of PLLA has a T_m of ~169°C [135], it can be concluded that the middle block has the effect of lowering the T_m of PLLA in the triblock; additionally the crystallite perfection (and

hence the T_m) could also be influenced by the LLA molar mass. The observed T_g seen in the DSC for the triblock is the T_g of random copolymer of CL and TMC. Since the T_g of homopolymers of PCL and PTMC are -60°C and -20°C respectively [30, 88], it is expected that the T_g of the random copolymer would lie between these two values as confirmed in Table 4.5

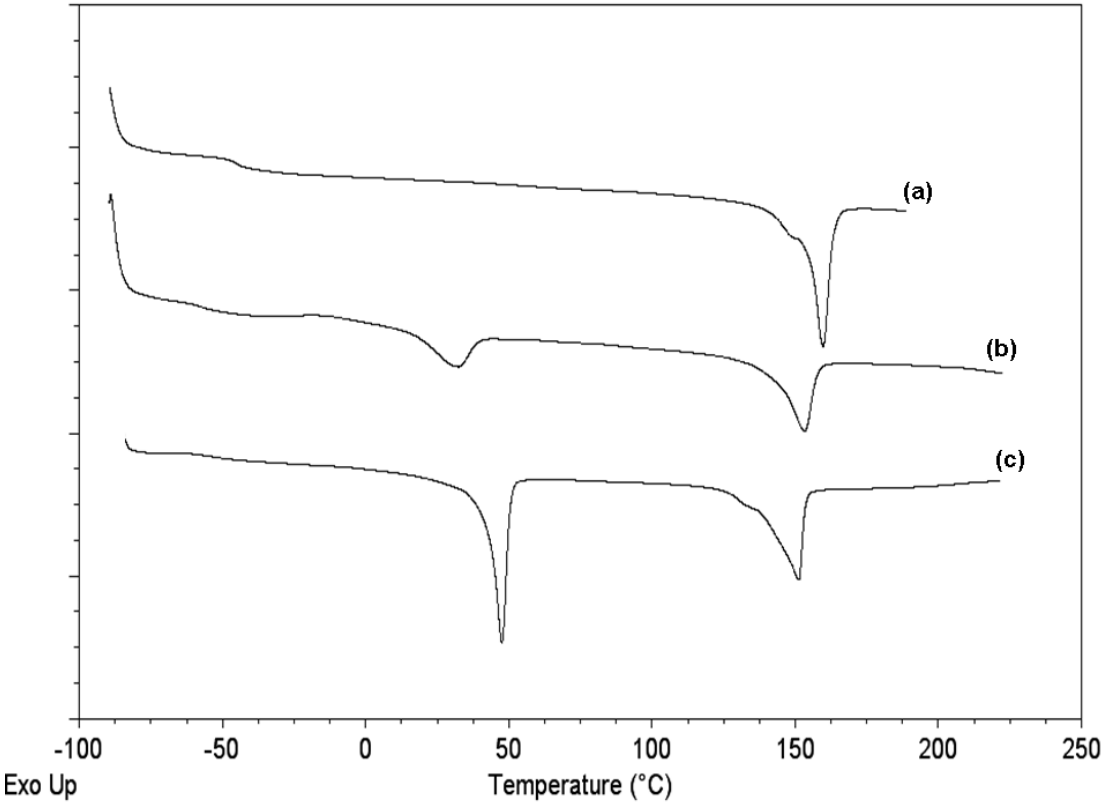

Figure 4.3 Typical DSC thermograms of triblock copolymers with middle block of: (a) CL:TMC 50:50 (**A7**), (b) CL:TMC 75-25 (**B4**), and (c) CL:TMC 90-10 (**C1**).

For mechanical properties, Table 4.5 shows that the molar ratio and molar mass of the triblock copolymers influence the measured properties significantly. For polymer **A1** with targeted molar ratio CL:LLA of 1:0.38, the resulting polymer film was too weak to be measured by Instron, despite having a medium molar mass in the group. At the

other extreme, polymer **A9** with CL:LLA 1:3 is a brittle polymer. Meanwhile, for polymer **A2-A8**, it was observed that the tensile strength and the maximum elongation clearly depended on their molar mass. From Table 4.5 it can be seen that the polymer **A8** exhibits good mechanical properties with elongation up to 520% as shown in Figure 4.4(c). Notice the absence of a measurable yield stress in the stress-strain curve. In this group, this polymer exhibits the highest elongation to break. Its elastomeric nature will be discussed further in a later section.

4.2.2.2 PLLA-b-poly(CL-co-TMC)-b-PLLA with CL:TMC 75:25

Table 4.6 Thermal and mechanical properties of various PLLA-*b*-poly(CL-*co*-TMC)-*b*-PLLA with CL:TMC 75:25 (Group B).

Polymer	T_g (°C)	T_m (°C)	ΔH (J/g)	Modulus (MPa)	Tensile Strength (MPa)	Max Strain, ε_b (%)
B1	-50	37 143	21.2 5.5	20.0 ± 2.8	4.4 ± 0.2	571 ± 36
B2	-52	39 147	21.6 12.4	19.6 ± 4.5	6.4 ± 0.5	725 ± 42
B3	-55	33 143	0.9 14.4	23.8 ± 1.6	7.9 ± 1.0	812 ± 23
B4	-57	37 150	9.4 18.7	32.0 ± 4	12.3 ± 0.5	1084 ±123

The random copolymer of PCL and PTMC with a molar ratio of 75:25 is a semi crystalline polymer with T_g around -58°C and T_m around 40°C. Therefore the triblock copolymer has two T_m, one from the poly(CL-*co*-TMC) block and other from the PLLA block, Figure 4.3(b). Again, Table 4.6 shows that the middle block affected the T_m of PLLA by lowering it from 169°C (T_m of pure PLLA) to around 140-150°C. Meanwhile, the T_g from the middle block is significantly lower compared to the

triblocks in group A (with middle block of CL:TMC 50:50). This was expected as PCL has a lower T_g compared to TMC and the CL content is higher in group B.

The DSC results showed an interesting effect of the end-block on the crystallinity of the mid-block. Increasing the CL:LLA ratio from 1:0.5 (**B1** and **B2**) to 1:1 (**B3** and **B4**) increases the crystallinity of hard-block as expected, but it also decreases the crystallinity of the soft-block quite significantly until the extent that polymer **B3** middle-block is almost amorphous. We attribute this to the fact that the increasing end-block crystallinity acts as a hindrance for packing of the mid-segment chains.

Considering the mechanical properties, a significant improvement in elongation-to-break (ε_b) can be seen by increasing the molar ratio of CL:TMC 50:50 to 75:25 for all polymers (compare Table 4.5 and Table 4.6). All the triblock copolymers with soft-block of CL:TMC 75:25 managed to reach elongation beyond 500%. If we consider only ε_b values only for assessing elastomeric character, it would appear that these polymers with CL:TMC ratio of 75:25 are superior to the 50:50 midblock polymers, at comparable overall molar mass. This is in spite of having measurable crystallinity of the mid-block for the 75:25 polymer: our data showed that polymer **B1** had a soft segment ΔH of 21.2 J/g, which translated into percentage crystallinity of as much as 15%, calculated using the heat of fusion (ΔH^0_f) of the totally crystalline PCL (139.5 J/g) [88]. Nevertheless, the triblock copolymer still exhibits 570% elongation. The highest elongation of the triblock copolymers with soft segment CL:TMC 75:25 was from polymer **B4**, with an elongation of 1084%. However, the presence of a pronounced yield stress in the stress strain curve, Figure 4.4(b), implies that the high elongations may not be fully recoverable, as there is also a possible contribution from

plastic deformation (which is non-recoverable) to this observed elongation. This non-recoverability is quantified using recovery from two different stresses, as discussed in the next section. Here we simply note that high elongations alone do not imply elastomeric behavior.

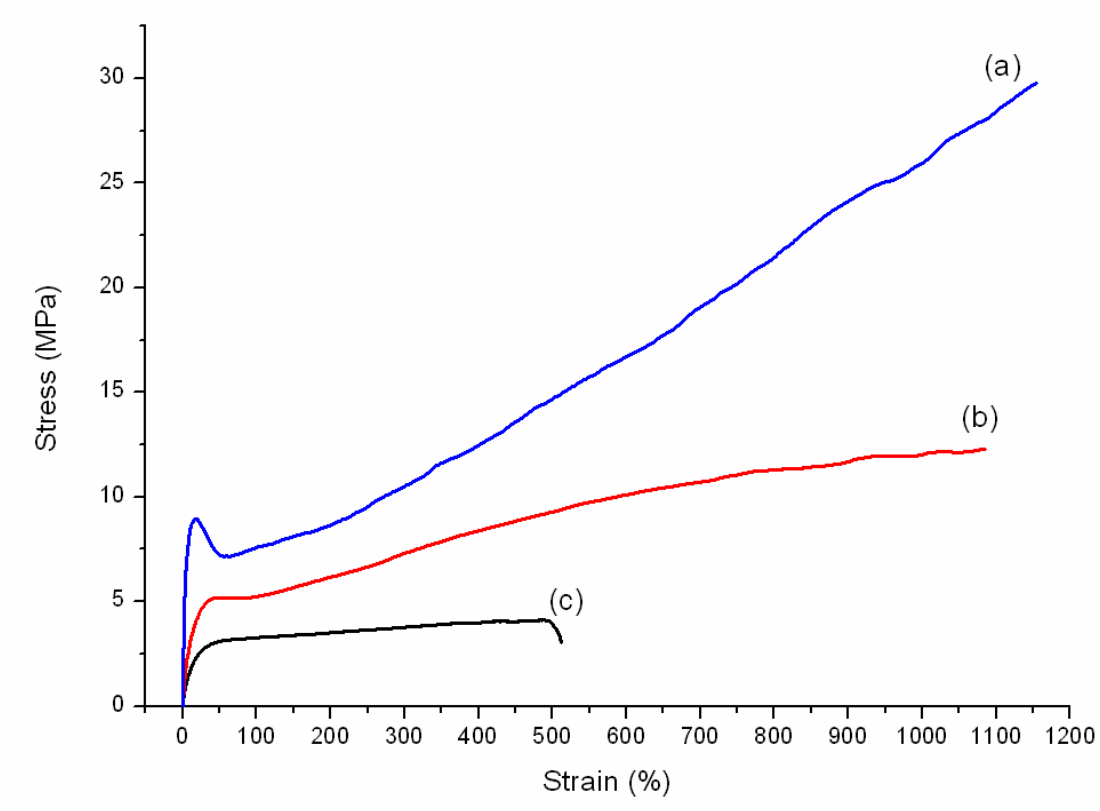

Figure 4.4 Stress strain measurements of the triblock copolymers: (a) CL:TMC 90:10 (**C2**), (b) CL:TMC 75:25 (**B4**), (c) CL:TMC 50:50 (**A8**).

4.2.2.3 PLLA-b-poly(CL-co-TMC)-b-PLLA with CL:TMC 90-10

Table 4.7 Thermal and mechanical properties of various PLLA-*b*-poly(CL-*co*-TMC)-*b*-PLLA with CL:TMC 90:10 (Group C).

Polymer	T_g (°C)	T_m (°C)	ΔH (J/g)	Modulus (MPa)	Tensile Strength (MPa)	Max Strain, ε_b (%)
C1	-56	48 151	25.2 19.9	72.3 ± 4.6	9.4 ± 2.0	67 ± 30
C2	-61	50 159	16.7 18.2	56.8 ± 18.0	29.5 ± 2.5	>1200

DSC results in Table 4.7 showed that for triblock copolymer with middle-block of CL:TMC 90:10, the T_m and crystallinity of the soft-block are higher than those with middle-block of CL:TMC 75:25 (compare Table 4.7 and Table 4.6). This confirms the role of TMC in the middle-block as a disruptor for PCL crystallinity.

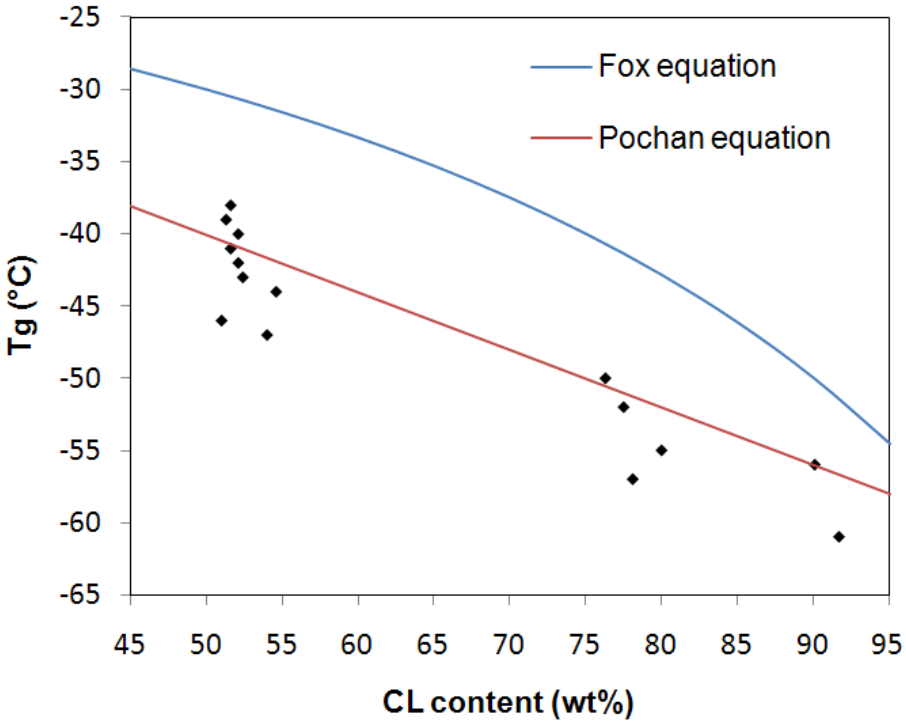

Figure 4.5 T_gs of all the triblocks as a function of CL content, plotted against Fox and Pochan equations

Gathering all the T_gs from Table 4.5, 4.6, and 4.7, one can plot the CL:TMC compositions versus the T_gs and compare them to the Fox equation [136] to estimate the T_gs of a copolymer based on the T_gs of the respective homopolymers:

$$\frac{1}{T_g} = \frac{w_1}{T_{g1}} + \frac{w_2}{T_{g2}}$$

Here w_1 and w_2 refer to the weight fraction of the two comonomers and T_{g1} and T_{g2} refer to the glass transition temperatures of the two corresponding homopolymers. Looking at Figure 4.5 apparently Fox equation does not fit the experimental data, as the experimental T_gs are significantly lower. Another equation that is commonly used is the Pochan equation [137]:

$$T_g = w_1 T_{g1} + w_2 T_{g2}$$

It can be seen that Pochan equation fits the experimental data better; indicating that single amorphous phase exist in soft segment of the triblock copolymer and the heat capacity increments for PCL and PTMC are similar.

For the mechanical properties, polymer **C2** exhibits very high elongations, very high modulus and tensile strength (Table 4.7). However, the presence of a yield point (a point where a decrease in stress is observed with increasing strain) at around 25% elongation in Figure 4.4(a), again implies plastic, non-recoverable deformation contributing substantially to the overall elongation. Clearly, crystallinity of the mid-block influences the observed mechanical properties, particularly with respect to the extent of plastic deformation in the polymer.

4.2.3 Elastomeric Properties

To get a better assessment of elastomeric behavior, we used creep and recovery measurements. Ideal elastomers are able to recover almost completely regardless of the level of stress applied during the creep test. We subjected each triblock polymer to low and high stresses (corresponding to 30% and 80% of their maximum tensile stress up to 200% elongation respectively) for creep and recovery measurements. In this test, we have estimated recovery using:

$$Recovery = \frac{L_M - L_R}{L_M - L_0} \times 100\%$$

where, L_M is maximum sample length at elongation, mm; L_R - sample length after recovery, mm; L_0 - initial length of sample, mm.

The reason for the choice of these two stresses is as follows: if the polymer is truly elastomeric, recovery values should be independent of the creep stress imposed [138]. If the higher stress is close to the yield stress, then we are likely to see less recovery for those polymers which may exhibit high ε_b, but with yielding (or plastic deformation) behavior contributing to this high ε_b.

Table 4.8 Creep and recovery of various PLLA-*b*-poly(CL-*co*-TMC)-*b*-PLLA copolymers.

CL:TMC	Polymer	Recovery at 30% of maximum tensile stress (%)	Recovery at 80% of maximum tensile stress (%)
50:50	**A4**	78 ± 1	83 ± 1
	A8	78 ± 2	78 ± 1

	B1	73 ± 5	62 ± 2
75:25	**B3**	75 ± 3	46 ± 1
	B4	72 ± 4	41 ± 2
90:10	**C2**	70 ± 4	54 ± 2
	SBS	87 ± 2	82 ± 4

Table 4.8 shows the creep and recovery results obtained from triblock copolymers of varying CL:TMC compositions and targeted molar mass. From the results obtained from the triblock copolymers under low stress, we can see that all the copolymers, regardless of mid-block composition, are able to recover more than 70% of their maximum strain induced during creep. When the test is performed under high stress, however, only the copolymers with mid-segment of CL:TMC 50:50 are able to obtain recovery values similar to the recovery at the low stress level, whereas the other copolymers showed significant decreases in recovery.

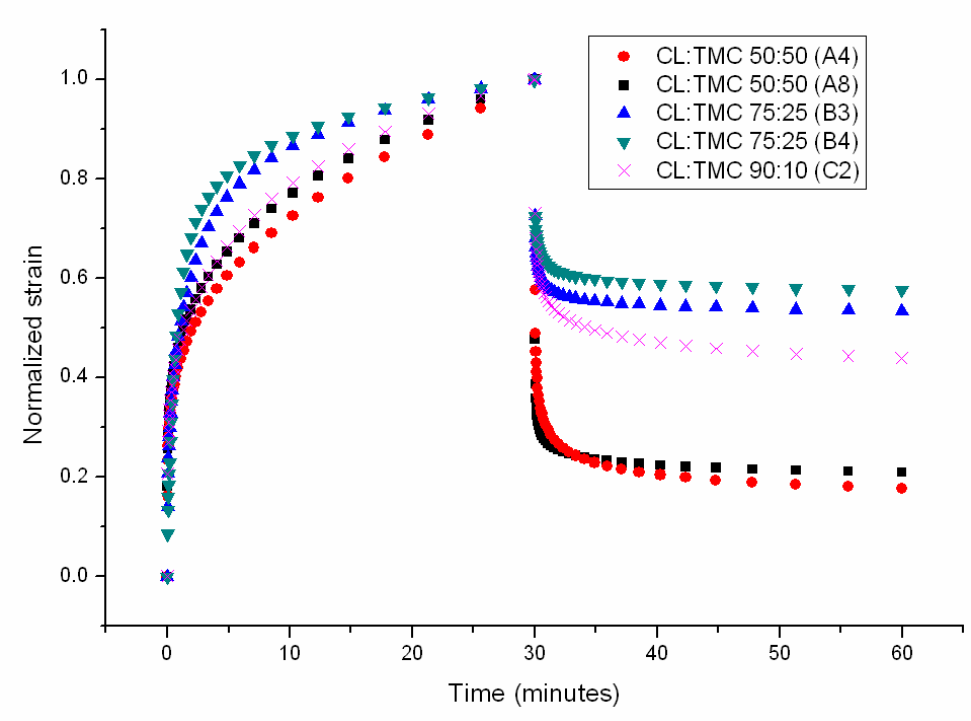

Figure 4.6 Typical creep and recovery curves of various triblock copolymers at 80% of maximum tensile stress.

Figure 4.6 shows the creep and recovery curves obtained from some of the triblock copolymers. Clearly at the higher stress, there is plastic deformation contributing to the creep, which is not recoverable at the temperature of the experiment. We note here that elastomeric behavior is confirmed when recovery levels are reasonably high, and are more or less independent of the imposed stress levels. When recovery decreases with imposed stress, it is a confirmation of the onset of plastic deformation in the sample, which is not recoverable. Creep and recovery of poly(styrene-b-butadiene-b-styrene) (SBS), a well known (non-biodegradable) thermoplastic elastomer, was also performed, and is shown in Table 4.8 for comparison. Thus, although our polymers do not exactly match the SBS polymer for recovery, polymers **A4** and **A8** come very close, and may be considered to be elastomeric. In fact, for recovery at higher stress level, polymer **A4** is shown to have a better recovery compared to SBS.

The difference in recovery behavior among the various polymers is due to the contribution of plastic deformation to the elongation or to creep. Triblocks with CL:TMC ratios greater than 1:1 exhibit higher amounts of plastic deformation, which are non-recoverable, when the imposed creep stress approaches the yield stress. Structurally, we propose that this plastic deformation is due to the presence of crystallinity in the mid-block. From our DSC results, we confirmed that there is crystallinity of PCL in the middle block for CL:TMC 75:25 and CL:TMC 90:10 triblock copolymers. Under creep, it is possible that the PCL crystallites undergo slippage (yielding). This result in permanent (plastic) deformation and upon recovery, only the amorphous region in the middle block is able to recover. On the contrary, CL:TMC 50:50 being completely amorphous in its middle block is able to deform during creep and recover upon removal of stress.

Instead of measuring recovery as a function of applied stress, we can also use the Instron to evaluate recovery after different strain (or elongation) levels. Upon cycling from low to high elongation, the loss of recovery can be quantified by the hysteresis level. Such cyclic loading test results are in agreement with the creep results. According to the DMA results, CL:TMC 50:50 polymers can recover better, especially at higher tensile stress, compared to CL:TMC 75:25 polymers. Figure 4.7 (Instron results) shows that for 100% elongation, CL:TMC 50:50 (**A4**) could recover to 82% while CL:TMC 75:25 (**B3**) recovered only 77%. For elongation to 200%, CL:TMC 50:50 (**A4**) managed to retain 82% recovery while CL:TMC 75:25 (**B3**) recovery dropped to 63%. At 300% elongation, CL:TMC 50:50 (**A4**) dropped by negligible amount to 81% while the CL:TMC 75:25 (**B3**) recovery dropped further to 60%. One point to take note here is that all these recovery percentage values were considered as instantaneous values (no recovery period was applied after the deformation of the polymer). The CL:TMC 50:50 (**A4**) triblock achieved a similar recovery value compared to some other TMC triblocks [117, 139] with applied recovery period up to 16 hours. Furthermore their recovery tests were done based on only 50% elongation which may not be sufficient to define the characteristic of an elastomer. Therefore, we believe that the elastomeric properties of our triblock are superior in terms of instantaneous recovery and recovery at high elongation.

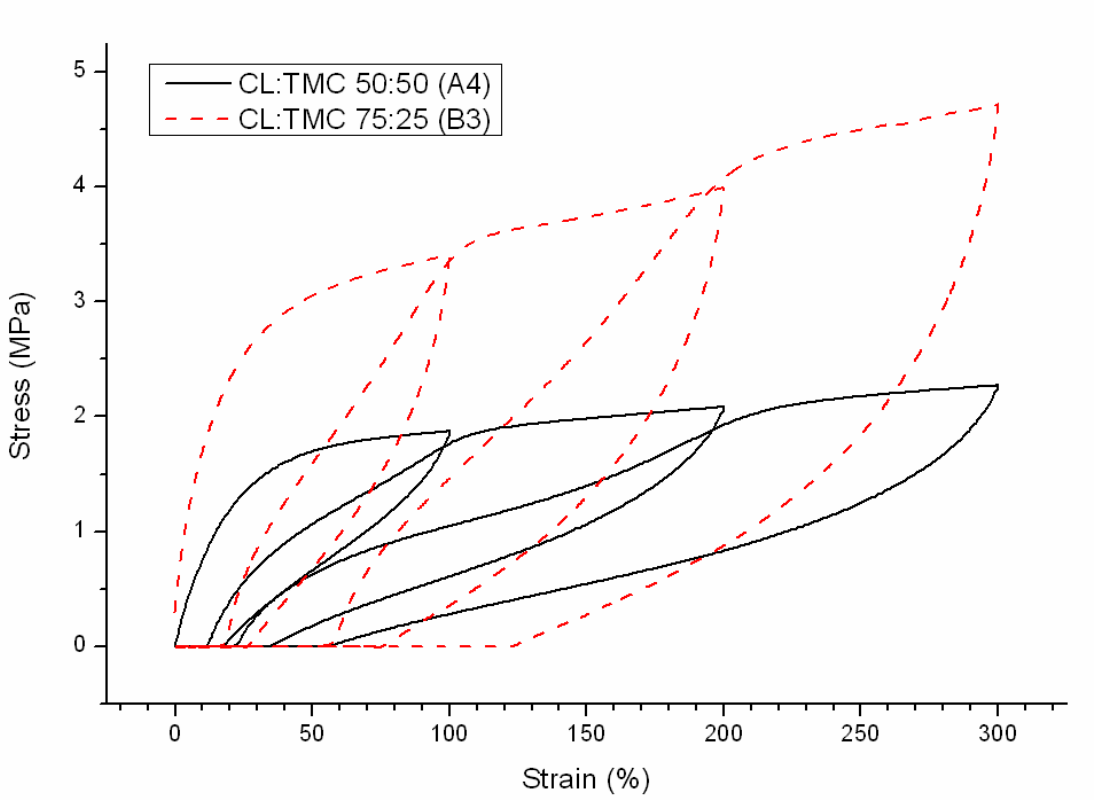

Figure 4.7 Cyclic loading test for two triblock copolymers: CL:TMC 50:50 (**A4**) and CL:TMC 75:25 (**B3**).

4.2.4 Biodegradation Properties

In vitro biodegradability test were conducted for four copolymers of varying soft segment CL:TMC and hard segment LLA composition: polymer **A8**, polymer **B2**, polymer **B4** and polymer **C2**. Figure 4.8 reports data up to sixteen weeks showing the change in molar mass with degradation time. During first 4 weeks the degradation rate is very fast for all the copolymers and then the rates slow down. The degradation rate of **C2** is highest, which has the highest starting molar mass (M_n=101k g·mol^{-1} PDI=1.29), while the remaining copolymers (**A8**, **B2** and **B4**) have lower values at the beginning (M_n=30-56k g·mol^{-1}). This apparent faster rate of initial degradation is due to the larger number of hydrolysable segments in the starting polymer. The

observations suggest that hydrolysis is occurring in the middle block as well as in the end-blocks, since (except for polymer **C2**) all the polymers have roughly the same molar mass of the mid-block.

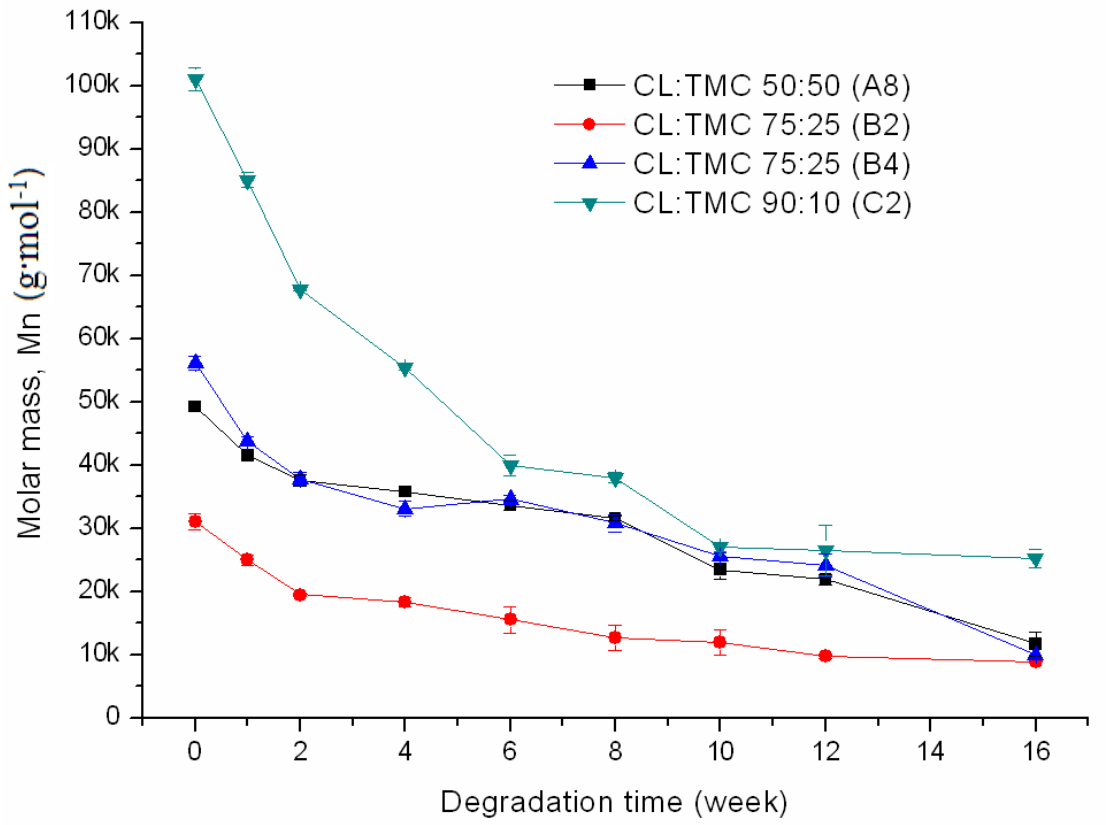

Figure 4.8 Molar mass change in degradation studies of four different triblock copolymers in PBS buffer 1M (pH=7.4) at 37°C.

The mass loss change for all the copolymers are compared in Figure 4.8 (data up to sixteen weeks only are reported). It shows a steady increase in mass loss occurring early for all polymers except polymer **B2**. In general, this behavior is along expected lines, with mass loss being inversely proportional to starting molar mass. We have shown in earlier studies [140] that mass loss occurs when the molar mass reaches a value between 20,000 and 10,000. This happens quicker for polymers with lower starting molar mass, as confirmed in this study.

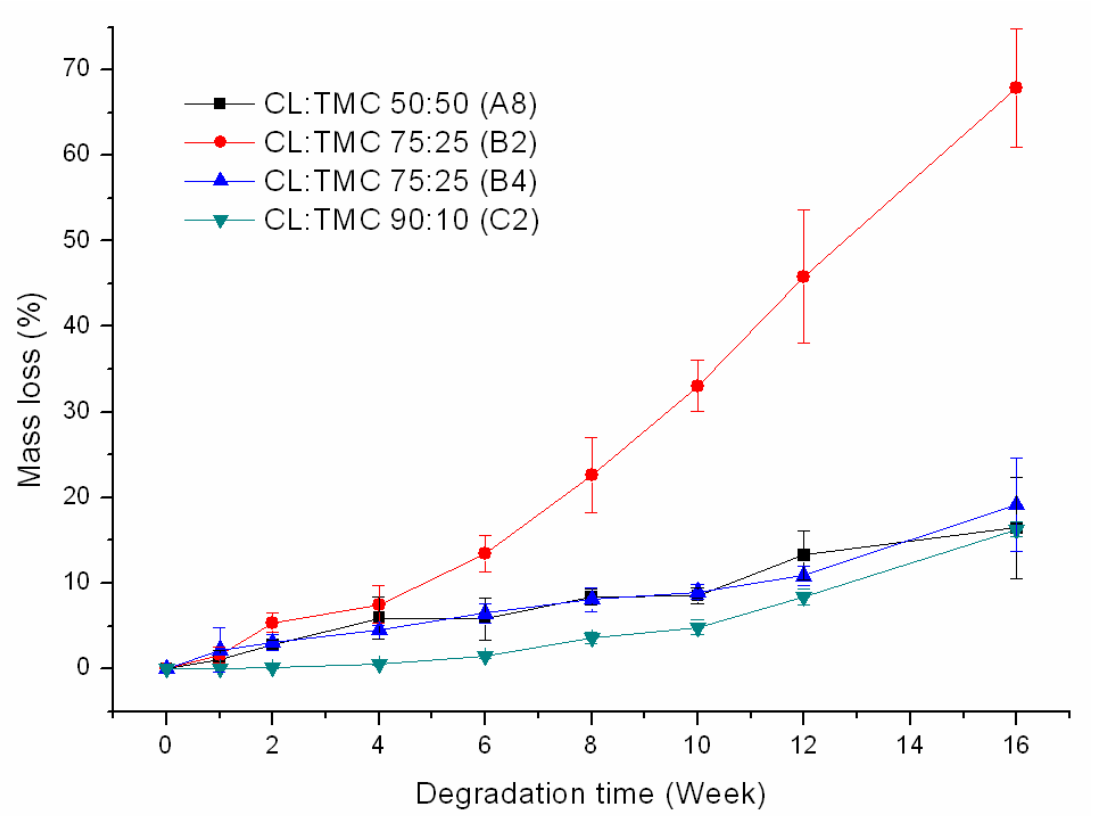

Figure 4.9 Mass loss change in degradation studies of four different triblock copolymers in PBS buffer 1M (pH=7.4) at 37°C.

To determine where the hydrolysis is predominant (i.e. middle segment or end block), we carried out ^{1}H NMR analysis on some selected degraded polymer samples, in $CDCl_3$ solution. The composition of the copolymers was determined by normalizing the protons of the methylene group alpha to the ester moieties of the PCL at 4.05 ppm (triplet) and the proton of the lactoyl methane peak (quartet) centered at 5.15 ppm. The increase in ratio of LLA to CL peaks (Table 4.9) along with degradation time indicates poly(CL-*co*-TMC) segments are degrading away at a faster rate than that of PLLA segments for all the copolymers. Molar mass change or mass change observed for this set of copolymers thus may be attributed to random chain scission of the soft middle segment of poly(CL-*co*-TMC).

Table 4.9 ^{1}H NMR analysis of the degraded samples

CL:TMC 50:50 (**A8**)				
Week	M_n (g·mol^{-1})	Molar ratio CL	TMC	LLA
0	49200	1	0.830	1.350
8	31600	1	0.833	1.350
16	11700	1	0.812	1.516

CL:TMC 75:25 (**B2**)				
Week	M_n (g·mol^{-1})	Molar ratio CL	TMC	LLA
0	31100	1	0.291	0.378
8	12700	1	0.306	0.403
16	8800	1	0.291	0.515

CL:TMC 75:25 (**B4**)				
Week	M_n (g·mol^{-1})	Molar ratio CL	TMC	LLA
0	56100	1	0.283	0.846
2	30800	1	0.288	0.866
10	10000	1	0.309	0.933

CL:TMC 90:10 (**C2**)				
Week	M_n (g·mol^{-1})	Molar ratio CL	TMC	LLA
0	101000	1	0.091	0.737
2	38000	1	0.081	0.745
10	25200	1	0.091	0.783

4.3 Summary

In this Chapter, various triblock copolymers made of CL, TMC and LLA were synthesized by the ring-opening copolymerization, using stannous octoate as catalyst and propanediol as initiator. We have characterized these triblocks and shown that they exhibit thermoplastic elastomeric behavior when the middle segment is completely amorphous, and the overall polymer molar mass is reasonably high. Our study showed that the molar ratio of CL:TMC is the single most crucial parameter in determining the mechanical properties of the copolymers, along with the molar mass of the PLLA end blocks. At 50:50 CL:TMC ratio, the middle segment is amorphous, and this ratio gives a thermoplastic elastomer with good recovery values and elongations-to-break. As the CL:TMC ratio increases, the middle segment becomes more crystalline, increasing modulus and elongations-to-break, but decreasing recovery (or elastomeric character).

Chapter 5 Effects of Having a Random Copolymer as Hard-Block

In *Chapter 4*, we synthesized triblock copolymers that have elastomeric properties. Triblock copolymers with soft block of CL:TMC 75:25 managed to reach a very high elongation, with some degree of recovery, while triblock copolymers with CL:TMC 50:50 had a better recovery property, with less elongation to break. One way to improve the elongation or recovery of the triblock is by changing the structure of the hard block. Lipik et al. [141] have reported elastomers based on diblock copolymers that incorporate a random copolymer of PLLA and PCL as their hard block over a certain range of compositions where the segment length of PLA and PCL are defined to be within limits. In this chapter, we will also investigate the effect of adding PCL into the PLLA hard-block of the triblock copolymer. So basically, what we have here is an A-B-A triblock copolymer, with B block consisting of a random copolymer of PCL and PTMC, while and an A block consisting of a random copolymer of PLLA and PCL.

Total of eight triblock copolymers have been synthesized, which were categorized under two different groups. Similar to *Chapter 4*, the grouping is based on CL:TMC ratio in the soft-block which were 50:50 and 75:25 (Table 5.1 and 5.2). Within each group, the ratio of CL to TMC in the soft-block was kept constant and the molar ratio between LLA and CL in the hard block was varied within that group to study their effects on elastomeric character.

Thus, in each table, the second column designates the molar percentage of CL in the hard-block (with relative to LLA). The third column designates the target overall molar ratio of all monomers inside the triblock, hence the reduced TMC content relative to CL although the CL:TMC ratio in the soft-block was kept constant.

5.1 Molar Mass and Structural Properties

5.1.1 Poly(LLA-*co*-CL)-*b*-poly(CL-*co*-TMC)-*b*-poly(LLA-*co*-CL) with CL:TMC 50:50

Table 5.1 Molar mass and molar ratio of various poly(LLA-*co*-CL)-*b*-poly(CL-*co*-TMC)-*b*-poly(LLA-*co*-CL) with CL:TMC 50:50 (Group D).

Polymer	Molar % of CL in hard-block	feed ratio CL:TMC:LLA	molar ratio[a] CL:TMC:LLA	M_n[b] ($g \cdot mol^{-1}$)	PDI[b]
D1	0	1 : 1 : 1.50	1 : 0.83 : 1.35	49200	1.22
D2	10	1 : 0.87 : 1.17	1 : 0.77 : 1.07	44500	1.34
D3	20	1 : 0.77 : 0.92	1 : 0.72 : 0.83	40100	1.49
D4	30	1 : 0.69 : 0.72	1 : 0.67 : 0.72	31400	1.44

[a] Determined by ^{1}H NMR analysis

[b] Obtained by SEC analysis

Table 5.1 shows various A-B-A triblock copolymers with the B block made of a random copolymer of CL and TMC at a molar ratio of 50:50, and the A block made of random copolymer of LLA and CL. Four triblocks with different CL molar percentage content in the hard-block ranging from 0% until 30% were successfully

synthesized. The number-average molar mass (M_n) obtained from the SEC analysis varied from 31400 to 49200 g·mol^{-1}.

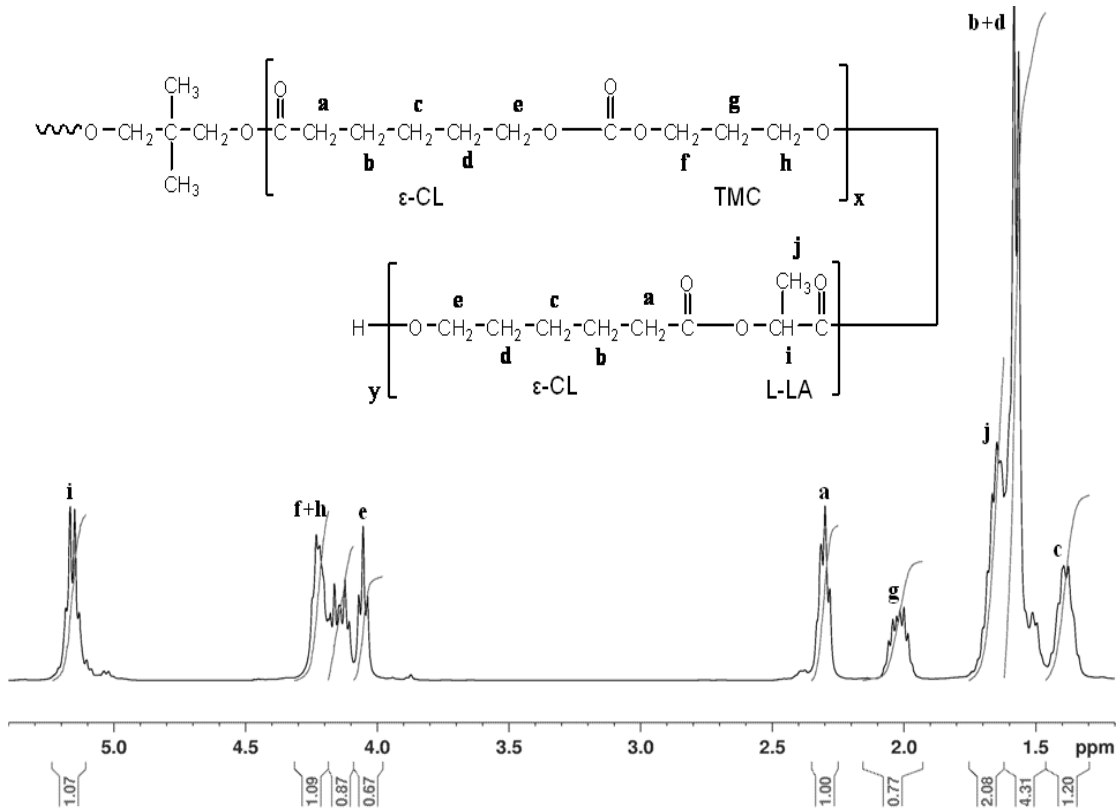

Figure 5.1 Structure of the triblock copolymer and its ^{1}H NMR spectrum for CL:TMC 50:50 (**D2**) in $CDCl_3$.

The typical ^{1}H NMR spectrum of the triblock copolymer is shown in Figure 5.1. The spectrum of triblock **D2** is very similar to the spectrum of triblock **D1** which has been characterized on previous chapter. The methylene protons from PCL: (**a**), (**b+d**), (**c**) and (**e**) are shown at 2.31, 1.66, 1.39, and 4.05 ppm respectively. Also, methylene protons from PTMC (**f+h**), and (**g**) are shown at 4.23 and 2.04 ppm, respectively. The methane (**i**) and methyl protons (**j**) from the PLLA are shown at 5.16 and 1.64 ppm respectively. The peak splitting in the region between (**f+h**) and (**e**) peaks suggested randomization of PCL and PTMC inside the soft block. Monomer composition of the

copolymer was determined from the integration ratio between proton signals (**a**), (**g**), and (**i**) (as the results are included in Table 5.1). It can be seen that the synthesized triblocks are having molar ratio close to their feed ratio. An interesting observation here suggested that the addition of CL to the PLLA hard-block helped the LLA to reach its targeted ratio. Triblock **D1** with 0% CL in the hard-block is having LLA molar ratio slightly less than targeted (feed ratio), while **D4** with 30% CL in the hard-block having LLA molar ratio exactly the same as targeted. This might be attributed to the fact that CL has a faster polymerization rate compared to LLA [142].

5.1.2 Poly(LLA-*co*-CL)-*b*-poly(CL-*co*-TMC)-*b*-poly(LLA-*co*-CL) with CL:TMC 75:25

Table 5.2 Molar mass and molar ratio of various poly(LLA-*co*-CL)-*b*-poly(CL-*co*-TMC)-*b*-poly(LLA-*co*-CL) with CL:TMC 75:25 (Group E).

Polymer	Molar % of CL in hard-block	feed ratio CL:TMC:LLA	molar ratio[a] CL:TMC:LLA	M_n[b] ($g \cdot mol^{-1}$)	PDI[b]
E1	0	1 : 0.33 : 1	1 : 0.28 : 0.85	56100	1.40
E2	10	1 : 0.30 : 0.81	1 : 0.26 : 0.70	50500	1.51
E3	30	1 : 0.26 : 0.54	1 : 0.23 : 0.48	40300	1.70
E4	50	1 : 0.22 : 0.33	1 : 0.18 : 0.33	40300	1.41

[a] Determined by ^{1}H NMR analysis

[b] Obtained by SEC analysis

Table 5.2 shows four triblock copolymers with a middle block of random copolymer with CL:TMC molar ratio of 75:25. Four different molar ratio of CL to LLA in the hard block were targeted, and their molar mass ranged from 40300 to 56100. Similar to group D, ^{1}H NMR data also showed good agreement for molar ratio composition,

with triblock **E1** having a slightly less than targeted LLA molar ratio and triblock **E4** having the same LLA molar ratio as targeted.

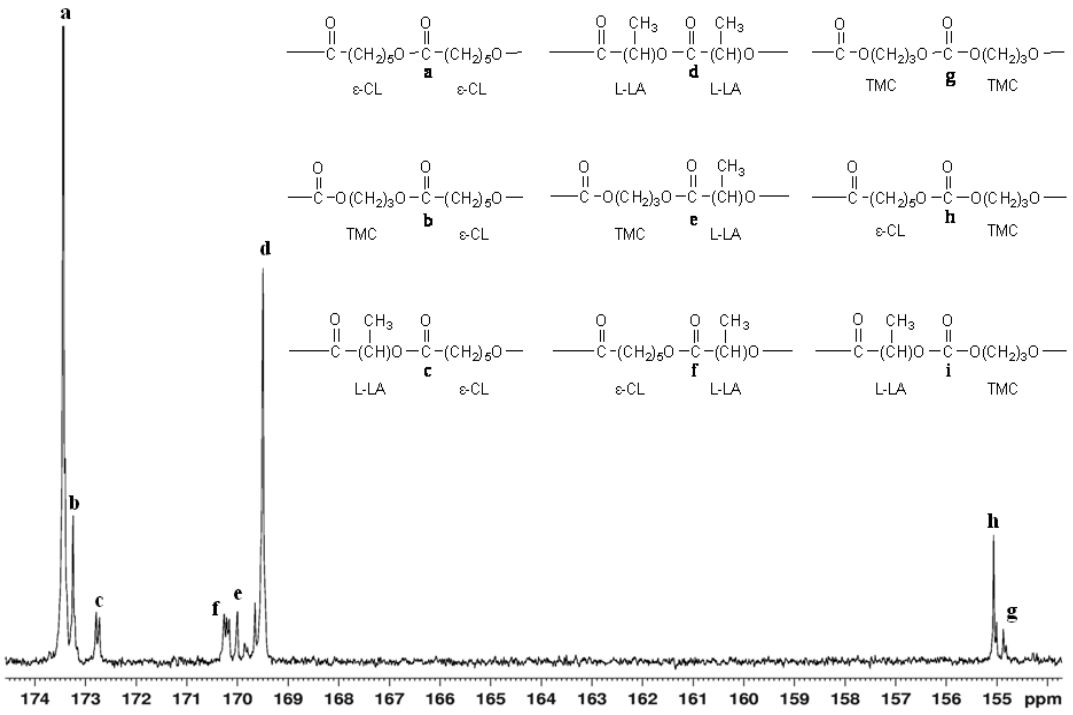

Figure 5.2 ^{13}C NMR spectrum from region of carbonyl carbon atoms of CL:TMC 75:25 (**E4**) in $CDCl_3$ and their peaks assignment.

Overall, ^{13}C NMR spectra show that the chemical shift of the triblock copolymers with additional CL in the hard-block were in a good agreement with the spectrum from a terpolymer of CL, TMC, and PLLA reported by Jia et al [134] and were very similar to the triblock copolymer without CL in the hard-block from the *Chapter 4* (Figure 4.2 page 52). It can be observed from Figure 5.2 the CO signal from CL carbonyl atom in the soft-block showed a dyad splitting into peak (**a**) (CL-CL dyad) and peak (**b**) (CL-TMC dyad), which suggest that the soft-block made of CL:TMC of 75:25 (group E) is a random copolymer. A noticeable difference compared to triblock **B3** (Figure 4.2, *Chapter 4*) without CL in the hard-block is the splitting of (CL-LLA)

dyad peak (**c**) as well as (LLA-CL) dyad peak (**f**) which suggests a more complex interaction between CL and LLA due to the addition of CL inside the PLLA hard-block. From the L-lactide carbonyl signals, it can be observed that there was indeed a certain amount of transesterification on the L-lactide block during the polymerization, as shown by a cluster of small peaks (**e**) and (**f**) located to the left of (LLA-LLA) dyad peak (**d**). Nevertheless, the low intensity of peaks (**e**) and (**f**) compared to peak **(d)** has shown that our copolymer is a triblock instead of a multiblock or random copolymer.

5.2 Thermal and Mechanical Properties

5.2.1 Poly(LLA-*co*-CL)-*b*-poly(CL-*co*-TMC)-*b*-poly(LLA-*co*-CL) with CL:TMC 50:50

Table 5.3 Thermal and mechanical properties of various poly(LLA-*co*-CL)-*b*-poly(CL-*co*-TMC)-*b*-poly(LLA-*co*-CL) with CL:TMC 50:50 (Group D).

Polymer	Molar % of CL in hard-block	T_g (°C)	T_m (°C)	ΔH (J/g)	Modulus (MPa)	Tensile Strength (MPa)	Max Strain, ε_b (%)
D1	0	-49	149	19.1	12.5 ± 0.8	4.5 ± 0.6	520 ± 81
D2	10	-48	139	11.0	10.0 ± 0.3	4.7 ± 0.1	914 ± 29
D3	20	-45	138	11.8	9.1 ± 0.3	2.5 ± 0.1	300 ± 20
D4	30	-39	112	1.3	too weak	too weak	too weak

Clearly, at a ratio of 50:50 CL:TMC, all the synthesized soft-blocks were amorphous, as no melting of the PCL could be measured, Figure 5.3(a) and 5.3(b). The hard-block was crystalline in all cases: Table 5.3 shows that the T_m of the hard-block in the copolymers ranged between 112°C to 149°C. Since it is reported that the

homopolymer of PLLA has a T_m of ~169°C [135], it can be concluded that the middle block has the effect of lowering the T_m of PLLA in the triblock, as discussed in *Chapter 4*. Furthermore, the addition of CL in the PLLA block clearly has the effect of lowering the T_m as well as the crystallinity of the hard-block. The observed T_g seen in the DSC for the triblock is the T_g of random copolymer of CL and TMC. Considering that the T_g of homopolymers of PCL and PTMC are -60°C and -20°C respectively [30, 88], it expected that the T_g of the random copolymer would lie between these two values as confirmed in Table 5.3. An interesting observation here was the effect of having CL in the hard-block to the T_g of the soft-block. Instead of lowering the T_g as when the CL content of the mid-block is increased (compare the T_gs of triblock CL:TMC 50:50 with CL:TMC 75:25, and with CL:TMC 90:10 in *Chapter 4*), it seems that adding CL to the hard-block will increase the T_g of the soft-block. This might be due to the possibility that when CL is presence in the hard-block, the CL in the hard block is "attached" to the CL in the mid-block, thereby restraining the motion of the mid-block, and effectively increasing T_g.

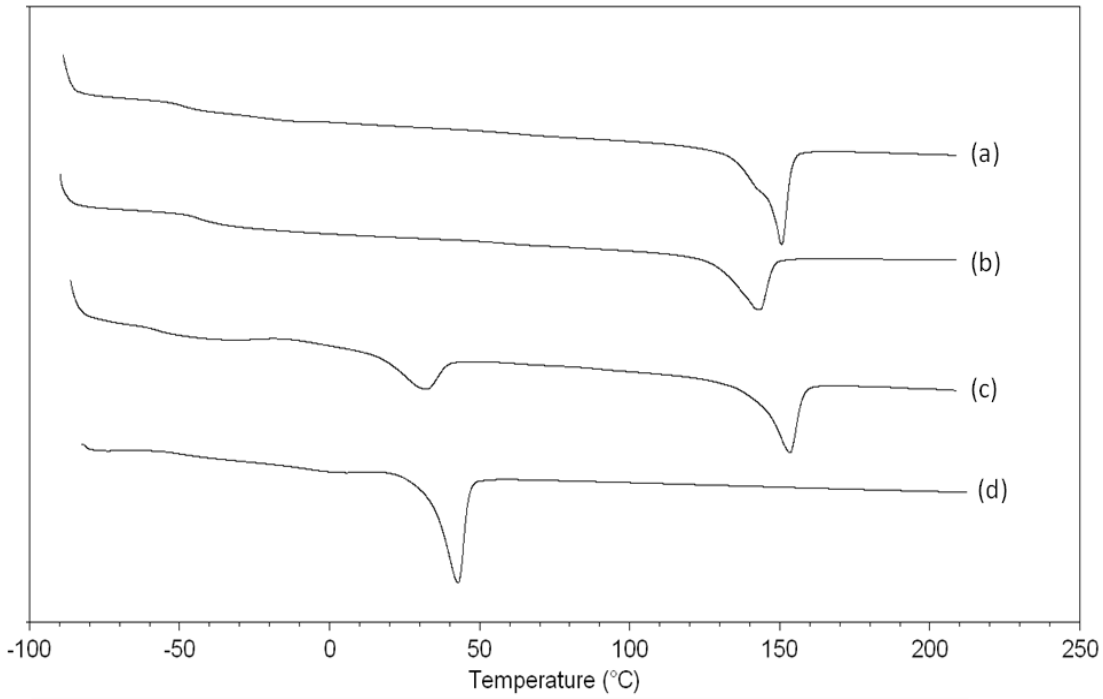

Figure 5.3 DSC thermograms of triblock copolymers with middle block of: (a) CL:TMC 50:50 (**D1**), (b) CL:TMC 50:50 (**D2**), (c) CL:TMC 75:25 (**E1**), and (d) CL:TMC 75:25 (**E4**).

For mechanical properties, Table 5.3 shows that the amount of CL in the PLLA hard-block influences the measured properties. Triblock **D1** is an elastic polymer which already exhibits good mechanical properties with elongation up to 520%, but by adding 10% CL inside the hard-block (triblock **D2**), it increases the elongation up to 914% without much change on the modulus and tensile strength, as can be seen from Figure 5.4(a) and 4(b). When we compare **D2** to the triblock **A2** from *Chapter 4*, the higher elongation observed for **D2** is particularly significant, as the molar mass of **D2** is in fact lower than that of **D1**. Adding more than 10% CL into the hard-block resulted in decrease of all mechanical properties including the elongation as can be seen from triblock **D3**. Finally triblock **D4** with 30% CL in poly(LLA-*co*-CL) was too

soft and weak to be measured mechanically, most probably due to the very low crystallinity of the hard-block.

5.2.2 Poly(LLA-*co*-CL)-*b*-poly(CL-*co*-TMC)-*b*-poly(LLA-*co*-CL) with CL:TMC 75:25

Table 5.4 Thermal and mechanical properties of various poly(LLA-*co*-CL)-*b*-poly(CL-*co*-TMC)-*b*-poly(LLA-*co*-CL) with CL:TMC 75:25 (Group E).

Polymer	Molar % of CL in hard-block	T_g (°C)	T_m (°C)	ΔH (J/g)	Modulus (MPa)	Tensile Strength (MPa)	Max Strain, ε_b (%)
E1	0	-57	31 153	8.1 12.8	32 ± 4	12.3 ± 0.5	1084 ± 123
E2	10	-55	32 146	13.1 12.4	18.0 ± 0	8.0 ± 0.4	934 ± 108
E3	30	-51	36 125	25.3 4.4	11.8 ± 2.4	>5.1	>1200
E4	50	-49	43	20.8	15.1 ± 1.1	>3.9	>1200

Preliminary study showed that random copolymer of PCL and PTMC with molar ratio 75:25 is a semi crystalline polymer with T_g around -58°C and T_m around 40°C. Therefore the triblock copolymer **E1** has 2 T_m, one from the poly(CL-*co*-TMC) soft-block and other from the PLLA block, Figure 5.3(c). By adding PCL inside the PLLA block, it can be observed from triblock **E2**, **E3**, and **E4** that the T_m and crystallinity of the soft-block increased while the T_m and crystallinity of the hard-block decreased (Table 5.4). When the CL content in the PLLA-block reached 50%, the poly(LLA-*co*-CL) block became an amorphous hardblock, as can be seen in Figure 5.3(d). Meanwhile, same as group D, the T_g from the soft-block increased as the amount of CL in poly(LLA-*co*-CL) block increased.

Looking only at the thermal properties, one might argue that adding CL to the PLLA block has the same effect as increasing the CL content in the poly(CL-*co*-TMC), but that is not the case if we look at the mechanical properties. From the previous chapter, triblock with an increased CL content in poly(CL-*co*-TMC) soft-block has a characteristic of a stiff polymer with high modulus and low elongation (group C, *Chapter 4*), while looking at triblock **E2**, **E3**, and **E4**, increasing the CL content seems to enhance the elastomeric character of the triblock by lowering the modulus and increasing the elongation. The significant decrease in modulus and yield strength can be seen between triblock **E1** and **E4** in Figure 5.4(c) and 5.4(d). An interesting result is found on triblock **E4**, despite having a completely amorphous poly(LLA-*co*-CL) hard-block, the elongation of **E4** is the highest among all the synthesized triblock. One possible explanation is that for polymer **E4**, the semi-crystalline poly(CL-*co*-TMC) now acts as a hard-block, which is responsible for anchoring during polymer chain stretching and the amorphous poly(LLA-*co*-CL) block acts as to effectively increase branching of the main chain, and hence perhaps the degree of entanglement of the overall network. It is also possible that chain slippage in the crystalline regions (plastic flow) may also contribute to the high elongations, as explained in the next section.

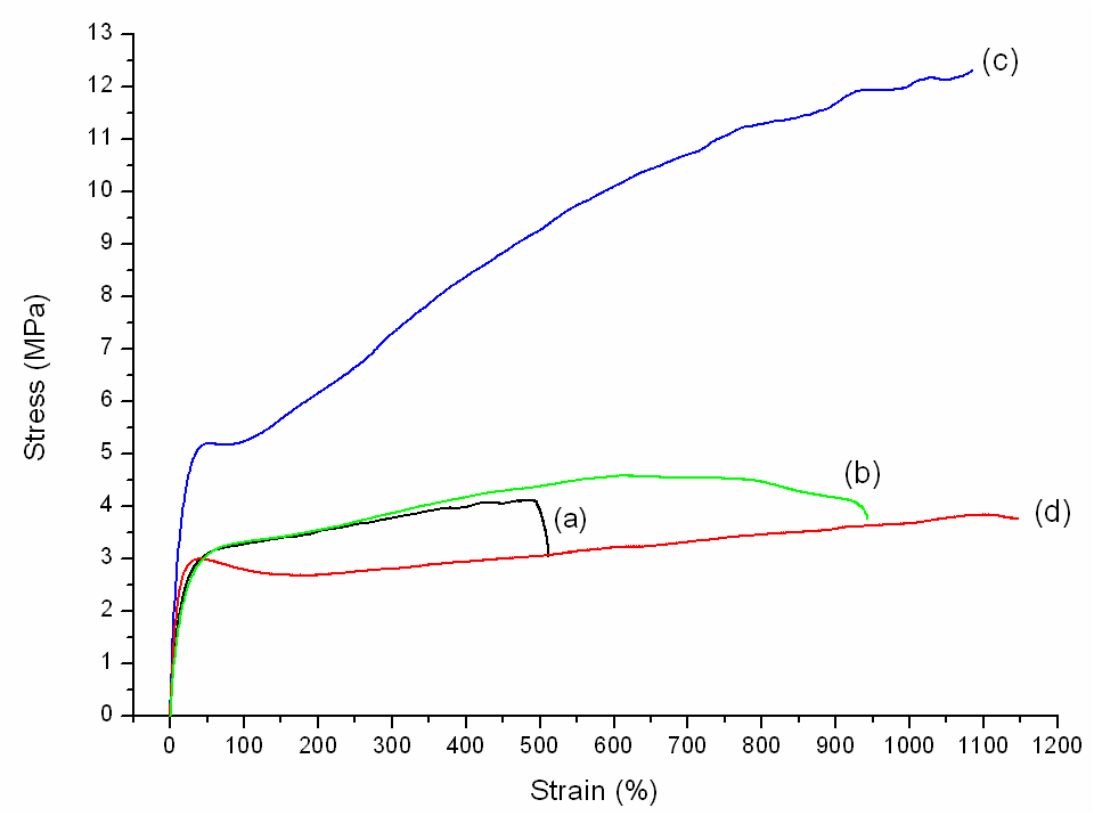

Figure 5.4 Stress strain measurement of the triblock copolymers: (a) CL:TMC 50:50 (**D1**), (b) CL:TMC 50:50 (**D2**), (c) CL:TMC 75:25 (**E1**), and (d) CL:TMC 75:25 (**E4**)

Considering the mechanical properties, it can be seen generally that group E with soft-block CL:TMC 75:25 has a better elongation-to-break (ε_b) compared to group D with soft-block CL:TMC 50:50 for all polymers (compare Table 5.3 and Table 5.4). If we consider only ε_b values only for assessing elastomeric character, it would appear that these polymers with CL:TMC ratio of 75:25 are superior to the 50:50 midblock polymers. The highest elongation of the triblock copolymers with soft segment CL:TMC 75:25 was from triblock **E4**, with an elongation of more than 1200%. However, the presence of a pronounced yield stress in the stress strain curve, Figure 5.4(d), implies that the high elongations may not be fully recoverable, as there is also a possible contribution from plastic deformation (which is non-recoverable) to this

observed elongation. This non-recoverability is quantified using recovery from two different stresses, see below. Here we simply note that high elongations alone do not imply elastomeric behavior.

5.3 Elastomeric Properties

To get a better assessment of elastomeric behavior, we used creep and recovery measurements. Ideal elastomers are able to recover almost completely regardless of the level of stress applied during the creep test. We subjected each triblock polymer to low and high stresses (corresponding to 30% and 80% of their maximum tensile stress up to 200% elongation respectively) for creep and recovery measurements. In this test, we have estimated recovery using:

$$\text{Recovery} = \frac{L_M - L_R}{L_M - L_0} \times 100\ \%,$$

where, L_M is maximum sample length at elongation, mm; L_R - sample length after recovery, mm; L_0 - initial length of sample, mm.

The reason for the choice of these two stresses is as follows: if the polymer is truly elastomeric, recovery values should be independent of the creep stress imposed. If the higher stress is close to the yield stress, then we are likely to see less recovery for those polymers which may exhibit high ε_b, but with yielding (or plastic deformation) behavior contributing to this high ε_b.

Table 5.5 Creep and recovery of various poly(LLA-*co*-CL)-*b*-poly(CL-*co*-TMC)-*b*-poly(LLA-*co*-CL) triblock copolymers.

	Polymer	Recovery at 30% of maximum tensile stress (%)	Recovery at 80% of maximum tensile stress (%)
CL:TMC 50:50	**D1**	78 ± 2	78 ± 1
	D2	63 ± 1	74 ± 2
CL:TMC 75:25	**E1**	72 ± 4	41 ± 2
	E2	80 ± 1	54 ± 2
	E3	65 ± 3	67 ± 1
	E4	67 ± 2	69 ± 1

Table 5.5 shows the creep and recovery results obtained from triblock copolymers of different CL:TMC compositions and different PCL content inside PLLA. The results obtained from the triblock containing CL:TMC 50:50 clearly shows that adding PCL into PLLA reduces recovery percentage for both the low and high stress. However, it is again proven that triblocks based on CL:TMC 50:50 manages to retain their recovery properties at higher stress level (**D1** and **D2**). For triblock with CL:TMC 75:25, adding 10% of CL into PLLA will increase the recovery for low and high stress (triblock **E2**), but adding 30% of PCL will significantly reduce the recovery for low stress (triblock **E3**). With 50% PCL (**E4**), the recovery property for low stress level and high stress level is similar to triblocks from CL:TMC 50:50 which does not show a significant difference between low stress level and high stress level.

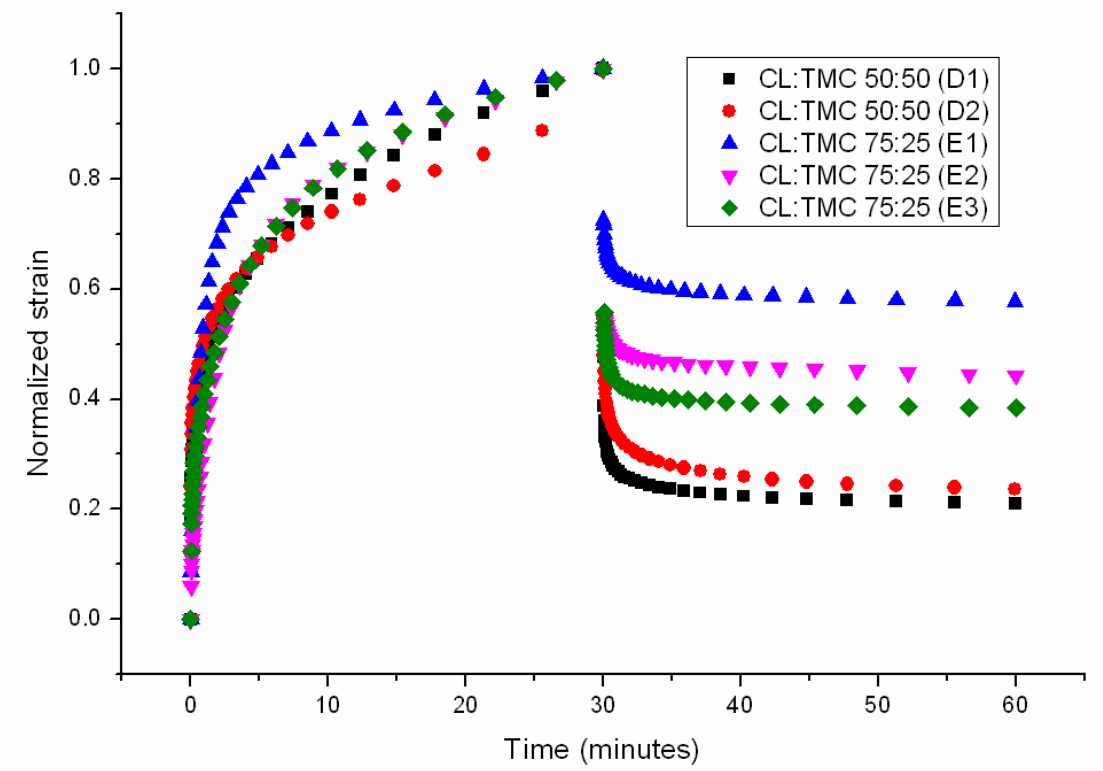

Figure 5.5 Typical creep and recovery curves of various poly(LLA-*co*-CL)-*b*-poly(CL-*co*-TMC)-*b*-poly(LLA-*co*-CL) triblock copolymers at 80% of maximum tensile stress.

Figure 5.5 shows the creep and recovery curves obtained from some of the triblock copolymers. Clearly at the higher stress, there is plastic deformation contributing to the creep, which is not recoverable at the temperature of the experiment. We note here that elastomeric behavior is confirmed when recovery levels are reasonably high, and are more or less independent of the imposed stress levels. When recovery decreases with imposed stress, it is a confirmation of the onset of plastic deformation in the sample, which is not recoverable.

The difference in recovery behavior among the various polymers arises from the contribution of plastic deformation to the elongation or to creep. Triblocks with

CL:TMC ratios greater than 1:1 exhibit higher amounts of plastic deformation, which are non-recoverable, when the imposed creep stress approaches the yield stress. Structurally, we propose that this plastic deformation is due to the presence of crystallinity in the mid-block. From our DSC results, we confirmed that there is crystallinity of PCL in the middle block for CL:TMC 75:25 triblock copolymers. Under creep, it is possible that the PCL crystallites undergo slippage (yielding). This result in permanent (plastic) deformation and upon recovery, only the amorphous region in the middle block is able to recover. On the contrary, CL:TMC 50:50 being completely amorphous in its middle block is able to deform during creep and recover upon removal of stress.

Table 5.6 Cyclic loading and recovery of various poly(LLA-*co*-CL)-*b*-poly(CL-*co*-TMC)-*b*-poly(LLA-*co*-CL) triblock copolymers.

	Polymer	Instantaneous recovery (%) after		
		100% ε_b	200% ε_b	300% ε_b
CL TMC 50:50	**D1**	77 ± 1	76 ± 0	74 ± 0
	D2	83 ± 0	80 ± 0	77 ± 0
CL TMC 75:25	**E1**	60 ± 3	50 ± 3	46 ± 2
	E2	74 ± 1	66 ± 1	64 ± 1
	E3	77 ± 0	70 ± 0	68 ± 0
	E4	81 ± 1	71 ± 1	66 ± 1

Instead of measuring recovery as a function of applied stress, we can also use the Instron to evaluate recovery after different strain (or elongation) levels. Upon cycling from low to high elongation, the loss of recovery can be quantified by the hysteresis level. Table 5.6 which contains cyclic loading results shows that generally triblocks with soft-block of CL:TMC 50:50 are having a better recovery compared to CL:TMC

75:25. By adding CL in the PLLA hard-block, we can observe an increase in the recovery for both CL:TMC 50:50 and 75:25. Triblock **D1** was having an increase of 3-6% in recovery by adding 10% CL in the LLA hard-block (triblock **D2)** while triblock **E1** had a significant increase of 20-21% of recovery by adding 50% CL in the PLLA hard-block (triblock **E4**), and their cyclic loading curves can be seen in Figure 5.6. One point to take note here is that all these recovery percentage values were considered as instantaneous values (no recovery period was applied after the deformation of the polymer). The CL:TMC 50:50 (**D2**) triblock achieved a similar recovery value compared to some other TMC triblocks [117, 139] with applied recovery period up to 16 hours. Furthermore their recovery tests were done based on only 50% elongation which is not sufficient to define the characteristic of an elastomer.

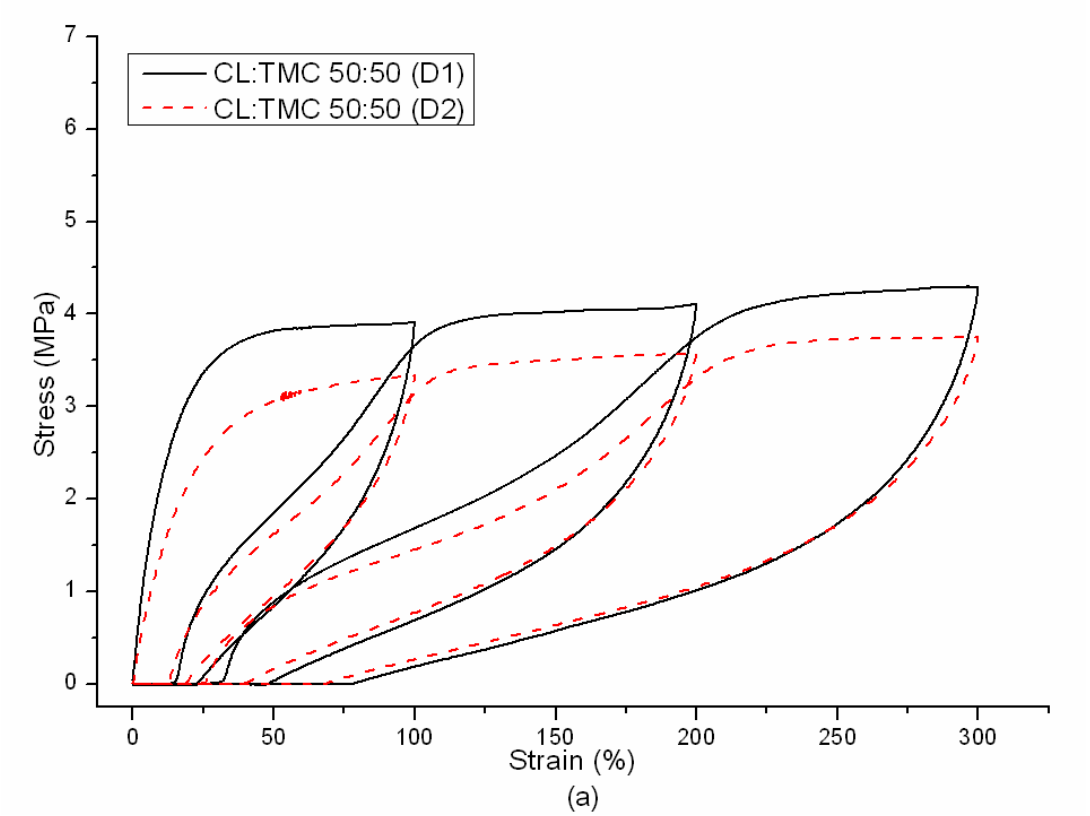

(a)

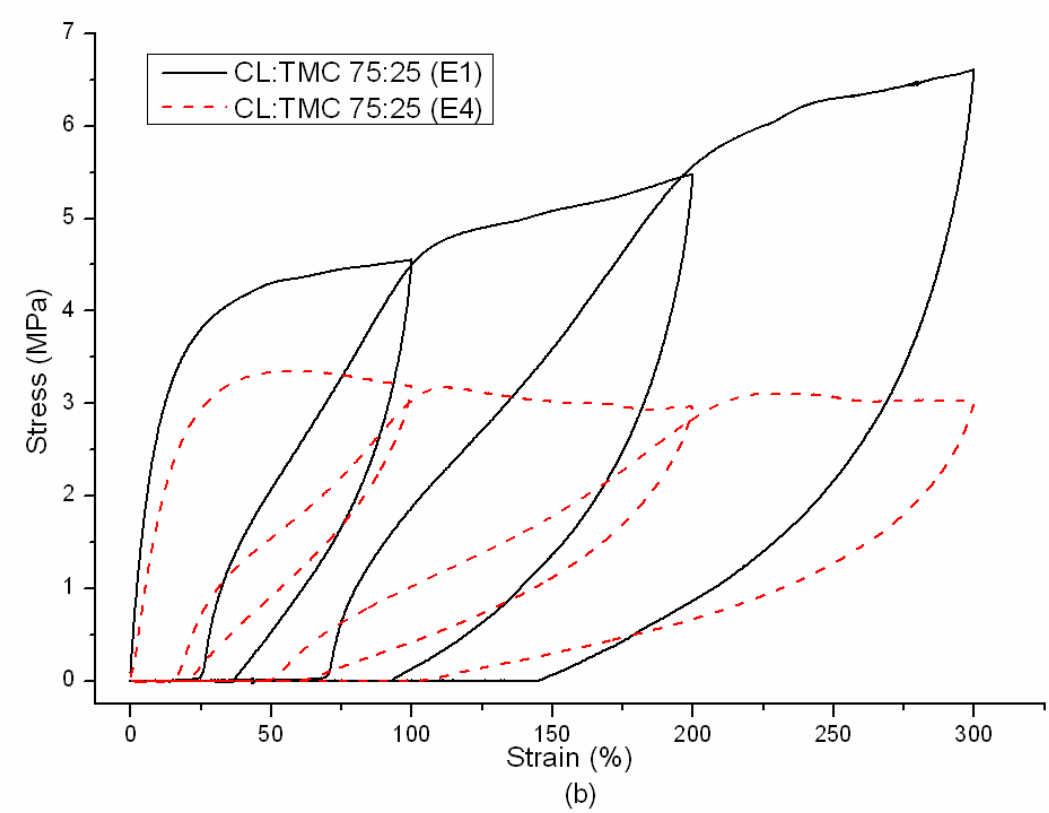

Figure 5.6 Cyclic loading test for four triblock copolymers: (a) CL:TMC 50:50 (**D1**) and (**D2**), (b) CL:TMC 75:25 (**E1**) and (**E4**).

In summary, different effects were observed as a result of adding CL into the PLLA hard block. With respect to the elongation, for triblock with CL:TMC 50:50 soft block, adding a little amount of PCL improves its elongation while too much PCL will completely soften the triblock. For triblock with CL:TMC 75:25 soft block, adding CL into PLLA will increase the elongation even until 50% CL inside the PLLA. In terms of recovery properties, both CL:TMC 50:50 and 75:25 triblock generally showed a reduction in creep recovery property but the instantaneous recovery property is significantly increased.

In order to understand why there can be a different trend between creep recovery and cyclic test result, we have to consider the difference between these two tests. In creep recovery, the triblock are subjected to a long term stress whereby in cyclic test, short term stress are introduced to the triblock. The addition of CL into PLLA hard block makes the entire polymer more flexible, but still there is some anchoring. So, with cyclic test which is completed within a short time, the overall result reflects that the triblock is flexible yet elastomeric. With creep test, the triblock is hold to a constant stress for a longer period of time, which causes more realignment of the polymer chains and perhaps chain slippage. This realignment of PCL in the hard block and the soft block give rise to crystals formation, which in turn will cause the triblock to be less flexible.

5.4 Biodegradation Properties

In vitro biodegradability tests were conducted for four triblock copolymers; triblock **D1, D2**, **E1,** and **E3**. In Figure 5.7 we report data up to sixteen weeks showing the change in molar mass with degradation time. During first 2 weeks the degradation rate is very fast for all the copolymers and then the rates slow down. Comparing the triblocks with the same soft-block, we can see that the addition of the CL into PLLA block will slow the degradation rate. Triblock **D1** has an initial M_n higher than triblock **D2** with 10% CL inside the hard-block, and by the end of the sixteenth week, it had a lower M_n compared to triblock **D2.** The same trend can be observed between triblock **E1** and **E3.** This can be simply attributed to the fact that copolymerization of PLLA with PCL has the effect of decreasing PLLA hydrolysis rate [143].

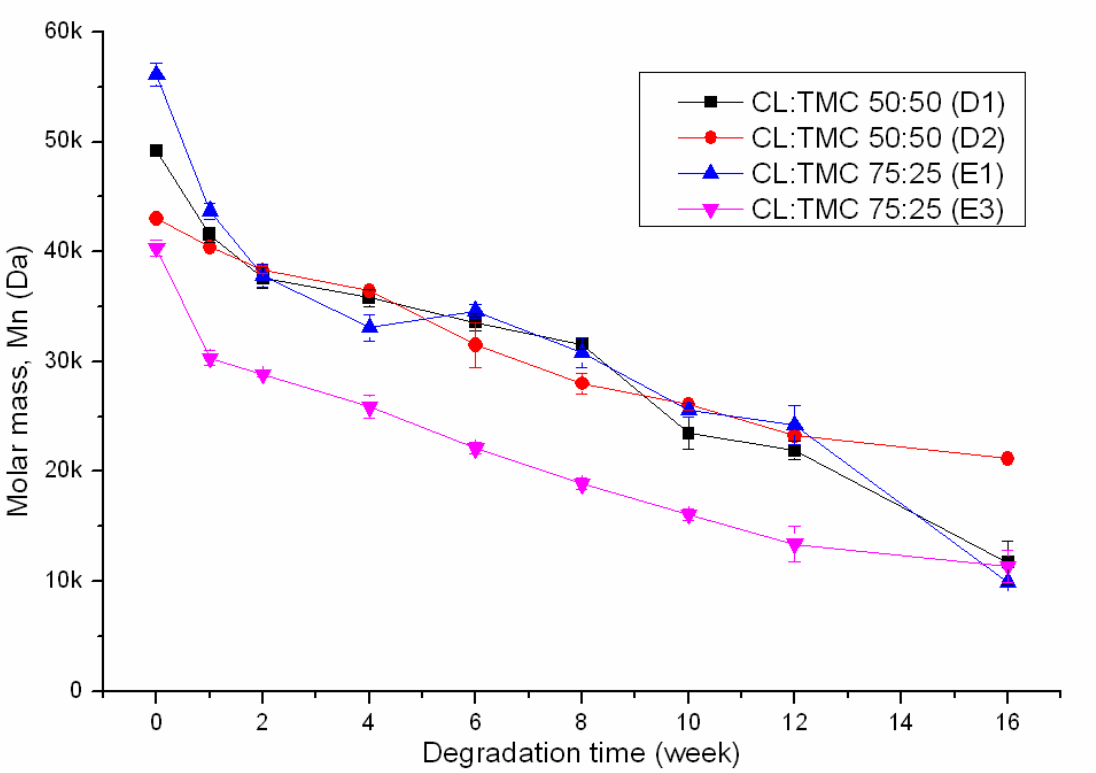

Figure 5.7 Molar mass change in degradation studies of four different triblock copolymers in PBS buffer 1M (pH=7.4) at 37°C.

5.5 Summary

In this Chapter, some modifications were done to some of the selected triblock copolymers from *Chapter 4*. Retaining the same basic middle blocks of poly(CL-*co*-TMC) copolymer, the PLLA end-segment crystallinity was disrupted to examine its effect on elastomeric behavior. A series of triblock copolymers comprising end block of PLLA modified with PCL, and random copolymer of PCL and PTMC as soft segment were synthesized. DSC data show that PCL disrupted the crystallinity of PLLA, making the hard block to be completely amorphous when the PCL content is 50%. Correspondingly, the addition of CL into PLLA block enhances the elongation

of the triblock considerably. With regards to the elasticity, however, creep test results show that adding CL to PLLA block seems to reduce the "equilibrium" recovery, while cyclic test results shows that the instantaneous recovery increased significantly with more CL inside PLLA block. It was also observed that the degradation rate of triblock with added CL inside the PLLA was slower compared to triblock with pure PLLA hard block. This can be simply caused by the fact that PCL has a slower degradation rate compared to PLLA in general.

Chapter 6 Deformation Induced Elasticity

Chapter 5 showed that by adding PCL into PLLA hard-block, and thus reducing the crystallinity of the hard-block, an increase in instantaneous recovery percentage was observed. This contradicts the general agreement which states that in order to have a good elastomeric property, the hard-block needs to be a highly crystalline polymer. Furthermore, it has been observed that the triblock with CL inside PLLA hard-block will have an enhanced elasticity after being exposed to high elongation. This prompts us to do a more thorough investigation on the elastomeric properties especially the structural properties of the triblock copolymers.

Four triblocks with CL:TMC 75:25 soft-block from *Chapter 5* were chosen for characterization using DSC, WAXD, AFM, and Instron cyclic test. They were triblocks **E1**, **E2**, **E3**, and **E4** which have hard-blocks of PLLA random-copolymerized with 0, 10, 30, and 50% PCL respectively.

6.1 Structure Characterization

The phase structure of the multiblock copolymers was investigated by DSC (refer to Table 5.4, *Chapter 5*) to probe on the state of phase separation and the existing phases presented. The DSC thermograms are shown in Figure 6.1.

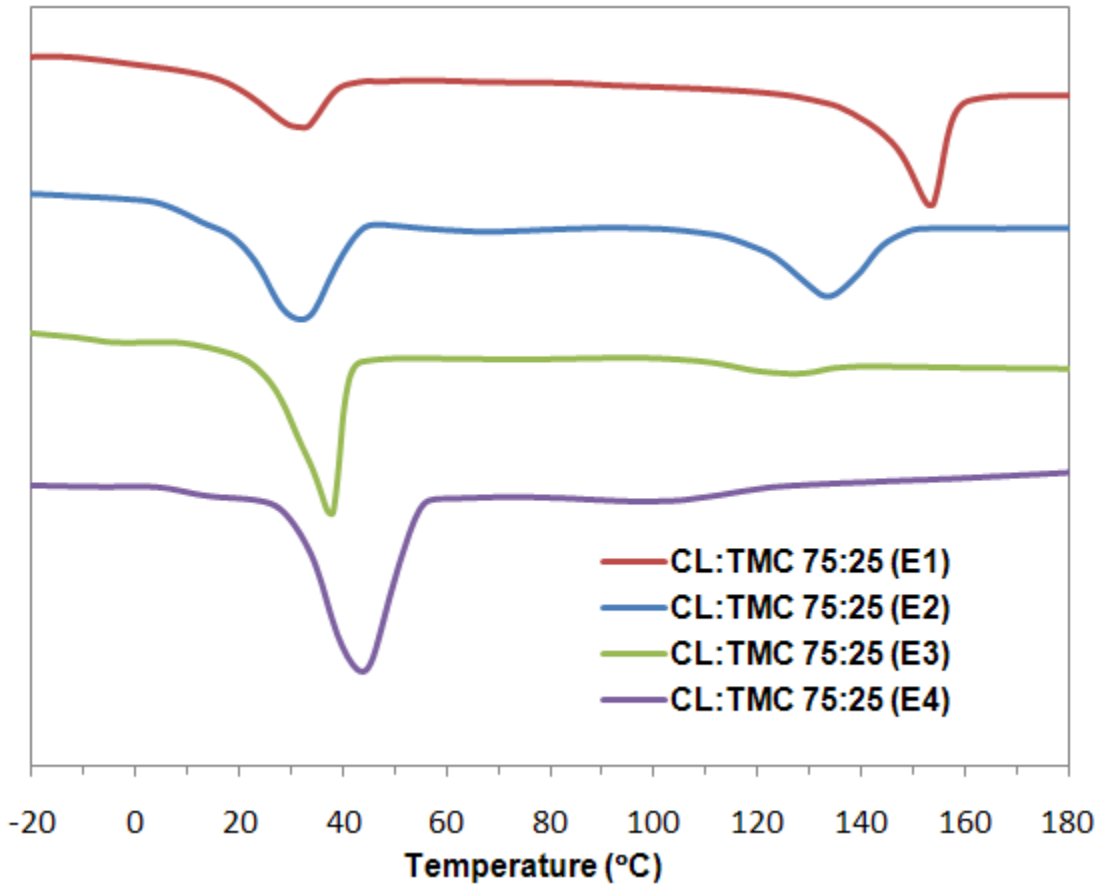

Figure 6.1 DSC thermograms of the triblock copolymer with various contents of CL in the hard segment.

As can be seen in Figure 6.1, two melting peaks were observed at 31 and 153 °C when the PCL content in the hard segment is nil (triblock **E1**), which are due to the presence of PLLA crystallites in the hard segment and PCL crystallites in the soft segment correspondingly. Both of the melting temperatures are lower than those of their homopolymers, suggesting the formation of less perfect crystals. As the content of PCL increases in the hard segment, it is evident that the end-segment crystalline morphology gradually changes, i.e., PLLA melting endotherm diminishes gradually and shifts to lower temperature whereas there is a pronounced shift of PCL melting endotherm to a higher temperature. Particularly, for sample **E3**, only a small and ill-

defined melting endotherm of PLLA was detected in the DSC thermograms. We hypothesize that this effect is due to the disturbance of PLLA crystallization by the PCL blocks, especially when the PCL content in the hard segment is high. During the sample preparation, PCL crystallizes first due to its lower crystallization temperature, followed by crystallization of PLLA segments. The earlier crystallization of PCL component is expected to restrict the mobility of PLLA chains, resulting in the suppression of PLLA crystal formation in the hard segment.

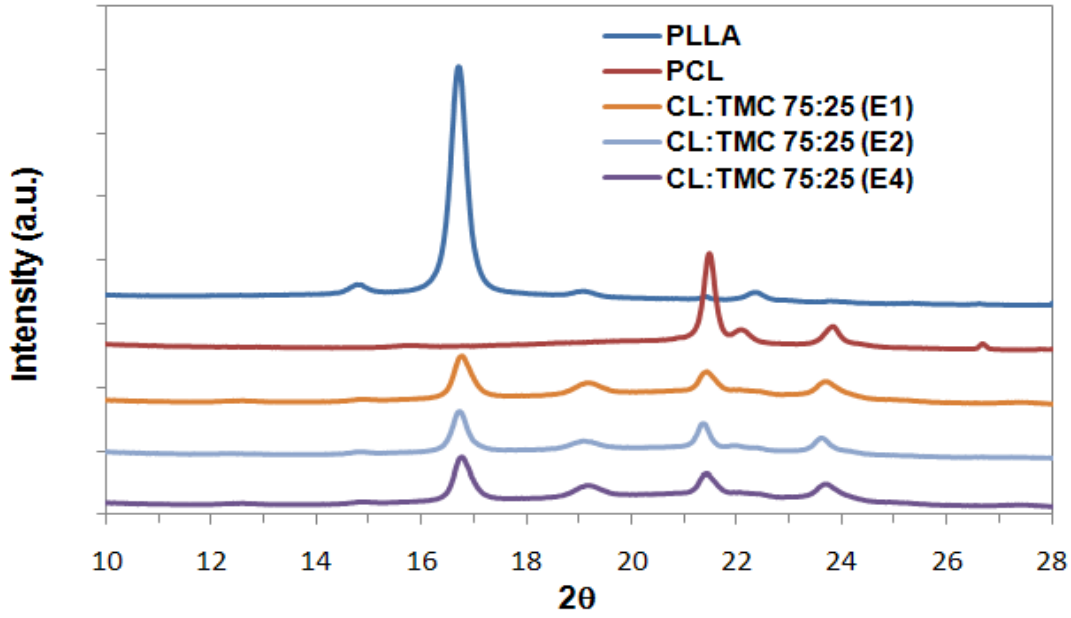

Figure 6.2 WAXD spectra of the triblock copolymers with various contents of CL in the hard segment.

The crystalline structures of the copolymers were examined by using WAXD. X-ray diffraction patterns of PLLA and PCL homopolymers are shown in Figure 6.2 together with those of the copolymers with poly(LLA-*co*-CL) hard-block. PLLA exhibits two diffraction peaks at 2θ = 16.8 and 19.2°, and PCL at 2θ = 21.4 and 23.8°. In the copolymers, all of them present a summation of both PLLA and PCL

diffraction peaks, indicating that both blocks are able to crystallize and form separate crystal phases even when the PCL content in the hard segment is high. Generally, with increasing hard segment PCL content, it was observed that the full width at half maximum (FWHM) of PLLA diffraction peak (2θ = 16.8°) increases, suggesting that the size of PLLA crystals decreases with increasing PCL content. These findings indicate that with poly(LLA-*co*-CL) hard segment, the crystallization ability of PLLA is restricted by the presence of PCL, which is in agreement with the DSC results.

In term of morphology, atomic force microscopy (AFM) in tapping mode was employed to elucidate the micro-phase separated structure at nanoscale levels. Figure 6.3 illustrates the phase images of the copolymers with various molar content of PCL in the hard segment.

Typically, the light regions correspond to hard phase material and the dark regions correspond to soft phase material [144-145]. In these images there is visual evidence for the appearance of microphase-separated structure in all the copolymers being studied. The hard phase is ascribed to the crystalline PLLA phase while the soft phase can be ascribed to the crystalline PCL or a mixed-phase of crystalline PCL and amorphous TMC. In Figure 6.3(a), when the hard segment PCL content is nil, there is clear phase separation between the hard crystallized PLLA and the soft segment phase; however, there is intermixing of hard phase with small regions of soft phase, which causes the drop in their T_ms as discussed before. In addition, when the PCL content in hard segment increases, we observe different crystals shape in the hard phase domains.

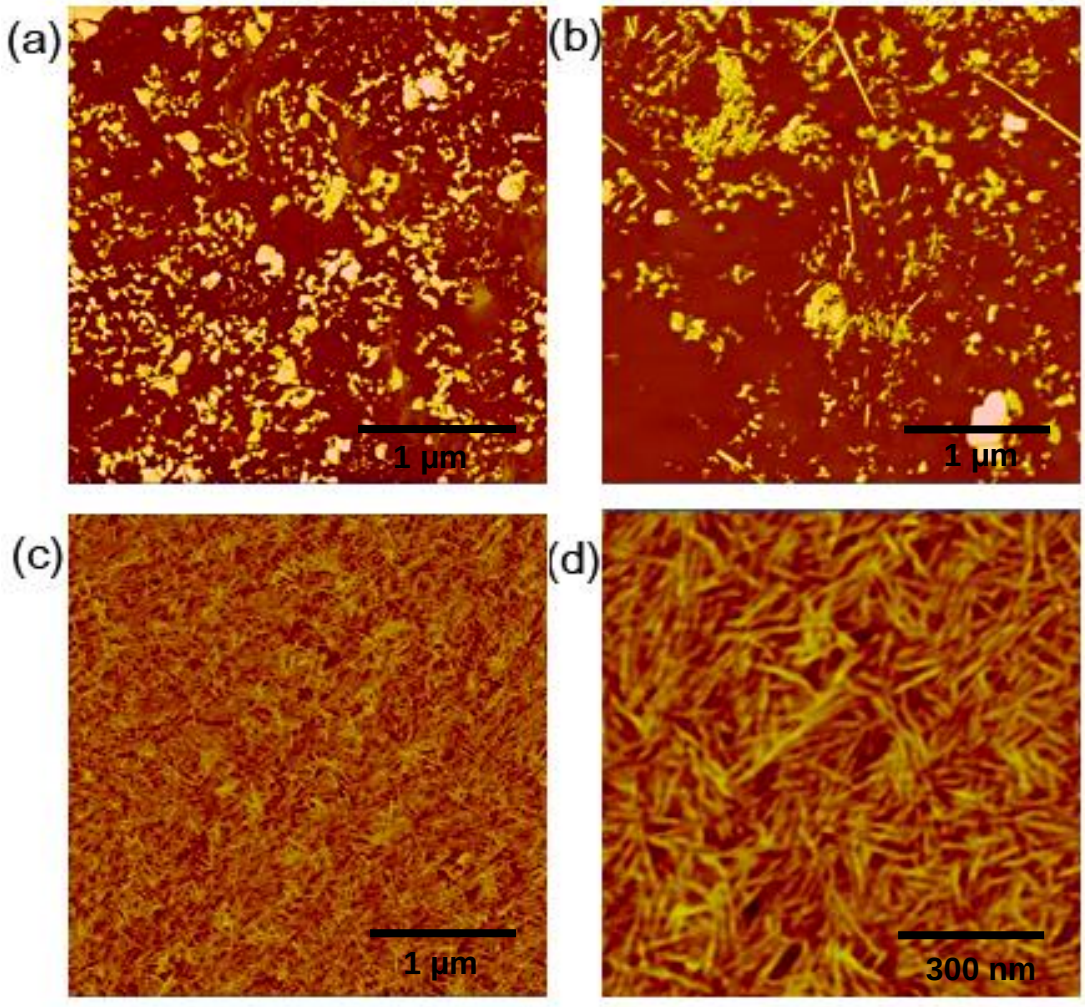

Figure 6.3 AFM images (phase contrast) of triblock copolymers. (a) **E1**, (b) **E2**, (c) and (d) **E4**.

6.2 Mechanical Cyclic Behavior of Triblock Copolymer

The stress – strain responses for the copolymers during the cyclic uniaxial tensile tests are shown in Figure 6.4. In the first cycle, the stress – strain curve during extension exhibited an apparent yield point, followed by a rubbery plateau, and the onset of strain hardening when the strain level exceeds 100% elongation. It is generally accepted that the yield point is associated with the 'permanent' set behavior [146]. At the end of the first cycle, this permanent set was manifested in the non-recoverable

strain. In the second and subsequent cycles, the sample exhibited an almost completely elastic behavior whereby there is no evidence of a yield point and very little permanent set; this is particularly true of polymer **E4**. Moreover, the stress – strain responses in the second and higher cycles were nearly identical, implying little change in the hard domain continuity [147]. However, it was clearly observed that there is substantial change in the shape of the curve between the first and second cycles, leading to a substantially lower stress in cycle 2 (implying a significantly lower initial modulus). These changes indicate structural changes in the crystalline domains during the first cycle of deformation, as discussed later.

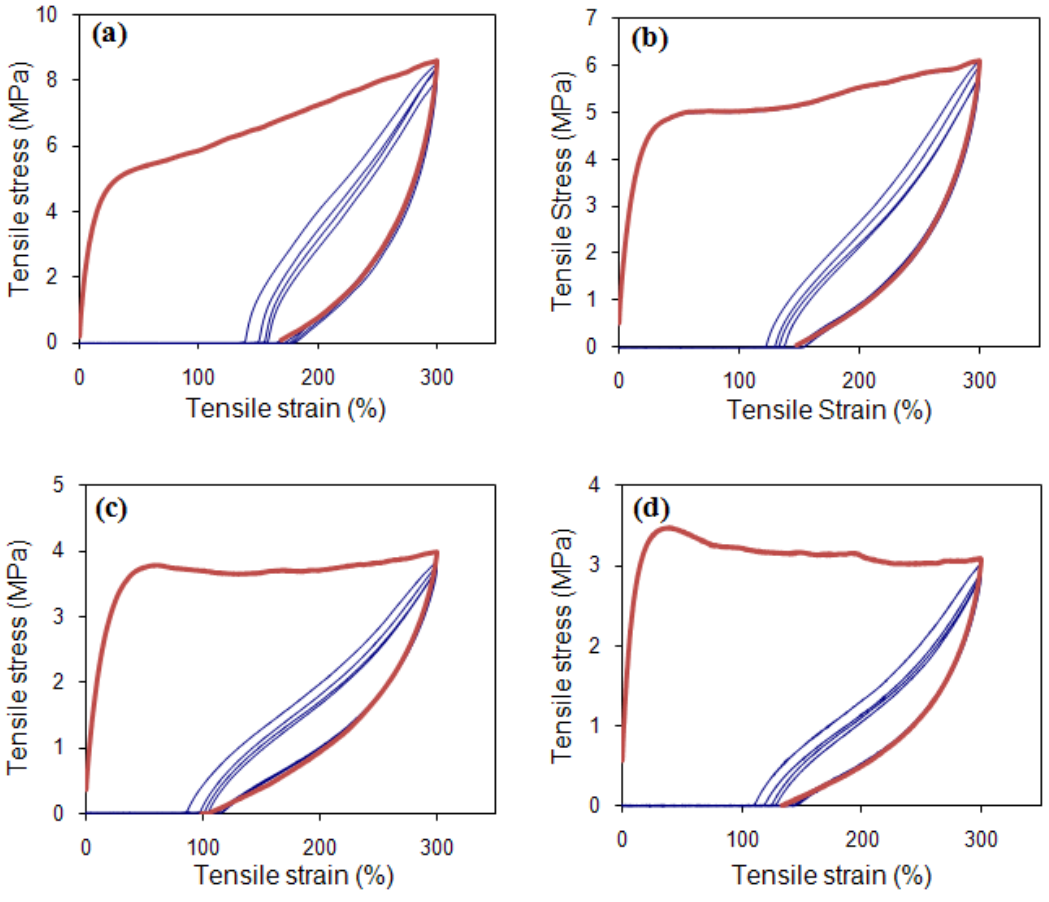

Figure 6.4 Stress - strain behavior of triblock copolymers at cyclic tests up to five cycles: (a) **E1**, (b) **E2**, (c) **E3**, and (d) **E4**. Red curve indicates the path of 1st cycle while blue curves indicate the path of the 2nd cycle onwards.

One interesting observation is that the non-recoverable strain varies with the hard segment PCL content. The strain recovery data are presented as fractional recovery in Figure 6.5, for ease of comparison. Fractional strain recovery is defined by the following equation:

$$Fractional\ strain\ recovery = \frac{\varepsilon_m - \varepsilon_p(N)}{\varepsilon_m - \varepsilon_p(N-1)}$$

where $\varepsilon_p(N)$ represents the residual strain value where the stress returns to zero in the N-th cycle and ε_m represents the maximum strain. Fractional strain recovery is the ratio of recoverable strain to deformed strain in each cycle *N*.

Several interesting points are noted in Figure 6.5:

(a) The strain recovery reaches 85 ~ 95% after the first cycle and it is larger than 95% for polymer **E4**.

(b) The strain recovery following 300% elongation is higher than that following 100% elongation for polymer **E4**.

(c) It is shown that strain recovery increases significantly with the addition of PCL into the hard segment.

Interestingly, incorporating PCL in the hard segment enables the polymer to exhibit the "DIE" effect and this contrasts with the behaviors of PLLA and PCL homopolymers, which essentially do not show any strain recovery when the applied strain goes beyond 100%.

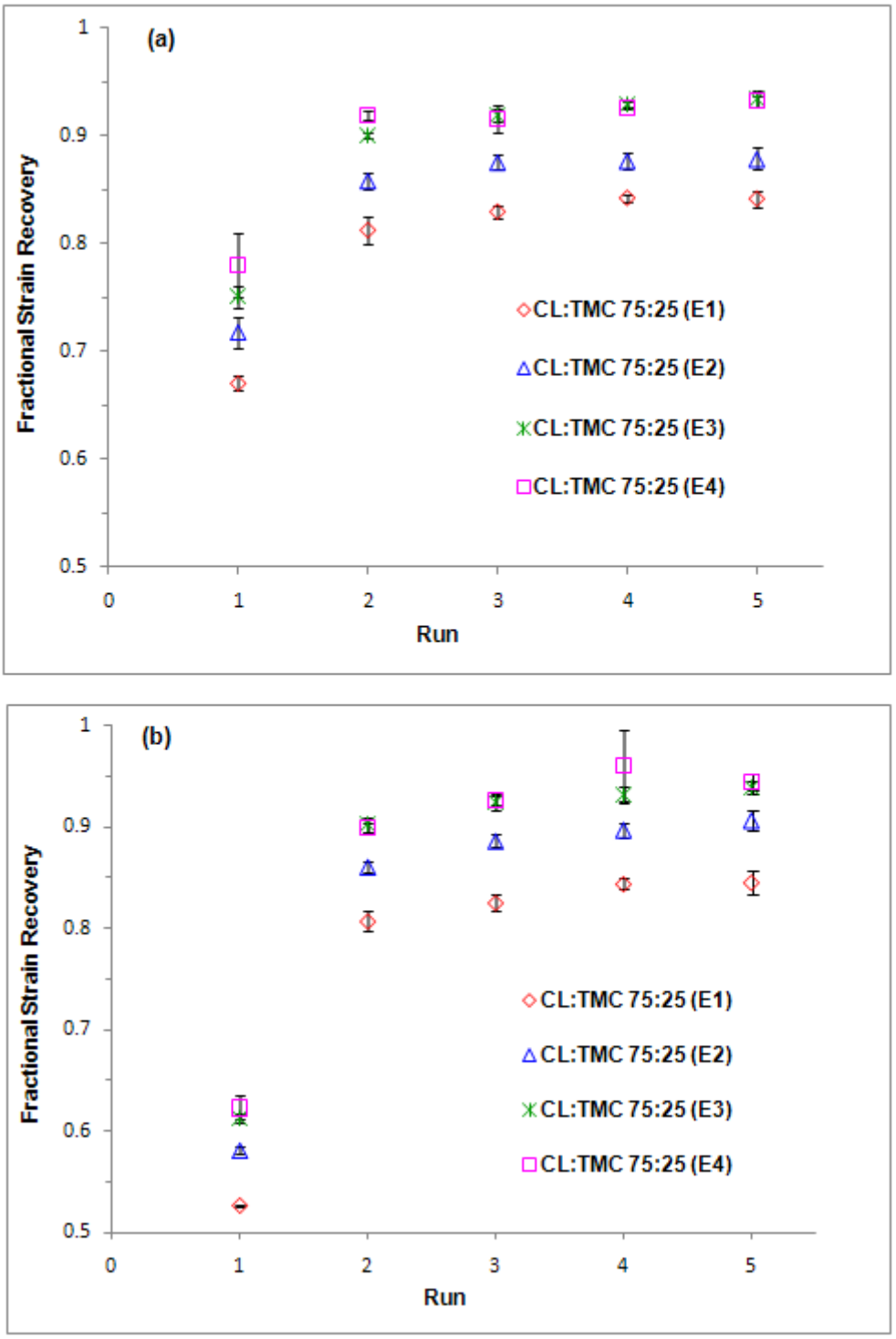

Figure 6.5 Fractional strain recovery data for the triblock copolymers series subjected to (a) 100% elongation and (b) 300% elongation in the cyclic tests.

In order to better understand the structure changes that happened during the cyclic deformation, the stress – strain curve and selected WAXD patterns in sample **E4** during stretching and retraction in the first and second cycles are shown in Figure 6.6 (Only first and second cycles are discussed as those in the higher cycles are identical to the second cycle). The arrow indicates the strain value where the image was taken. It is seen that the WAXD image at strain zero is completely isotropic with a broad amorphous halo superimposed with three sharp crystal reflection rings. The first reflection ring at $2\theta = 16.5°$ is attributed to the (110)/(200) reflection of PLLA crystal. Moreover, the second and third reflection rings at $2\theta = 21.4°$ and $23.8°$ have been attributed to (110) and (200) reflections of PCL crystal, respectively.

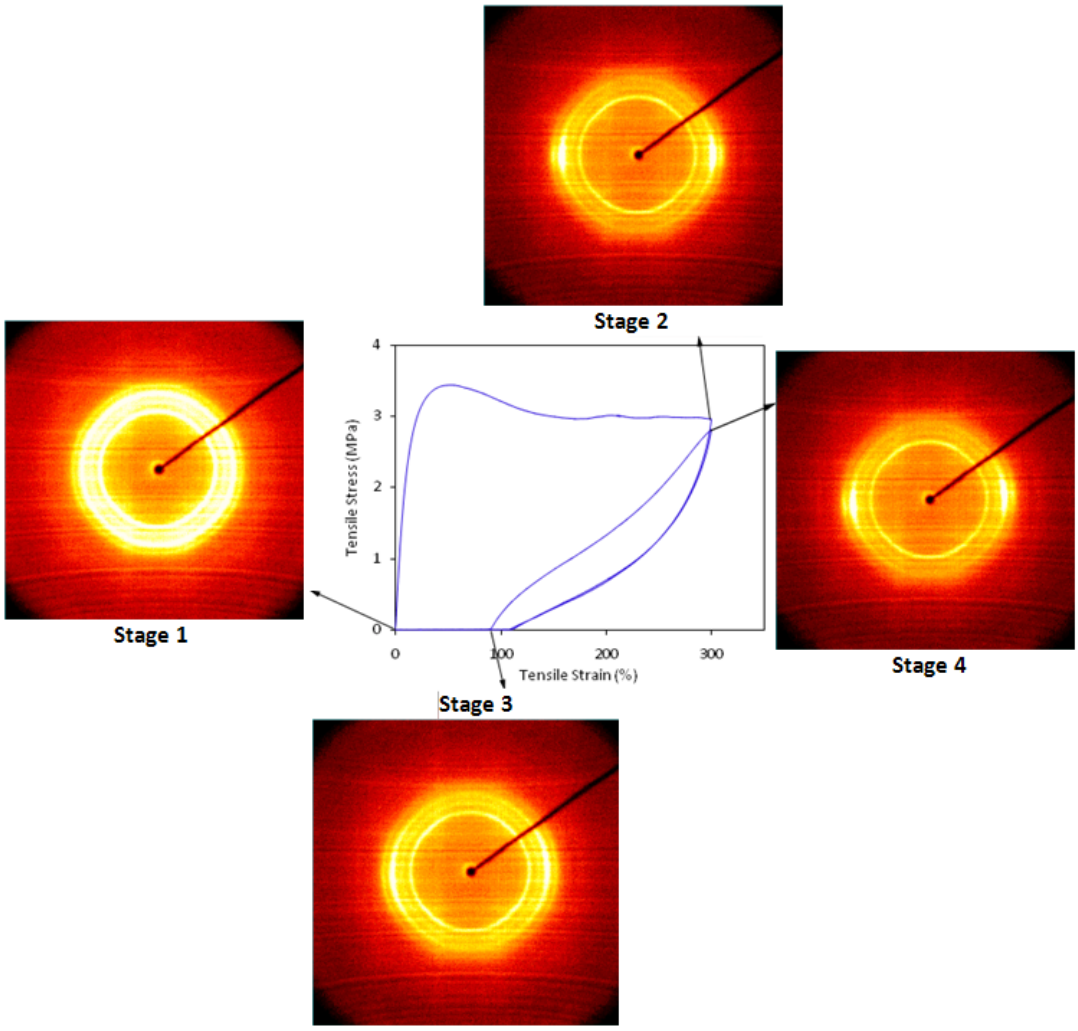

Figure 6.6 The stress – strain curve and selected WAXD patterns collected during stretching and retraction of triblock copolymer **E4** in the first and second cycles. Each image was taken at the average strain indicated by the arrows.

Upon deformation, structural anisotropy is seen in the WAXD image. The isotropic (110) PCL crystal ring is found to converge on the equator with stretching, which indicates that the PCL crystals present in both soft and hard segments were gradually oriented along the stretching direction and the diffraction arc intensified. Upon retraction, the orientation of the PCL crystallites showed partial recovery resulting in a less sharp PCL diffraction arc on the equator. In contrast, the reflection ring from

the PLLA crystals was not affected by deformation and retraction. This is clear evidence that during this deformation, only the PCL crystallites are being oriented in the stretching direction.

For clearer illustration, the corresponding azimuthal profiles for both the PCL (110) and PLLA (110)/(200) reflections at different stages are displayed in Figure 6.7. The azimuthal angle at 270° refers to the equatorial axis. At stage 1 (strain zero), PCL crystals are randomly distributed with azimuthal intensity being constant. Upon stretching to 300% strain elongation (stage 2), the intensity maxima appear, indicating a significant increase in the degree of orientation in the PCL crystalline region. Subsequently there is substantial drop in intensity upon retraction (stage 3), consistent with the partial recovery. During stretching in the second cycle (stage 4), the intensity maxima become azimuthally narrower again. On the other hand, the azimuthal intensity of PLLA (110)/(200) crystal reflection is flat and constant throughout all the stages, indicating that the PLLA crystals were not affected by deformation and remained randomly distributed. This result is surprising as it is generally believed that the permanent set in the first deformation cycle is associated with the fragmentation or reorganization of the hard domains in typical thermoplastic elastomers [147-149]. However, the WAXD results demonstrated here show that the PLLA crystals in the hard domains remain intact while the PCL crystals are being oriented during stretching, contributing to the permanent set observed in the first cycle.

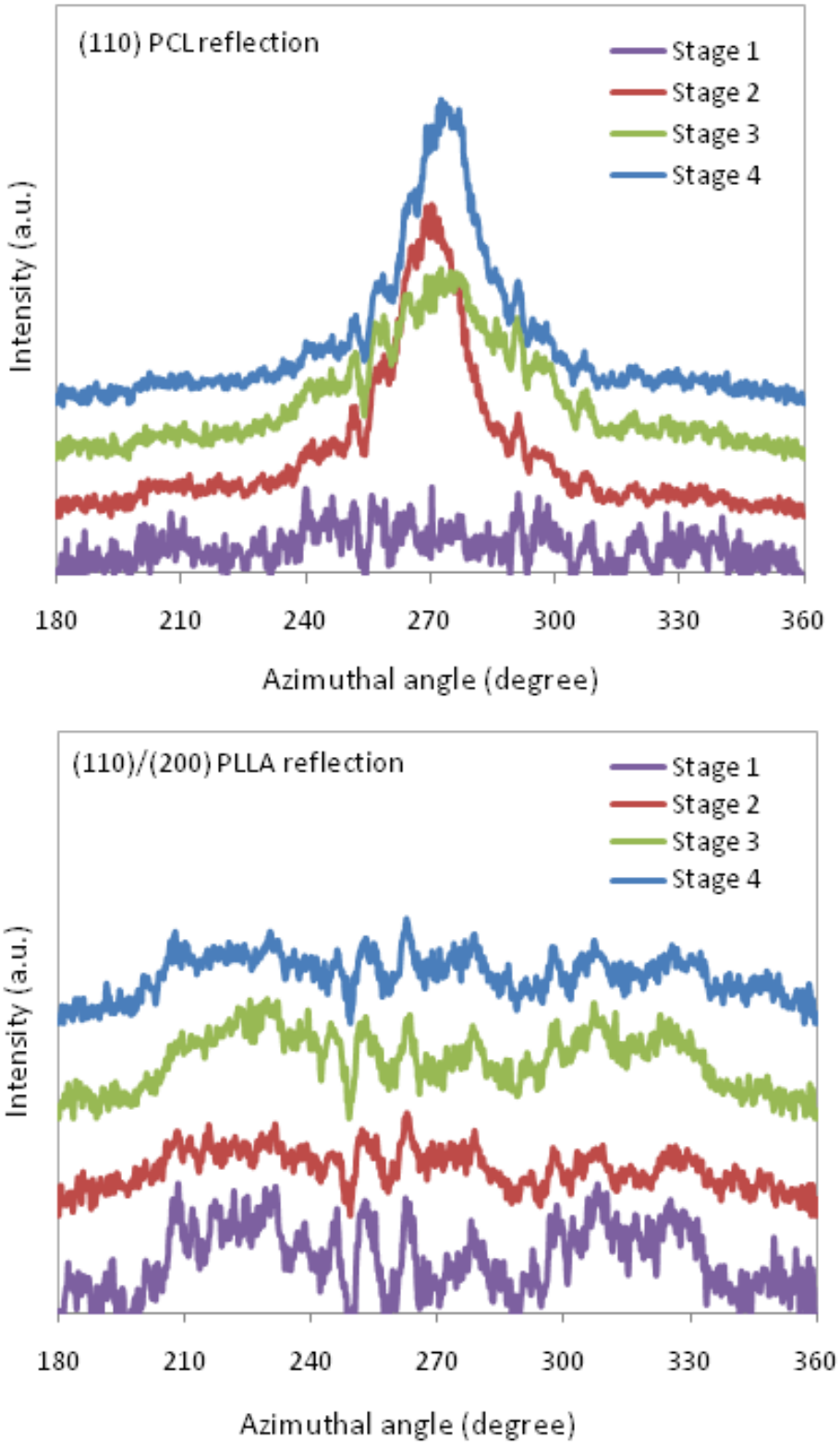

Figure 6.7 Azimuthal profiles of (110)/(200) PLLA and (110) PCL reflections for copolymer E4 at different stages during the cyclic test. The stage numbers correspond to those in Figure 6.6.

For characterization of the influence of hard segment PCL content on the strain recovery, Herman's orientation function for PCL crystals, $P_{2,CL}$, has been calculated and is shown in Table 6.1. Bonart [150] reported that the orientation of segments depended on the hard domain morphology. In addition, Albertsson et al. [139] have observed the same phenomena (the DIE effect) and mentioned that it could probably be due to a reorientation of macromolecules. In our study, during first cycle, PCL crystallites in both the soft and hard segments are being oriented in the stretching direction. Upon recovery, some of these crystallites return to their unoriented state; the residual orientation of these crystallites is the reason for the permanent set. In the second cycle, there is not much re-orientation of PCL crystals for **E1**, while **E3** and **E4** (which have higher PCL content in the hard segment) show more orientation of the PCL crystals. This orientation is however, more recoverable. Thus, it is reasonable to assume that the end-segment PCL crystals are more likely to recover their orientation than the middle segment PCL crystals due to the morphological difference of PLLA in the end-segment. It is likely that the residual oriented crystals after cycle 1 (in all 3 polymers), merely act as extra crosslink points during cycle 2, leading to better recovery overall after first cycle. Figure 6.8 illustrates the structural changes involved during the deformation in the first and second cycles.

Table 6.1 Calculated $P_{2,CL}$ values of PCL crystals at various stages in the cyclic test.

Stage	State	Polymer		
		E1	**E3**	**E4**
1	Undrawn	0	0	0
2	300% strain (1st cycle)	0.44	0.49	0.90
3	Recovered	0.44	0.36	0.36
4	300% strain (2nd cycle)	0.42	0.48	0.87
5	Recovered (end of 2nd cycle)	0.42	0.37	0.38

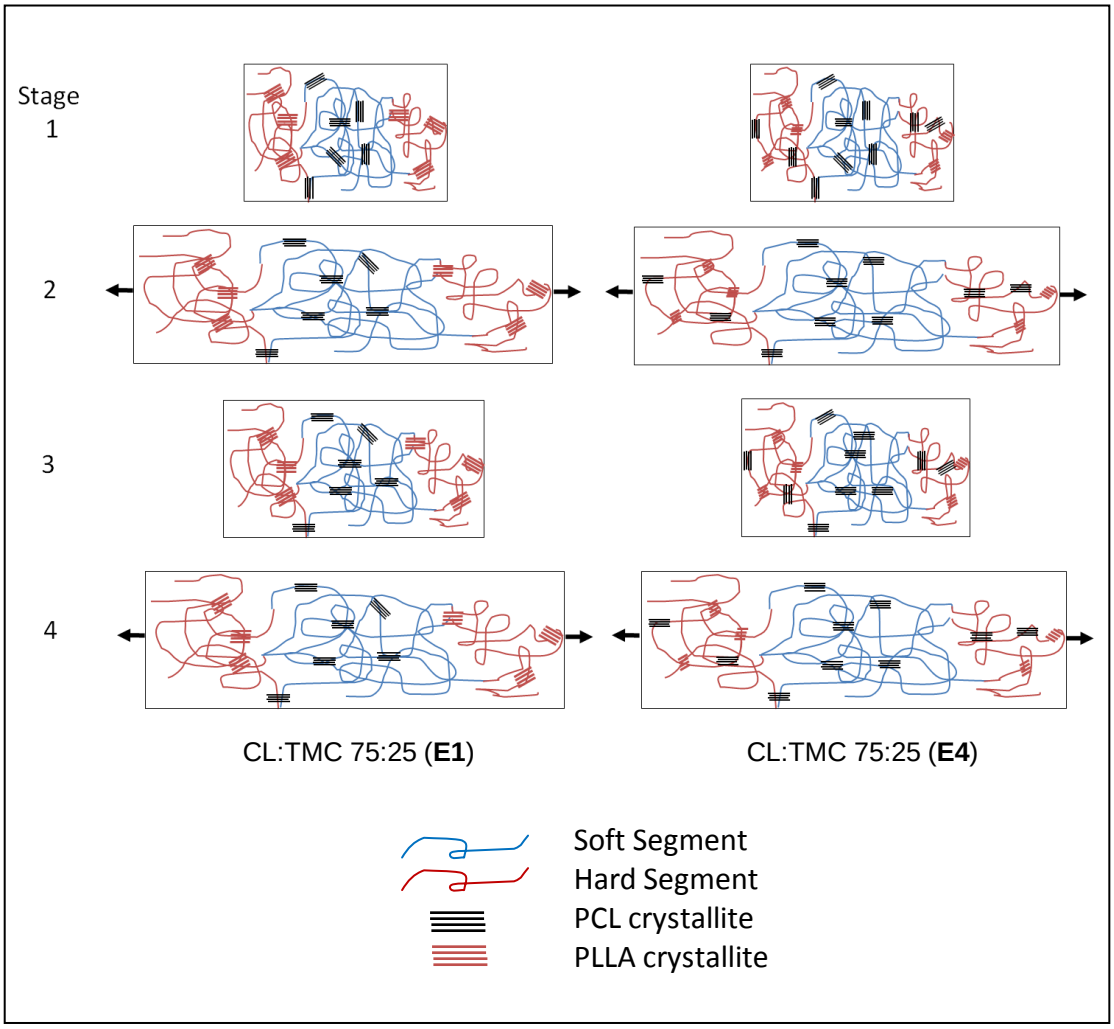

Figure 6.8 Schematic diagram to illustrate the structural changes involved during extension and retraction in the cyclic deformation. Note the negligible PLLA crystals orientation in the hard domains during the stretching while the PCL crystals are being oriented

6.3 Summary

In this chapter, more thorough characterizations of the copolymers in *Chapter 5* were done to investigate the increase in elasticity for these triblock copolymers with PCL

inside PLLA hard block. DSC and WAXD results allow concluding that PLLA crystallization is restricted by the presence of PCL segment chains in the hard segment. Furthermore, it has also been demonstrated by AFM that these triblock copolymers show more extensive phase separation and morphology of PLLA hard domain changes when the hard segment PCL content increases. Interestingly, it was found that although the recovery after the first elongation is low, the recovery increases during subsequent cycles (hence the name, "deformation-induced elasticity"). This phenomenon has been observed also with another copolymer [139], although its origins were not rationalized. Using WAXD and orientation measurements, we were able to relate the DIE effect to the influence of the PCL crystallinity and orientation changes with addition of PCL to the end-block.

Chapter 7 Starblock Copolymer of ε-Caprolactone, Trimethylene Carbonate, and L-Lactide

In the previous chapters, attempts were to make biodegradable thermoplastic elastomers using the classical triblock copolymer approach. Several triblock copolymers have been found to have good elastomeric properties, and further refinement of their mechanical properties was carried out by modifying the hard block. Another way to create a BTPE is by having an entirely different structure from the triblock. Recently, starblock homo- and copolymers have become an interesting alternative to their linear counterpart. This chapter discusses the synthesis of four-armed starblock copolymer, using random poly(CL-*co*-TMC) as the soft block, and PLLA as the hard block.

Several starblock copolymers have been synthesized using pentaerythritol. Basically there are two groups of starblock copolymers, one is for copolymers with soft block made of random copolymer of PCL and PTMC with CL:TMC 50:50 (group SA) and the other groups with CL:TMC 75:25 (group SB). Within the group, the amount of hard block was varied to study the elastomeric properties. Preliminary study was done by synthesizing the poly(CL-*co*-TMC) soft block only, one each for CL:TMC 50:50 and CL:TMC 75:25.

7.1 Molar Mass and Structural Properties

Table 7.1 Molar ratio and molar mass of various PLLA-*b*-poly(CL-*co*-TMC) starblock copolymers.

Polymer	feed ratio CL:TMC:LLA	molar ratio[a] CL:TMC:LLA	M_n[b] ($g \cdot mol^{-1}$)	PDI[b]	M_n[c] P(CL-*co*-TMC) ($g \cdot mol^{-1}$)	M_n[c] PLLA ($g \cdot mol^{-1}$)
SA0	1 : 1 : 0	1 : 0.90 : 0	20700	1.11	20700	-
SA1	1 : 1 : 0.38	1 : 0.94 : 0.21	20100	3.36	17700	2400
SA2	1 : 1 : 0.75	1 : 0.83 : 0.50	26300	1.24	19300	7000
SA3	1 : 1 : 1.50	1 : 0.94 : 1.28	29700	1.31	15800	13900
SA4	1 : 1 : 3.00	1 : 0.93 : 2.64	37000	2.15	13100	23900
SB0	1 : 0.33 : 0	1 : 0.26 : 0	40200	1.98	40200	-
SB1	1 : 0.33 : 0.25	1 : 0.28 : 0.16	29600	2.72	25600	4000
SB2	1 : 0.33 : 0.50	1 : 0.30 : 0.37	42900	1.89	31300	11600
SB3	1 : 0.33 : 1.00	1 : 0.31 : 0.84	47800	1.93	26200	21600
SB4	1 : 0.33 : 2.00	1 : 0.33 : 1.83	66800	1.91	23800	43000

[a] Determined by ^{1}H NMR analysis

[b] Obtained by SEC analysis

[c] Block length calculated from the M_n by SEC and ^{1}H NMR result

Table 7.1 shows various compositions of four-armed star-copolymer with PCL and PTMC at a molar ratio of 50:50 and 75:25. **SA0** and **SB0** were the soft block of star copolymer without the PLLA hard block. For each group, the feed ratio of the soft block was kept constant while hard block was increased. From SEC results, it can be observed that molar mass increases as the amount of lactide increases, with an exception on **SA1** and **SB1** due to the very low PLLA content. Looking further at column 6, we can see that the molar mass of the poly(CL-*co*-TMC) soft blocks of **SA1**-**SA4** and **SB1**-**SB4** star copolymers are relatively stable although they seem to be always lower than **SA0** and **SB0.** Meanwhile from column 7, we can see that the

molar mass of PLLA hard block is increasing proportionally according to the molar ratio.

A very high conversion of monomer can only be achieved through anionic polymerization. Although with coordination-insertion, molar mass could still be controlled, but the conversion would not be as high as anionic polymerization as it depends on the nature of initiator being used, as well as the catalyst. This is shown in the fact that from the experiment the polymer's molar mass obtained was rather low. Impurities in the reactants and reactions system affect polymerization and contribute to the low molar mass polymer obtained. Environmental condition, e.g. humidity, also adds effect to the reaction, even though all the experiments were done in inert conditions. The catalyst used, stannous octoate, is a strong transesterification agent. If the temperature of the system reaches 150^{o}C, polymer backbiting is very likely to happen, especially when the polymerization lasts more than 10 hrs [151]. This is also the possible reason why the results obtained are in a rather broad PDI (1.24-3.36).

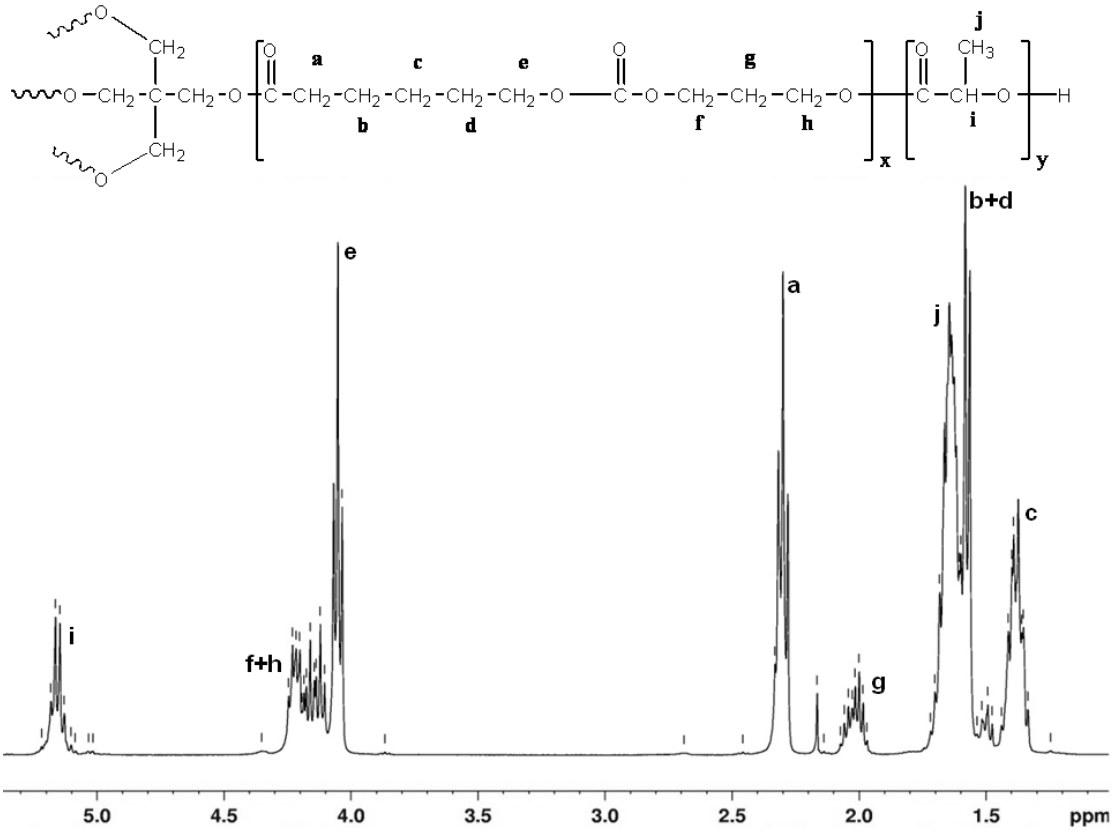

Figure 7.1 ^{1}H NMR Spectrum and structure of four-armed star-shaped copolymer CL:TMC 75:25 **SB2**

Figure 7.1 illustrates the details of representative ^{1}H NMR spectra of star-shaped copolymer of CL, TMC, and LLA (starblock **SB2**). The signals of methylene protons from PCL are shown at 2.33, 1.6, 1.35, and 4.04 ppm for (**a**), (**b+d**) (**c**), and (**e**) respectively. While methylene protons from PTMC at 4.23 and 2.02 ppm are assigned to (**f+h**) and (**g**) respectively. Finally for PLLA, methyne proton (**i**) is displayed at 5.16 ppm and methyl protons (**j**) is shown at 1.65 ppm. The peak splitting on the region of (**f+h**) and (**e**) peaks suggests that random copolymerization of PCL and PTMC occurred. Randomization of PCL and PTMC is preferable as both PCL and PTMC will serve as the matrix in this thermoplastic elastomer. While the homopolymer of PCL is crystalline and PTMC is amorphous, introducing PTMC into

PCL will reduce PCL's crystalline properties and provide better mechanical properties. Polymers with microcrystalline regions are tougher and have higher impact resistance [152]. Moreover, PTMC is able to reach more elongation compared to PCL, thus randomization of these two polymers will produce a tougher, flexible polymer as preferred in the matrix of thermoplastic elastomer.

From the above ^{1}H NMR spectra, the copolymer's composition could be determined by looking at the integration ratio between the proton signals of PCL (**a**), PTMC (**g**), and PLLA (**i**). The copolymer's composition obtained from ^{1}H NMR spectra is shown in Table 7.1. For copolymers with PCL: PTMC 75:25 and 50:50, the results show us that the molar ratio between PCL, PTMC and PLLA are generally quite close to our target.

7.2 Thermal and Mechanical Properties

The DSC characterization of the four armed star-shaped copolymers is given in Table 7.2. From this table we can see that copolymers with different compositions apparently have different thermal properties. Some trends that we may deduce from the experimental results are as follows. Firstly, as the hard block composition increases, the T_ms generally increase which is expected because increasing the amount of crystalline PLLA will increase the crystallinity of the polymer. As previously discussed, molar mass plays a significant role in determining the properties of a polymer, including thermal and mechanical properties. Thus, some discrepancies in the trend observed are probably related to the molar mass obtained during

polymerization. Nonetheless, there are still quite a number of remarkable points we could notice from the results.

Table 7.2 Thermal and mechanical properties of various PLLA-*b*-poly(CL-*co*-TMC) star copolymers

Polymer	M_n[a] ($g \cdot mol^{-1}$)	T_g (°C)	T_m (°C)	ΔH (J/g)	Modulus (MPa)	Tensile Strength (MPa)	Max Strain, ε_b (%)
SA0	20700	-52	-	-	-	-	-
SA1	20100	-36	-	-	Too weak	Too weak	Too weak
SA2	26300	-33	-	-	Too weak	Too weak	Too weak
SA3	29700	-34	144	13.9	4.6	1.9	603
SA4	37000	-43	157	27.6	Too brittle	Too brittle	Too brittle
SB0	40200	-54	36	33.8	-	-	-
SB1	29600	-49	37	40	3.2	1.5	253
SB2	42900	-51	128	5.7	3.5	4.5	> 980
SB3	47800	-52	147	17.8	12.6	5.8	291
SB4	66800	-54	162	25.7	44.4	9.2	276

[a] Obtained by SEC analysis

For **SA** group whereby CL:TMC is 50:50 it was expected that there will be no melting point from the soft block, as the soft block (**SA0**) was proven to be completely amorphous. And for the star block copolymer with low amount of PLLA (**SA1** and **SA2**), there were no melting point of PLLA observed.

If we see the T_ms of the **SB** group with CL:TMC 75:25, there are two distinct T_ms which are 37°C (from poly(CL-*co*-TMC) block: **SB1**) and those between 128°C-162°C (from PLLA block: **SB2**, **SB3**, and **SB4**). However, it must be noted that these two T_ms did not co-exist for any of the copolymers. It is reported that when the crystalline segment in block copolymers is relatively short and the content is

relatively low, one of melting endotherms in the block copolymers decreases and finally disappears, which results in the decreasing overall crystallinity [151]. Since poly(CL-*co*-TMC) is randomly copolymerized, the crystalline segment would be relatively short. For the entire SA group, there is no PCL crystallinity: in addition, the PCL crystallinity in the soft block disappears when the PLLA amount increases, as seen for **SB2**, **SB3**, and **SB4**.

Degree of crystallinity of a polymer can be expressed in the heat of fusion (ΔH), and from these two samples it is clear that the heat of fusion decreased as we increased PLLA into the copolymers. Some research groups also suggest that the PLLA segments have higher tendency in retaining their crystalline array [151, 153]. A suppression of the melting temperatures may also happen due to the increased complexity of crystallization when two crystalline segments exist in a polymer [154]. Short or low molar mass arms and greater number of end-groups like in star-shaped copolymers may also disrupt the crystal formation. Thus in the copolymers with considerable amount of PLLA, the low melting temperature was not observed. This melting temperature disappearance phenomenon is also indicating that poly(CL-*co*-TMC) crystalline segments were phase mixed with the PLLA. Phase mixing is affected by the number of arms in star-shaped copolymer. As the number of arms increases, the mixing extent also increases, and phase mixing causes crystalline imperfection which therefore decreases the melting point [151].

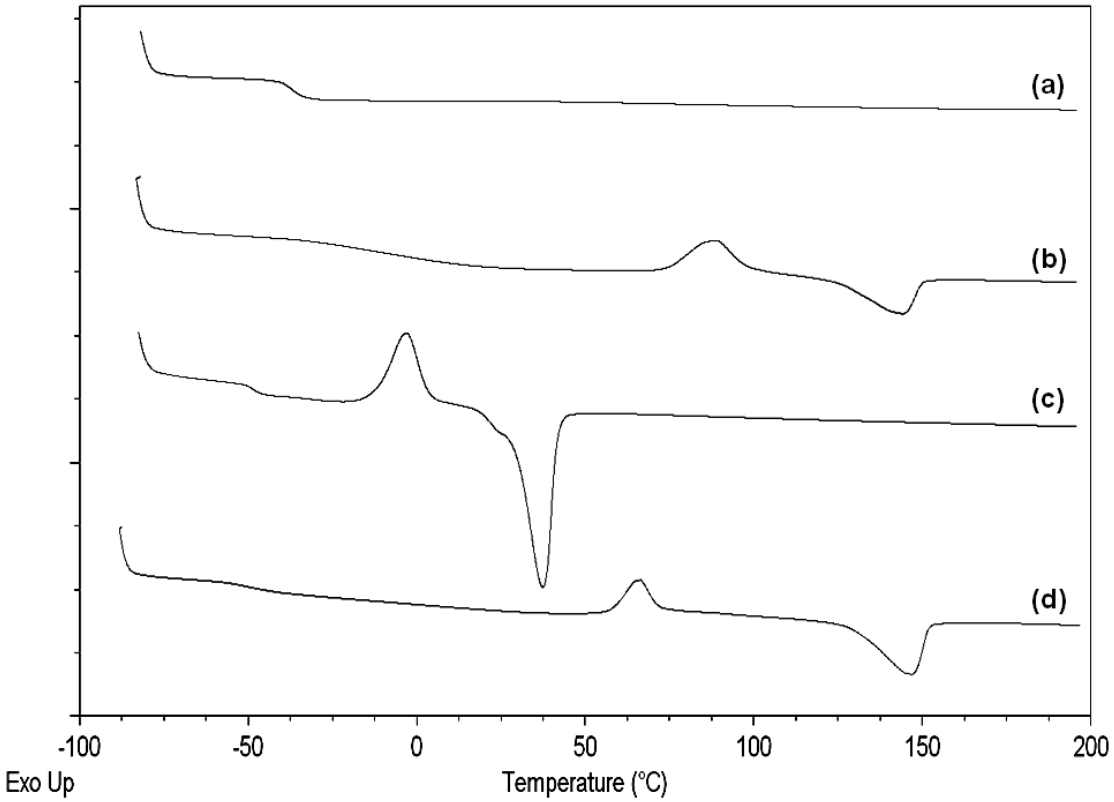

Figure 7.2 Comparison of DSC thermograms of various star-shaped copolymers: (a) **SA1**, (b) **SA3**, (c) **SB1**, and (d) **SB3**

In term of glass transition temperature (T_g), copolymers with a lower CL to TMC ratio have higher T_g (Figure 7.2). This result is expected as the T_g of PTMC (around -20^{o}C) is higher than PCL. Thus reducing the amount of PCL will increase its T_g. The experimental results show that only a single T_g observed in all copolymers' compositions. T_g of PLLA is not observed in the DSC either due to overlapping of the T_g of PLLA (40-60^{o}C) with the melting point of PCL or due to the low amount of PLLA inside the copolymer. This single T_g detection from DSC which is apparently between that of PCL and PTMC confirms our previous premise from ^{1}H NMR result that this star copolymer's soft block is a random copolymer [115].

Good mechanical properties (e.g. elasticity) of TPEs is possible to be achieved through physical cross-linking as it requires the phase separation of the hard and soft segments into separate domains [117]. As only single T_g is observed, it suggests that there is a lack of phase separation between the soft and hard segments which tells us the reason why most of the copolymers do not have significant elasticity.

As previously discussed, polymers with microcrystalline regions show higher elongations. Thus the experimental result is consistent in that the copolymers with CL:TMC ratio of 75:25 provide better mechanical properties than CL:TMC ratio of 50:50 as shown in Table 7.2. It appears that for both groups, there is a certain composition which yields a very good mechanical property. For CL:TMC 75:25, it was **SB2** (Figure 7.3b) with elongation of more than 980% which has molar mass of hard block close to half of the soft block molar mass according to Table 7.1. The rest of the copolymers in the group had lower elongations, between 250-300%. For copolymer with soft block of CL:TMC 50:50 the mechanical properties variation was even more extreme. Among the four copolymers, only **SA3** (Figure 7.3a) can be measured using the Instron machine and had a satisfactory elongation of 600%, while the rest were either too weak/sticky or too hard/brittle.

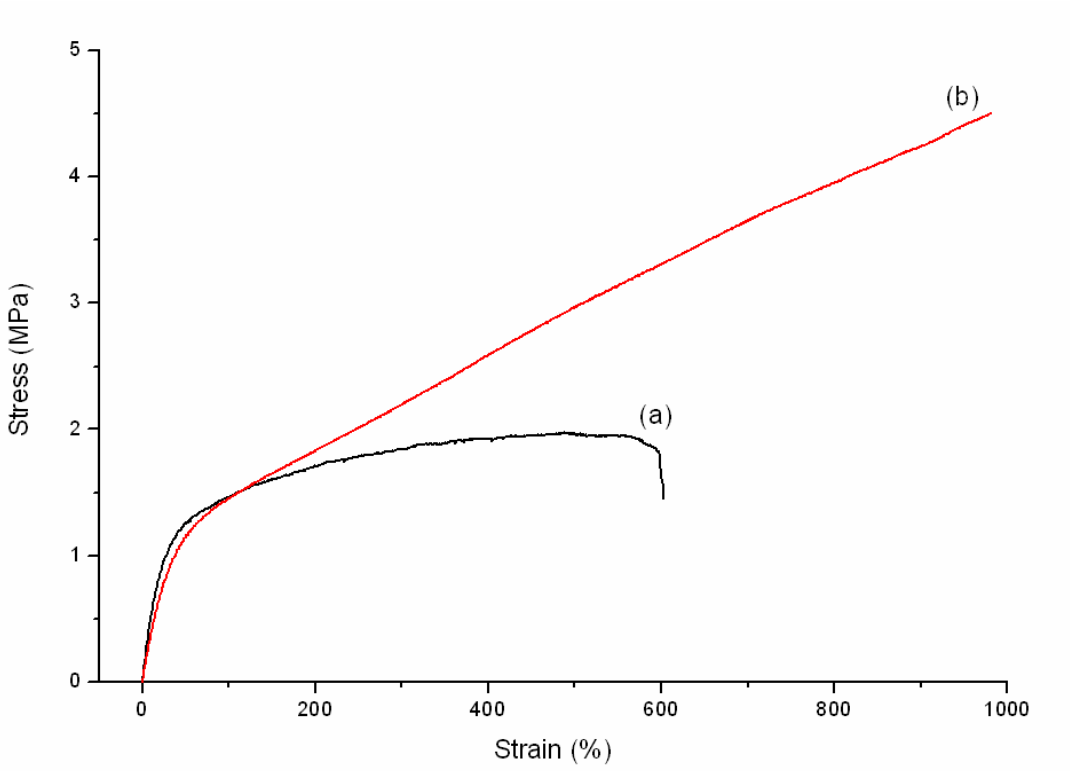

Figure 7.3 Stress-strain Curve of four armed star-shaped copolymers, (a) CL:TMC 50:50 **SA3**, (b) CL:TMC 75:25 **SB2**

PLLA is hard and brittle, while PCL and PTMC are tough [115]. Therefore, the star-shaped copolymers synthesized possessed mechanical properties that are roughly a combination of those of PLLA, PCL and PTMC. The elongations to break and the tensile strengths of the copolymers are dependent on the PLLA content in the copolymers. Copolymers with too high PLLA content are hard and brittle. This is because of the high T_g (and T_m) of the PLLA relative to the testing (ambient) temperature. On the other hand, those with low PLLA content are too weak. In this case, poor mechanical properties could be related to the absence of crystalline phases which act as physical cross-links.

Although there were only two copolymers with relatively good elongation, we can note one interesting feature: there was no yielding at all for both **SA3** and **SB2** in their stress-strain curves as we can see in Figure 7.3. Especially for **SB2** which has soft block of CL:TMC 75:25, this is a remarkable result since for their triblock counterpart, all triblock copolymers with soft block of CL:TMC 75:25 will still show a small degree of yielding. The absence of yield point will show that these two copolymers have a good recovery property which will be discussed in the next section.

7.3 Elastomeric Properties

From the previous discussion, we have seen that there are a few star-shaped copolymers synthesized which have good mechanical properties. To further characterize their properties in term of elasticity, cyclic test was performed. Two samples (**SA3** and **SB2**) were tested and both samples were chosen based on their ability to reach a high elongation.

Figure 7.4 below shows the cyclic test results, we can observe that for starblock **SA3**, the instantaneous recovery after 100%, 200%, and 300% elongation was 79%, 77%, and 73% while for starblock **SB2**, the instantaneous recovery after 100%, 200%, and 300% elongation was 81%, 68%, and 66%, respectively. Compared to the triblock copolymers, whereby generally triblocks with soft block of CL:TMC 50:50 have better recovery properties than CL:TMC 75:25, we can see here that for the starblock copolymer, **SB2** with soft block CL:TMC 75:25 managed to have a better recovery

property after 100% elongation. This could be due to the thermal properties of both starblocks. Starblock **SB2** with a much lower T_g of -50 °C will have a more flexible chains which allow it to recover better. However it also has a lower T_m and crystallinity compared to starblock **SA3** which cause it to be less recoverable at higher elongations, where the PLLA hard block starts to play the role as anchoring points.

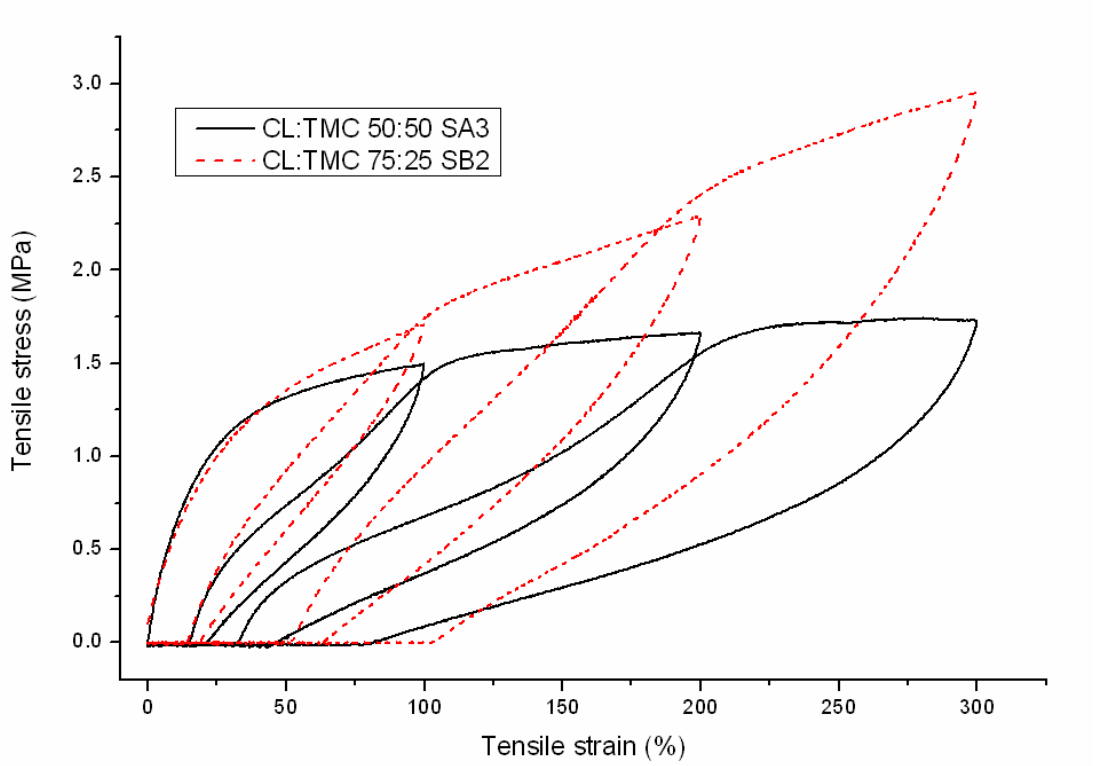

Figure 7.4 Cyclic testing on two star block copolymers, CL:TMC 50:50 **SA3** and CL:TMC 75:25 **SB2.**

7.4 Summary

In this chapter, another interesting copolymer system was explored, a branched BTPE based on copolymers of poly(CL-*co*-TMC) as soft block and PLLA as hard block were synthesized by ring opening polymerization using $SnOct_2$ catalyst and

pentaerythritol as initiator. The soft block poly(CL-*co*-TMC) was randomly polymerized and the molar ratio of the reacting monomers in these star-shaped copolymers was quite well controlled. Molar mass plays a significant role in determining the polymer's property. The molecular structures, thermal properties, as well as mechanical properties of the star-shaped copolymers changed considerably with composition. The mechanical properties of the star-shaped copolymers were determined by molar ratio of CL and TMC. Elastic properties were determined by the amount of microcrystalline regions present in the soft block as well as the amount of hard block in the composition.

Chapter 8 Conclusions and Recommendations

8.1 Conclusions

From *Chapter 1*, it was understood that intensive research for biodegradable thermoplastic elastomers has just started recently and there are not many commercial elastomeric biodegradable/biocompatible materials in the market today. Most of currently available biodegradable thermoplastic elastomers are polyurethanes, which contain urethane (OCONH) linkages. These versatile polymers have been used as implant materials for over 20 years but when they biodegrade in the body, the diamines produced are highly toxic. Synthesizing BTPE using a triblock copolymer made of biodegradable monomer will eliminate this problem.

Many research groups have claimed to have synthesized elastomeric biodegradable triblock copolymers, but their definition of elastomeric revolved only on a large elongations. Many of these have relied on high elongations only to claim elastomeric character; this can be misleading if the high elongations are attained through plastic deformations. For this reason, recovery measurements are essential to establishing true elastomeric behavior. Moreover, it is also important to measure recovery after both low and high elongations, or after both low and high imposed stresses. For example, some groups used only 50% elongations to measure the recovery properties, while others have applied long recovery period. Thus, the main goal of this thesis was

to synthesize copolymers with elastomeric properties and relate the range of elastomeric compositions to structure and properties.

8.1.1 Triblock Copolymer from CL, TMC, and L-lactide

We have shown that triblock copolymers of CL, TMC, and L-lactide exhibit thermoplastic elastomeric behavior when the middle segment is completely amorphous, and the overall polymer molar mass is reasonably high. These copolymers were synthesized by the ring-opening copolymerization, using stannous octoate as catalyst and propanediol as initiator. The ^{1}H NMR results showed that the molar ratios of the reacting monomers were preserved in the final polymer. The molecular structures, thermal properties, as well as the mechanical properties of the triblocks changed considerably with composition. Our study showed that the molar ratio of CL:TMC is the single most crucial parameter in determining the mechanical properties of the copolymers, along with the molar mass of the PLLA end blocks. At 50:50 CL:TMC ratio, the middle segment is amorphous, and this ratio gives a thermoplastic elastomer with good recovery values and elongations-to-break. As the CL:TMC ratio increases, the middle segment becomes more crystalline, increasing modulus and elongations-to-break, but decreasing recovery (or elastomeric character).

8.1.2 Effects of Having a Random Copolymer as Hard-Block

Retaining the same basic middle blocks of poly(CL-*co*-TMC) copolymer, the PLLA end-segment crystallinity was disrupted to examine its effect on elastomeric behavior. A series of triblock copolymers comprising end block of PLLA modified with PCL, and random copolymer of PCL and PTMC as soft segment were synthesized. DSC

data show that PCL disrupted the crystallinity of PLLA, making the hard block to be completely amorphous when the PCL content is 50%. Correspondingly, the addition of CL into PLLA block enhances the elongation of the triblock considerably. With regards to the elasticity, however, creep test results show that adding CL to PLLA block seems to reduce the "equilibrium" recovery, while cyclic test results shows that the instantaneous recovery increased significantly with more CL inside PLLA block. It was also observed that the degradation rate of triblock with added CL inside the PLLA was slower compared to triblock with pure PLLA hard block. This can be simply caused by the fact that PCL has a slower degradation rate compared to PLLA in general.

8.1.3 Deformation Induced Elasticity

The increase in elasticity for triblock copolymers with PCL inside PLLA hard block has led us to do a more thorough characterization of these copolymers. DSC and WAXD results allow concluding that PLLA crystallization is restricted by the presence of PCL segment chains in the hard segment. Furthermore, it has also been demonstrated by AFM that these triblock copolymers show more extensive phase separation and morphology of PLLA hard domain changes when the hard segment PCL content increases. Interestingly, it was found that although the recovery after the first elongation is low, the recovery increases during subsequent cycles (hence the name, "deformation-induced elasticity"). This phenomenon has been observed also with another copolymer [139], although its origins were not rationalized. Using WAXD and orientation measurements, we were able to relate the DIE effect to the influence of the PCL crystallinity and orientation changes with addition of PCL to the end-block.

8.1.4 Starblock Copolymer of CL, TMC, and LLA

Another interesting copolymer system was also explored, a branched BTPE based on copolymers of poly(CL-*co*-TMC) as soft block and PLLA as hard block were synthesized by ring opening polymerization using $SnOct_2$ catalyst and pentaerythritol as initiator. The soft block poly(CL-*co*-TMC) was randomly polymerized and the molar ratio of the reacting monomers in these star-shaped copolymers was quite well controlled. Molar mass plays a significant role in determining the polymer's property. The molecular structures, thermal properties, as well as mechanical properties of the star-shaped copolymers changed considerably with composition. The mechanical properties of the star-shaped copolymers were determined by molar ratio of CL and TMC. Elastic properties were determined by the amount of microcrystalline regions present in the soft block as well as the amount of hard block in the composition.

8.1.5 Comparison of all the Elastomeric Copolymers

Table 8.1 Properties of various elastomeric copolymers sorted by their recovery value

Polymer	molar ratio[a] CL:TMC:LLA	M_n[b] ($g \cdot mol^{-1}$)	T_g (°C)	T_m (°C)	ΔH (J/g)	Max Strain, ε_b (%)	Instant Recovery[c] (%)
D2	1 : 0.77 : 1.07	44500	-48	139	11	914	83
A4	1 : 0.85 : 0.66	43600	-47	140	8.4	421	82
E4	1 : 0.18 : 0.33	40300	-49	43	20.8	>1200	81
SB2	1 : 0.30 : 0.37	42900	-51	128	5.7	> 980	81
SA3	1 : 0.94 : 1.28	29700	-34	144	13.9	603	79
E3	1 : 0.23 : 0.48	40300	-51	36 125	25.3 4.4	>1200	77

B3	1 : 0.25 : 1.03	41600	-55	33 143	0.9 14.4	812	77
D1	1 : 0.83 : 1.35	49200	-49	149	19.1	520	77
E2	1 : 0.26 : 0.70	50500	-55	32 146	13.1 12.4	934	74
E1	1 : 0.28 : 0.85	56100	-57	31 153	8.1 12.8	1084	60

[a] Determined by ^{1}H NMR analysis

[b] Obtained by SEC analysis

[c] Measured by Instron after 100% elongation

A few trends and conclusions may be stated based on Table 8.1:

1. The three types of triblock (i.e. random poly(CL-*co*-TMC) mid-block with PLLA end-block; the poly(CL-*co*-TMC) midblock with poly(LLA-*co*-CL) end block; and the starblock copolymer with poly(CL-*co*-TMC) midblock and PLLA end segments) all show good recovery over certain composition ranges; hence it was possible to make elastomers from these three copolymer types.
2. Although these are all elastomeric, the elongations-to-break do vary with polymer type. Specifically, it appears that using a randomized PLLA end-block enhances total elongation to break.
3. It is also clear that while an amorphous mid-segment is generally preferred for elastomeric character, a certain amount of crystallinity does not reduce elastomeric character.

These points are elaborated further below.

Looking at Table 8.1, we can see some of the copolymers sorted by their recovery percentage after 100% elongations, starting from the highest value. There are a few parameters that can affect the recovery percentage of the triblocks, but we believe that

the composition of the copolymers is the most important parameter. The best two copolymers, **D2** and **A4** have a targeted soft block of CL:TMC 50:50, which means the soft block is completely amorphous. On the other hand, starblock **SA3** and triblock **D1** both have targeted soft block CL:TMC 50:50 but their high PLLA content has restricted their recovery values to be lower than **D2** and **A4**.

The structure of the copolymer will also play a role in determining the property of a copolymer. A triblock with pure PLLA end-block will have a different property from triblock with end-block made of PLLA and PCL. Two copolymers with the same composition will have completely different properties if one is a triblock and the other is a starblock. Examples of these can be seen in the following discussion.

In the case of triblock **E4**, it manages to have a good recovery value despite of having middle block of CL:TMC 75:25 which has T_m of 42.7 °C and ΔH of 20.8 J/g. This is due to the end-block which is made of PLLA plus 50% PCL, resulting in a completely amorphous end-block. It is highly possible that this amorphous end-block enhanced the elasticity of the triblock while the semi-crystalline middle block helps to maintain the anchoring point during deformation.

Starblock **SB2** also manages to get a good recovery, although having a middle block of CL:TMC 75:25. From Table 8.1 it can be seen that there is no T_m of the middle block, whereby random copolymer of CL:TMC 75:25 is supposed to be semi-crystalline. The hypothesis is that due to its unique four-armed structure, the high density of PLLA crystals are hindering the formation of PCL crystal in the middle

block. This was supported by the fact that when the PLLA content is low, the middle block is still semi-crystalline (Table 7.2, *Chapter 7*).

Molar mass are also a parameter which affect the elastomeric properties. It is more related to the mechanical properties (e.g. elongations, tensile stress, and modulus) of the copolymer rather than the recovery value. For every copolymer synthesized, there will be a minimum molar mass requirement that has to be fulfilled in order for the copolymer to have a good mechanical property. Table 8.1 shows that almost all copolymers are having molar mass above 40000 $g \cdot mol^{-1}$. The only exception is starblock **SA3**, which again due to the four-armed structure manage to have a good elongation and recovery value. For comparison, triblock **A6** from *Chapter 4* is a triblock with similar composition and molar mass compared to **SA3**, but its elongation is only 60%.

8.2 Recommendations

8.2.1 Polymerization Conditions

In order to keep transesterification reaction at minimum, an inert atmosphere for polymerization is very important. Although we have tried our best to keep it as little as possible, the method used for synthesis in this work caused the polymerization mixture to get into contact with surrounding air, especially during the second block monomer addition. One way to completely prevent contact with surrounding atmosphere is to do the whole synthesis process inside a glove-box filled with inert gas.

8.2.2 Kinetics of Polymerization

A lot of parameters affect the polymerization results. In this work, some of the parameters like synthesis temperature and time, monomer concentration, catalyst amount are fixed for all the synthesis. In reality, there should be an optimum value for each of these parameters for different copolymers. In order to find those optimum values, a kinetic study of the polymerization should be done for the direct copolymerizations, whether it is the PLLA-b-poly(CL-co-TMC)-b-PLLA, the poly(LLA-*co*-CL)-*b*-poly(CL-*co*-TMC)-*b*-poly(LLA-*co*-CL), or the PLLA-*b*-poly(CL-*co*-TMC) starblock copolymers. By knowing the kinetics of these polymerizations, problem such as transesterification can be eliminated.

8.2.3 Ring Opening Polymerization of Other Monomers

The monomer combinations in this work are limited to CL, TMC, and LLA. There are still many biodegradable monomers that have potential as good thermoplastic elastomer. For example, instead of TMC with T_g of -20 °C, γ-butyrolactone with T_g of around -50 °C will make a better combination with PCL to be used as soft block. The problem now lies on the requirement of extreme synthesis conditions (20,000 atm and 165 °C) to polymerize γ-butyrolactone [155]. A more thorough research is needed in order to establish a way to polymerize γ-butyrolactone using an easier method such as by finding a suitable combination of catalyst and initiator.

8.2.4 Starblock Copolymers

Our study on starblock copolymer in this thesis has shown that this structure has a potential as a good BTPE candidate. More work has to be done in order to understand how different structure will affect the morphological, thermal, and mechanical properties of the copolymer by much. And it seems that due to the different structure from triblock, the optimum composition for triblock might not be the same for starblock. Furthermore, there are still different structures of starblock e.g. four-armed, three-armed, etc. Each of these structures is expected to give different properties.

8.2.5 Biocompatibility Study

The monomers used in this work, CL, TMC, and LLA have been used in biomedical field for quite some time now, and the copolymers of poly(CL-co-TMC), poly(CL-co-LLA), and poly(TMC-co-LLA) have also been investigated in vitro as well as in vivo and proven to be biocompatible and bioresorbable [156-158], especially for poly(CL-co-TMC) which exhibited the lowest degree of activation with few adhered platelets in haemo- and cyto-compatibility test [159]. There is hardly any reason why the triblock and the starblock copolymers of CL, TMC, and LLA will not show the same biocompatibility. Nevertheless, biocompatibility studies, accompanied by extensive biodegradation study can be done to confirm the viability of these BTPEs to be used as implantable biomedical devices.

References

[1] http://en.wikipedia.org/wiki/Elastomer.

[2] Odian G. Principles of Polymerization. 4th ed. Hoboken: John Wiley & Sons, Inc.; 2004.

[3] World Thermoplastic Elastomers, Industry Study with Forecasts for 2011 & 2016. The Freedonia Group; 2007.

[4] Ameduri B, Boutevin B. Update on fluoroelastomers: from perfluoroelastomers to fluorosilicones and fluorophosphazenes. Journal of Fluorine Chemistry 2005;126:221-9.

[5] Van der Mee L, Helmich F, de Bruijn R, Vekemans J, Palmans ARA, Meijer EW. Investigation of lipase-catalyzed ring-opening polymerizations of lactones with various ring sizes: Kinetic evaluation. Macromolecules 2006;39:5021-7.

[6] Amsden B. Curable, biodegradable elastomers: emerging biomaterials for drug delivery and tissue engineering. Soft Matter 2007;3:1335-48.

[7] Harris LG, Gorna K, Gogolewski S, Richards RG. Biodegradable polyurethane cytocompatibility to fibroblasts and staphylococci. J Biomed Mater Res Part A 2006;77A:304-12.

[8] Amsden B, Cheng YL. A Generic Protein Delivery System Based on Osmotically Rupturable Monoliths. J Control Release 1995;33:99-105.

[9] Gu F, Neufeld R, Amsden B. Sustained release of bioactive therapeutic proteins from a biodegradable elastomeric device. J Control Release 2007;117:80-9.

[10] Stegemann JP, Nerem RM. Phenotype modulation in vascular tissue engineering using biochemical and mechanical stimulation. Ann Biomed Eng 2003;31:391-402.

[11] Monson KL, Goldsmith W, Barbaro NM, Manley GT. Axial mechanical properties of fresh human cerebral blood vessels. J Biomech Eng-Trans ASME 2003;125:288-94.

[12] Tuominen J, Kylma J, Kapanen A, Venelampi O, Itavaara M, Seppala J. Biodegradation of lactic acid based polymers under controlled composting conditions and evaluation of the ecotoxicological impact. Biomacromolecules 2002;3:445-55.

[13] http://en.wikipedia.org/wiki/Thermoplastic_elastomer.

[14] Bonart R. Thermoplastic Elastomers. Polymer 1979;20:1389-403.

[15] Grady BP, Cooper SL. Thermoplastic Elastomers. In: James EM, Burak E, Frederick RE, editors. Science and Technology of Rubber (Third Edition). Burlington: Academic Press; 2005. p. 555-617.

[16] Calmon-Decriaud A, Bellon-Maurel V, Silvestre F. Standard Methods for Testing the Aerobic Biodegradation of Polymeric Materials. Review and Perspectives. In: Bellon-Maurel V, Calmon-Decriaud A, Chandrasekhar V, Hadjichristidis N, Mays J, Pispas S, et al., editors. Blockcopolymers - Polyelectrolytes - Biodegradation: Springer Berlin / Heidelberg; 1998. p. 207-26.

[17] Nayak PL. Natural oil-based polymers: Opportunities and challenges. J Macromol Sci-Rev Macromol Chem Phys 2000;C40:1-21.

[18] Siepmann J, Gopferich A. Mathematical modeling of bioerodible, polymeric drug delivery systems. Adv Drug Deliv Rev 2001;48:229-47.

[19] Coury AJ, Levy RJ, Ratner BD, Schoen FJ, Williams DF, Williams RL. Degradation of Materials in the Biological Environment. In: Ratner BD, Hoffman AS, Schoen FJ, Lemons JE, editors. Biomaterials Science, 2nd Edition: An Introduction to Materials in Medicine. San Diego: Academic Press; 2004. p. 243-81.

[20] Pol BJM, vanWachem PB, vanderDoes L, Bantjes A. In vivo testing of crosslinked polyethers .2. Weight loss, IR analysis, and swelling behavior after implantation. J Biomed Mater Res 1996;32:321-31.

[21] Tabata Y, Ikada Y. Phagocytosis of polymeric microspheres. In: Szycher M, editor. High Performance Biomaterials. Lancaster: Technomic Publishing Co Inc; 1991. p. 621-46.

[22] Salthouse TN. Cellular enzyme activity at the polymer–tissue interface: A review. J Biomed Mater Res 1976;10:197-229.

[23] Babior BM. Oxygen-Dependent Microbial Killing by Phagocytes .2. N Engl J Med 1978;298:721-5.

[24] Johnston RB. Oxygen-Metabolism And Microbicidal Activity of Macrophages. Federation Proceedings 1978;37:2759-64.

[25] Pitt CG, Chasalow FI, Hibionada YM, Klimas DM, Schindler A. Alipathic Polyesters .1. The Degradation of Poly(Epsilon-Caprolactone) Invivo. Journal of Applied Polymer Science 1981;26:3779-87.

[26] Benedict CV, Cameron JA, Huang SJ. Polycaprolactone Degradation by Mixed and Pure Cultures of Bacteria and a Yeast. Journal of Applied Polymer Science 1983;28:335-42.

[27] Albertsson AC, Edlund U. Novel release systems from biodegradable polymers. Abstr Pap Am Chem Soc 1998;216:044-POLY.

[28] Albertsson A, Varma I. Aliphatic polyesters. In: Doi Y, Steinbüchel A, editors. Biopolymers, Volume 4, Polyesters III - Applications and Commercial Products. Weinheim: Wiley-VCH; 2002. p. 25-52.

[29] Hakkarainen M, Albertsson AC, Karlsson S. Weight losses and molecular weight changes correlated with the evolution of hydroxyacids in simulated in vivo degradation of homo- and copolymers of PLA and PGA. Polymer Degradation and Stability 1996;52:283-91.

[30] Zhu KJ, Hendren RW, Jensen K, Pitt CG. Synthesis, Properties, and Biodegradation of Poly(1,3-trimethylene carbonate). Macromolecules 1991;24:1736-40.

[31] Albertsson AC, Eklund M. Influence of Molecular-Structure on the Degradation Mechanism of Degradable Polymers - In-Vitro Degradation of Poly(Trimethylene Carbonate), Poly(Trimethylene Carbonate-co-Caprolactone), and Poly(Adipic Anhydride). Journal of Applied Polymer Science 1995;57:87-103.

[32] Natta FJv, Hill JW, Carothers WH. Studies of Polymerization and Ring Formation. XXIII.1 ε-Caprolactone and its Polymers. Journal of the American Chemical Society 1934;56:455-7.

[33] Carothers WH, Dorough GL, Natta FJv. Studies of Polymerization and Ring Formation. X. The Reversible Polymerization of Six-Membered Cyclic Esters. Journal of the American Chemical Society 1932;54:761-72.

[34] Carothers WH, Van Natta FJ. Studies on polymerization and ring formation. III. Glycol esters of carbonic acid. Journal of the American Chemical Society 1930;52:314-26.

[35] Kricheldorf HR, Kreisersaunders I, Boettcher C. Polylactones .31. Sn(II)Octoate-Inititated Polymerization of L-lactide - A Mechanistic Study. Polymer 1995;36:1253-9.

[36] Duda A, Penczek S. Determination of the Absolute Propagation Rate Constants in Polymerization with Reversible Aggregation of Active Centers. Macromolecules 1994;27:4867-70.

[37] Degee P, Dubois P, Jerome R. Bulk polymerization of lactides initiated by aluminium isopropoxide .3. Thermal stability and viscoelastic properties. Macromolecular Chemistry and Physics 1997;198:1985-95.

[38] Jerome R, Henrioullegranville M, Boutevin B, Robin JJ. Telechelic Polymers - Synthesis, Characterization and Applications. Prog Polym Sci 1991;16:837-906.

[39] Pitt CG, Zhong-wei G. Modification of the rates of chain cleavage of poly([epsilon]-caprolactone) and related polyesters in the solid state. J Control Release 1987;4:283-92.

[40] Sosnowski S, Gadzinowski M, Slomkowski S. Poly(L,L-lactide) microspheres by ring-opening polymerization. Macromolecules 1996;29:4556-64.

[41] Gadzinowski M, Sosnowski S, Slomkowski S. Kinetics of the dispersion ring-opening polymerization of epsilon-caprolactone initiated with diethylaluminum ethoxide. Macromolecules 1996;29:6404-7.

[42] Dijkstra PJ, Du H, Feijen J. Single site catalysts for stereoselective ring-opening polymerization of lactides. Polymer Chemistry 2011;2:520-7.

[43] Brode GL, Koleske JV. Lactone polymerization and polymer properties. Journal of Macromolecular Science-Chemistry 1972;A 6:1109-44.

[44] Johns DB, Lenz RW, Luecke A. Lactones. In: Ivin KJ, Saegusa T, editors. Ring Opening Polymerization. London: Elsevier; 1984. p. 464.

[45] Kricheldorf HR, KreiserSaunders I. Polylactides - Synthesis, characterization and medical application. Macromol Symp 1996;103:85-102.

[46] Lofgren A, Albertsson AC, Dubois P, Jerome R. Recent advances in ring-opening polymerization of lactones and related-compounds. J Macromol Sci-Rev Macromol Chem Phys 1995;C35:379-418.

[47] Mecerreyes D, Jerome R, Dubois P. Novel macromolecular architectures based on aliphatic polyesters: Relevance of the "coordination-insertion" ring-opening polymerization. Macromolecular Architectures. Berlin: Springer-Verlag Berlin; 1999. p. 1-59.

[48] Saegusa T, Kobayashi S, Hayashi K. Polymerization via zwitterion 171 alternating co-polymerization of 2-phenylimino-1,3-dioxolane with beta-propiolactone. Macromolecules 1978;11:360-1.

[49] Bero M, Czapla B, Dobrzynski P, Janeczek H, Kasperczyk J. Copolymerization of glycolide and epsilon-caprolactone - 2 - Random copolymerization in the presence of tin octoate. Macromolecular Chemistry and Physics 1999;200:911-6.

[50] Duda A, Florjanczyk Z, Hofman A, Slomkowski S, Penczek S. Living pseudoanionic polymerization of epsilon-caprolactone - poly(epsilon-caprolactone) free of cyclics and with controlled end groups. Macromolecules 1990;23:1640-6.

[51] Kowalski A, Duda A, Penczek S. Polymerization of L,L-lactide initiated by aluminum isopropoxide trimer or tetramer. Macromolecules 1998;31:2114-22.

[52] Gilding DK, Reed AM. Biodegradable polymers for use in surgery - polyglycolic-poly(actic acid) homopolymers and copolymers .1. Polymer 1979;20:1459-64.

[53] Grijpma DW, Pennings AJ. Polymerization temperature effects on the properties of l-lactide and epsilon-caprolactone copolymers. Polymer Bulletin 1991;25:335-41.

[54] Dubois P, Ropson N, Jerome R, Teyssie P. Macromolecular engineering of polylactones and polylactides .19. Kinetics of ring-opening polymerization of epsilon-caprolactone initiated with functional aluminum alkoxides. Macromolecules 1996;29:1965-75.

[55] Kricheldorf HR, Berl M, Scharnagl N. Poly(lactones) .9. Polymerization mechanism of metal alkoxide initiated polymerizations of lactide and various lactones. Macromolecules 1988;21:286-93.

[56] Bero M, Kasperczyk J. Coordination polymerization of lactides .5. Influence of lactide structure on the transesterification processes in the copolymerization with epsilon-caprolactone. Macromolecular Chemistry and Physics 1996;197:3251-8.

[57] Veld P, Velner EM, VanDeWitte P, Hamhuis J, Dijkstra PJ, Feijen J. Melt block copolymerization of epsilon-caprolactone and L-lactide. Journal of Polymer Science Part a-Polymer Chemistry 1997;35:219-26.

[58] Lundberg RD, Cox EF. Lactones. In: Frish K, Reegen S, editors. Ring Opening Polymerization. New York: Marcell Dekker; 1969. p. 247.

[59] Ovitt TM, Coates GW. Stereoselective ring-opening polymerization of meso-lactide: Synthesis of syndiotactic poly(lactic acid). Journal of the American Chemical Society 1999;121:4072-3.

[60] Spassky N, Wisniewski M, Pluta C, LeBorgne A. Highly stereoelective polymerization of rac-(D,L)-lactide with a chiral Schiff's base/aluminium alkoxide initiator. Macromolecular Chemistry and Physics 1996;197:2627-37.

[61] Albertsson AC, Gruvegard M. Degradable high-molecular-weight random copolymers, based on epsilon-caprolactone and 1,5-dioxepan-2-one, with non-crystallizable units inserted in the crystalline-structure. Polymer 1995;36:1009-16.

[62] Albertsson AC, Lofgren A. Synthesis and characterization of poly(1,5-dioxepan-2-one-co-L-lactic acid) and poly(1,5-dioxepan-2-one-co-D,L-lactic acid) Journal of Macromolecular Science-Pure and Applied Chemistry 1995;A32:41-59.

[63] Dahlmann J, Rafler G, Fechner K, Mehlis B. Synthesis and properties of biodegradable aliphatic polyesters. British Polymer Journal 1990;23:235-40.

[64] Grijpma DW, Zondervan GJ, Pennings AJ. High molecular weight copolymers of L-lactide and epsilon-caprolactone as biodegradable elastomeric implant materials. Polymer Bulletin 1991;25:327-33.

[65] Kricheldorf HR, Meierhaack J. Polylactones, 22 ABA triblock copolymers of L-lactide and poly(ethylene glycol). Makromolekulare Chemie-Macromolecular Chemistry and Physics 1993;194:715-25.

[66] Kowalski A, Duda A, Penczek S. Kinetics and mechanism of cyclic esters polymerization initiated with tin(II) octoate, 1 Polymerization of epsilon-caprolactone. Macromolecular Rapid Communications 1998;19:567-72.

[67] Schwach G, Coudane J, Engel R, Vert M. More about the polymerization of lactides in the presence of stannous octoate. Journal of Polymer Science Part a-Polymer Chemistry 1997;35:3431-40.

[68] Kowalski A, Duda A, Penczek S. Mechanism of cyclic ester polymerization initiated with tin(II) octoate. 2. Macromolecules fitted with tin(II) alkoxide species observed directly in MALDI-TOF spectra. Macromolecules 2000;33:689-95.

[69] Kowalski A, Duda A, Penczek S. Kinetics and mechanism of cyclic esters polymerization initiated with tin(II) octoate. 3. Polymerization of L,L-dilactide. Macromolecules 2000;33:7359-70.

[70] Kricheldorf HR, Kreiser-Saunders I, Stricker A. Polylactones 48. SnOct(2)-initiated polymerizations of lactide: A mechanistic study. Macromolecules 2000;33:702-9.

[71] Ryner M, Stridsberg K, Albertsson AC, von Schenck H, Svensson M. Mechanism of ring-opening polymerization of 1,5-dioxepan-2-one and L-lactide with stannous 2-ethylhexanoate. A theoretical study. Macromolecules 2001;34:3877-81.

[72] Anneaux BL, Carpenter KA, Greene DD, Taylor MS, Shalaby M, Linden DE, et al. Effect of composition on physical properties of segmented copolylactides and BSR of suture braids therefrom. Trans Soc Biomater2003. p. 231.

[73] Mares F, Boyle Jr. WJ, Tang RT, Patel KM, Kotliar AM, Chiu T-h Polycarbonate-based block copolymers and devices. U.S. Patent 5531998, Jul 2, 1996.

[74] Shalaby SW High strength fibers of l-lactide copolymers, e-caprolactone, and trimethylene carbonate and absorbable medical constructs thereof. U.S. Patent 7192437, Mar 20, 2007.

[75] Kim YH, Kim SH, Park KD, Lee S-h Biodegradable triblock copolymers and process for their preparation. U.S. Patent 6476156, 2002.

[76] Boethling RS, Sommer E, DiFiore D. Designing small molecules for biodegradability. Chemical Reviews 2007;107:2207-27.

[77] Considine WJ. Organotin chemistry : VIII. The reaction of dibutyltin oxide with vic-glycols. Journal of Organometallic Chemistry 1966;5:263-6.

[78] Mehrotra RC, Gupta VD. Preparation and properties of some organotin compounds : I. Dibutyltin glycolates. Journal of Organometallic Chemistry 1965;4:145-50.

[79] Kricheldorf HR, Boettcher C, Tonnes KU. Polylactones .23. Polymerization of racemic and meso d,l-lactide with various organotin catalysts stereochemical aspects. Polymer 1992;33:2817-24.

[80] Ouhadi T, Stevens C, Teyssié P. Mechanism of ε-Caprolactone polymerization by Aluminum Alkoxides. Die Makromolekulare Chemie 1975;1:191-201.

[81] Dubois P, Jacobs C, Jerome R, Teyssie P. Macromolecular engineering of polylactones and polylactides .4. Mechanism and kinetics of lactide homopolymerization by aluminum isopropoxide. Macromolecules 1991;24:2266-70.

[82] Bero M, Kasperczyk J, Jedlinski ZJ. Coordination polymerization of lactides .1. Structure determination of obtained polymers. Makromolekulare Chemie-Macromolecular Chemistry and Physics 1990;191:2287-96.

[83] Lofgren A, Albertsson AC, Dubois P, Jerome R, Teyssie P. Synthesis and characterization of biodegradable homopolymers and block-copolymers based on 1,5-dioxepan-2-one. Macromolecules 1994;27:5556-62.

[84] Lofgren A, Renstad R, Albertsson AC. Synthesis and characterization of a new degradable thermoplastic elastomer based on 1,5-dioxepan-2-one and epsilon-caprolactone. Journal of Applied Polymer Science 1995;55:1589-600.

[85] Mclain SJH, DE), Drysdale, Neville E. (Newark, DE) Yttrium and rare earth compounds catalyzed lactone polymerization. 1991.

[86] Stevels WM, Dijkstra PJ, Feijen J. New initiators for the ring-opening polymerization of cyclic esters. Trends in Polymer Science 1997;5:300-5.

[87] Stevels WM, Ankone MJK, Dijkstra PJ, Feijen J. Kinetics and mechanism of L-lactide polymerization using two different yttrium alkoxides as initiators. Macromolecules 1996;29:6132-8.

[88] Crescenzi V, Manzini G, Calzolari G, Borri C. Thermodynamics of fusion of poly-[beta]-propiolactone and poly-[epsilon]-caprolactone. comparative analysis of the melting of aliphatic polylactone and polyester chains. European Polymer Journal 1972;8:449-63.

[89] Middleton JC, Tipton AJ. Synthetic Biodegradable Polymers as Medical Devices. Medical Plastics and Biomaterials Magazine1998.

[90] Goldberg D. A review of the biodegradability and utility of poly(caprolactone). J Environ Polym Degrad 1995;3:61-7.

[91] Serrano MC, Pagani R, Vallet-Regí M, Peña J, Rámila A, Izquierdo I, et al. In vitro biocompatibility assessment of poly([var epsilon]-caprolactone) films using L929 mouse fibroblasts. Biomaterials 2004;25:5603-11.

[92] Kim MS, Hyun H, Cho YH, Seo KS, Jang WY, Kim SK, et al. Preparation of methoxy poly(ethyleneglycol)-block-poly(caprolactone) via activated monomer mechanism and examination of micellar characterization. Polymer Bulletin 2005;55:149-56.

[93] Schindler A, Jeffcoat R, Kimmel G, Pitt C, Wall M, Zweidinger R. Biodegradable polymers for sustained drug delivery. In: Pearce E, Schaefgen J, editors. Contemporary Topics in Polymer Science. New York: Plenum; 1977. p. 251-89.

[94] Habraken W, Zhang Z, Wolke JGC, Grijpma DW, Mikos AG, Feijen J, et al. Introduction of enzymatically degradable poly(trimethylene carbonate) microspheres into an injectable calcium phosphate cement. Biomaterials 2008;29:2464-76.

[95] Takahashi Y, Kojima R. Crystal structure of poly(trimethylene carbonate). Macromolecules 2003;36:5139-43.

[96] Jia YT, Kim HY, Gong J, Lee DR, Ding B, Bhattarai N. Synthesis and characterization of ABA-type block copolymers of trimethylene carbonate and epsilon-caprolactone. Polym Int 2004;53:312-9.

[97] Leenslag JW, Pennings AJ. Synthesis of high-molecular-weight poly(l-lactide) initiated with tin 2-ethylhexanoate. Makromolekulare Chemie-Macromolecular Chemistry and Physics 1987;188:1809-14.

[98] Middleton JC, Tipton AJ. Synthetic biodegradable polymers as orthopedic devices. Biomaterials 2000;21:2335-46.

[99] Bergsma JE, de Bruijn WC, Rozema FR, Bos RRM, Boering G. Late degradation tissue response to poly(-lactide) bone plates and screws. Biomaterials 1995;16:25-31.

[100] Martin DP, Williams SF. Medical applications of poly-4-hydroxybutyrate: a strong flexible absorbable biomaterial. Biochemical Engineering Journal 2003;16:97-105.

[101] Kulkarni RK, Pani KC, Neuman C, Leonard F. Polylactic acid for surgical implants. Archives of Surgery 1966;93:839.

[102] Hepburn C. Polyurethane Elastomers. London: Elsevier Applied Science; 1982.

[103] Guan JJ, Wagner WR. Synthesis, characterization and cytocompatibility of polyurethaneurea elastomers with designed elastase sensitivity. Biomacromolecules 2005;6:2833-42.

[104] Lendlein A, Colussi M, Neuenschwander P, Suter UW. Hydrolytic degradation of phase-segregated multiblock copoly(ester urethane)s containing weak links. Macromolecular Chemistry and Physics 2001;202:2702-11.

[105] Skarja GA, Woodhouse KA. Structure-property relationships of degradable polyurethane elastomers containing an amino acid-based chain extender. Journal of Applied Polymer Science 2000;75:1522-34.

[106] Storey RF, Hickey TP. Degradable polyurethane networks based on d,l-lactide, glycolide, epsilon-caprolactone, and trimethylene carbonate homopolyester and copolyester triols. Polymer 1994;35:830-8.

[107] Spaans CJ, de Groot JH, Dekens FG, Pennings AJ. High molecular weight polyurethanes and a polyurethane urea based on 1,4-butanediisocyanate. Polymer Bulletin 1998;41:131-8.

[108] Guan JJ, Sacks MS, Beckman EJ, Wagner WR. Synthesis, characterization, and cytocompatibility of efastomeric, biodegradable poly(ester-urethane)ureas based on poly(caprolactone) and putrescine. J Biomed Mater Res 2002;61:493-503.

[109] Tabor CW, Tabor H. Polyamines. Annu Rev Biochem 1984;53:749-90.

[110] Yilgor E, Yilgor I. Hydrogen bonding: a critical parameter in designing silicone copolymers. Polymer 2001;42:7953-9.

[111] Zhang JY, Beckman EJ, Piesco NP, Agarwal S. A new peptide-based urethane polymer: synthesis, biodegradation, and potential to support cell growth in vitro. Biomaterials 2000;21:1247-58.

[112] Coleman MM, Sobkowiak M, Pehlert GJ, Painter PC, Iqbal T. Infrared temperature studies of a simple polyurea. Macromolecular Chemistry and Physics 1997;198:117-36.

[113] Guelcher SA, Gallagher KM, Didier JE, Klinedinst DB, Doctor JS, Goldstein AS, et al. Synthesis of biocompatible segmented polyurethanes from aliphatic diisocyanates and diurea diol chain extenders. Acta Biomaterialia 2005;1:471-84.

[114] Hassan MK, Mauritz KA, Storey RF, Wiggins JS. Biodegradable aliphatic thermoplastic polyurethane based on poly(epsilon-caprolactone) and L-lysine diisocyanate. Journal of Polymer Science Part a-Polymer Chemistry 2006;44:2990-3000.

[115] Qian HT, Bei JZ, Wang SG. Synthesis, characterization and degradation of ABA block copolymer of L-lactide and epsilon-caprolactone. Polymer Degradation and Stability 2000;68:423-9.

[116] Kim JH, Lee JH. Preparation and properties of poly(L-lactide)-block-poly(trimethylene carbonate) as biodegradable thermoplastic elastomer. Polymer Journal 2002;34:203-8.

[117] Zhang Z, Grijpma DW, Feijen J. Triblock copolymers based on 1,3-trimethylene carbonate and lactide as biodegradable thermoplastic elastomers. Macromolecular Chemistry and Physics 2004;205:867-75.

[118] Mizutani M, Arnold SC, Matsuda T. Liquid, phenylazide-end-capped copolymers of epsilon-caprolactone and trimethylene carbonate: Preparation, photocuring characteristics, and surface layering. Biomacromolecules 2002;3:668-75.

[119] Pego AP, Poot AA, Grijpma DW, Feijen J. Copolymers of trimethylene carbonate and epsilon-caprolactone for porous nerve guides: Synthesis and properties. Journal of Biomaterials Science-Polymer Edition 2001;12:35-53.

[120] Matsuda T, Mizutani M, Arnold SC. Molecular design of photocurable liquid biodegradable copolymers. 1. Synthesis and photocuring characteristics. Macromolecules 2000;33:795-800.

[121] Kricheldorf HR, Rost S. Biodegradable multiblock copolyesters prepared from epsilon-caprolactone, L-lactide, and trimethylene carbonate by means of bismuth hexanoate. Macromolecules 2005;38:8220-6.

[122] Graessley WW. Viscosity and Flow in Polymer Melts and Concentrated Solutions. In: Mark JE, Eisenberg A, Graessley WW, Mandelkern L, Samulski ET, Koenig JL, et al., editors. Physical Properties of Polymers. 1st ed. Washington DC: American Chemical Society; 1984. p. 97-143.

[123] Jamshidi K, Hyon SH, Ikada Y. Thermal characterization of polylactides. Polymer 1988;29:2229-34.

[124] Puig CC, Odell JA, Hill MJ, Barham PJ, Folkes MJ. A comparison of blends of linear with branched polyethylenes prepared by melt mixing and by solution blending. Polymer 1994;35:2452-7.

[125] Kim SH, Han YK, Ahn KD, Kim YH, Chang T. Preparation of star-shaped polylactide with pentaerythritol and stannous octoate. Makromolekulare Chemie-Macromolecular Chemistry and Physics 1993;194:3229-36.

[126] Kim SH, Han YK, Kim YH, Hong SI. Multifunctional initiation of lactide polymerization by stannous octoate pentaerythritol. Makromolekulare Chemie-Macromolecular Chemistry and Physics 1992;193:1623-31.

[127] Argade AB, Peppas NA. Preparation and characterization of novel biodegradable triacrylate and tetraacrylate intermediates. Polymer Bulletin 1993;31:401-7.

[128] Dong CM, Qiu KY, Cu ZW, Feng XD. Synthesis of star-shapee poly(epsilon-caprolactone)-b-poly(DL-lactic acid-alt-glycolic acid) with multifunctional initiator and stannous octoate catalyst. Macromolecules 2001;34:4691-6.

[129] Joziasse CAP, Grablowitz H, Pennings AJ. Star-shaped poly (trimethylene carbonate)-co-(epsilon-caprolactone) and its block copolymers with lactide/glycolide: synthesis, characterization and properties. Macromolecular Chemistry and Physics 2000;201:107-12.

[130] Wong YS, Stachurski ZH, Venkatraman SS. Orientation and structure development in poly(lactide) under uniaxial deformation. Acta Materialia 2008;56:5083-90.

[131] Zhang YB, Leblanc-Boily V, Zhao Y, Prud'homme RE. Wide angle X-ray diffraction investigation of crystal orientation in miscible blend of poly(epsilon-caprolactone)/poly(vinyl chloride) crystallized under strain. Polymer 2005;46:8141-50.

[132] Albertsson AC, Eklund M. Synthesis of copolymers of 1,3-dioxan-2-one and oxepan-2-one using coordination catalysts. Journal of Polymer Science Part a-Polymer Chemistry 1994;32:265-79.

[133] Lipik VT, Widjaja LK, Liow SS, Abadie MJM, Venkatraman SS. Effects of transesterification and degradation on properties and structure of polycaprolactone-polylactide copolymers. Polymer Degradation and Stability 2010;95:2596-602.

[134] Jia YT, Shen XY, Gu XH, Dong J, Mu CX, Zhang YQ. Synthesis and characterization of tercopolymers derived from epsilon-caprolactone, trimethylene carbonate, and lactide. Polymers for Advanced Technologies 2008;19:159-66.

[135] Vasanthakumari R, Pennings AJ. Crystallization kinetics of poly(l-lactic acid). Polymer 1983;24:175-8.

[136] Fox TG. Bulletin of American Physical Society 1956;1:123.

[137] Pochan JM, Beatty CL, Pochan DF. Different approach for the correlation of the tg of mixed amorphous systems. Polymer 1979;20:879-86.

[138] Kong JF, Lipik V, Abadie MJM, Deen GR, Venkatraman SS. Biodegradable elastomers based on ABA triblocks: influence of end-block crystallinity on elastomeric character. Polym Int 2011:n/a-n/a.

[139] Andronova N, Albertsson AC. Resilient bioresorbable copolymers based on trimethylene carbonate, L-lactide, and 1,5-dioxepan-2-one. Biomacromolecules 2006;7:1489-95.

[140] Alexis F, Venkatraman S, Rath SK, Gan L-H. Some insight into hydrolytic scission mechanisms in bioerodible polyesters. Journal of Applied Polymer Science 2006;102:3111-7.

[141] Lipik VT, Kong JF, Chattopadhyay S, Widjaja LK, Liow SS, Venkatraman SS, et al. Thermoplastic biodegradable elastomers based on [epsilon]-caprolactone and l-lactide block co-polymers: A new synthetic approach. Acta Biomaterialia 2010;6:4261-70.

[142] Vanhoorne P, Dubois P, Jerome R, Teyssie P. Macromolecular Engineering of Polylactones and Polylactides .7. Structural-Analysis of Copolyesters of epsilon-Caprolactone and L- or D,L-Lactide Initiated by Al(OiPr)3. Macromolecules 1992;25:37-44.

[143] Hakkarainen M. Aliphatic polyesters: Abiotic and biotic degradation and degradation products. Degradable Aliphatic Polyesters2002. p. 113-38.

[144] Pospiech D, Komber H, Jehnichen D, Haussler L, Eckstein K, Scheibner H, et al. Multiblock copolymers of L-lactide and trimethylene carbonate. Biomacromolecules 2005;6:439-46.

[145] Rueda-Larraz L, d'Arlas BF, Tercjak A, Ribes A, Mondragon I, Eceiza A. Synthesis and microstructure-mechanical property relationships of segmented polyurethanes based on a PCL-PTHF-PCL block copolymer as soft segment. European Polymer Journal 2009;45:2096-109.

[146] Toki S, Sics I, Burger C, Fang DF, Liu LZ, Hsiao BS, et al. Structure evolution during cyclic deformation of an elastic propylene-based ethylene-propylene copolymer. Macromolecules 2006;39:3588-97.

[147] Myers SB, Register RA. Extensibility and Recovery in a Crystalline-Rubbery-Crystalline Triblock Copolymer. Macromolecules 2009;42:6665-70.

[148] Yi J, Boyce MC, Lee GF, Balizer E. Large deformation rate-dependent stress-strain behavior of polyurea and polyurethances. Polymer 2006;47:319-29.

[149] Yeh F, Hsiao BS, Sauer BB, Michel S, Siesler HW. In-Situ Studies of structure development during deformation of a segmented poly(urethane-urea) elastomer. Macromolecules 2003;36:1940-54.

[150] Bonart RJ. J Macromol Sci, Phys 1968;B2:115.

[151] Choi YR, Bae YH, Kim SW. Star-shaped poly(ether-ester) block copolymers: Synthesis, characterization, and their physical properties. Macromolecules 1998;31:8766-74.

[152] Allcock HR, Lampe FR, Mark JE. Contemporary Polymer Chemistry. 3rd ed. New Jersey: Prentice Hall; 2003.

[153] Younes H, Cohn D. Morphological-study of biodegradable peo/pla block copolymers. J Biomed Mater Res 1987;21:1301-16.

[154] Odelius K, Albertsson AC. Precision synthesis of microstructures in star-shaped copolymers of epsilon-caprolactone, L-lactide, and 1,5-dioxepan-2-one. Journal of Polymer Science Part a-Polymer Chemistry 2008;46:1249-64.

[155] Korte F, Glet W. Hochdruckreaktionen .2. Die polymerisation vongamma-butyrolacton und delta-valerolactam bei hohen drucken. Journal of Polymer Science Part B-Polymer Letters 1966;4:685-&.

[156] Pego AP, Van Luyn MJA, Brouwer LA, van Wachem PB, Poot AA, Grijpma DW, et al. In vivo behavior of poly(1,3-trimethylene carbonate) and copolymers of 1,3-trimethylene carbonate with D,L-lactide or epsilon-caprolactone: Degradation and tissue response. J Biomed Mater Res Part A 2003;67A:1044-54.

[157] Declercq HA, Cornelissen MJ, Gorskiy TL, Schacht EH. Osteoblast behaviour on in situ photopolymerizable three-dimensional scaffolds based on D, L-lactide, epsilon-caprolactone and trimethylene carbonate. J Mater Sci-Mater Med 2006;17:113-22.

[158] Lemmouchi Y, Perry MC, Amass AJ, Chakraborty K, Schacht E. A novel and versatile potassium-based catalyst for the ring opening polymerization of cyclic esters. Journal of Polymer Science Part a-Polymer Chemistry 2008;46:5348-62.

[159] Yang JA, Liu F, Tu S, Chen YW, Luo XL, Lu ZQ, et al. Haemo- and cytocompatibility of bioresorbable homo- and copolymers prepared from 1,3-trimethylene carbonate, lactides, and epsilon-caprolactone. J Biomed Mater Res Part A 2010;94A:396-407.

Appendix A

List of molar ratio of monomers, initiator, and catalyst used in all the syntheses

Polymer	Soft block M_n target (Da)	Hard block M_n target (Da)	Mol ratio [TMC]/[CL]	Mol ratio [LLA]/[CL]	Mol ratio [Initiator]/[CL]	Mol ratio $[Sn(Oct)_2]$/[CL]
A1	40k	10k	1	0.378	10.81×10^{-3}	5.4×10^{-3}
A2	20k	10k	1	0.751	21.62×10^{-3}	5.4×10^{-3}
A3	40k	20k	1	0.751	10.81×10^{-3}	5.4×10^{-3}
A4	80k	40k	1	0.751	5.41×10^{-3}	5.4×10^{-3}
A5	10k	10k	1	1.500	43.01×10^{-3}	5.4×10^{-3}
A6	20k	20k	1	1.500	21.62×10^{-3}	5.4×10^{-3}
A7	80k	80k	1	1.500	5.41×10^{-3}	5.4×10^{-3}
A8	40k	40k	1	1.500	10.81×10^{-3}	5.4×10^{-3}
A9	10k	20k	1	2.989	43.01×10^{-3}	5.4×10^{-3}
B1	40k	20k	0.333	0.515	7.41×10^{-3}	3.6×10^{-3}
B2	80k	40k	0.333	0.515	3.70×10^{-3}	3.6×10^{-3}
B3	40k	40k	0.333	1.030	7.41×10^{-3}	3.6×10^{-3}
B4	80k	80k	0.333	1.030	3.70×10^{-3}	3.6×10^{-3}
C1	40k	40k	0.111	0.871	6.26×10^{-3}	3.0×10^{-3}
C2	80k	80k	0.111	0.871	3.13×10^{-3}	3.0×10^{-3}

Polymer	Mol % CL in hard block	Mol ratio [TMC]/[CL]	Mol ratio [LLA]/[CL]	Mol ratio [CL[a]]/[CL]	Mol ratio [Initiator]/[CL]	Mol ratio $[Sn(Oct)_2]/[CL]$
D1	0	1	1.500	0	10.81×10^{-3}	5.4×10^{-3}
D2	10	1	1.382	0.154	10.81×10^{-3}	5.4×10^{-3}
D3	20	1	1.254	0.314	10.81×10^{-3}	5.4×10^{-3}
D4	30	1	1.124	0.482	10.81×10^{-3}	5.4×10^{-3}
E1	0	0.333	1.030	0	3.70×10^{-3}	3.6×10^{-3}
E2	10	0.333	0.945	0.105	3.70×10^{-3}	3.6×10^{-3}
E3	30	0.333	0.769	0.329	3.70×10^{-3}	3.6×10^{-3}
E4	50	0.333	0.574	0.574	3.70×10^{-3}	3.6×10^{-3}

[a]Mol of ε-caprolactone in the hard-block

Polymer	Soft block M_n target (Da)	Hard block M_n target (Da)	Mol ratio [TMC]/[CL]	Mol ratio [LLA]/[CL]	Mol ratio [Initiator]/[CL]	Mol ratio $[Sn(Oct)_2]/[CL]$
SA1	80k	20k	1	0.376	10.81×10^{-3}	5.4×10^{-3}
SA2	80k	40k	1	0.751	10.81×10^{-3}	5.4×10^{-3}
SA3	80k	80k	1	1.503	10.81×10^{-3}	5.4×10^{-3}
SA4	80k	160k	1	3.003	10.81×10^{-3}	5.4×10^{-3}
SB1	80k	20k	0.333	0.257	7.41×10^{-3}	3.6×10^{-3}
SB2	80k	40k	0.333	0.515	7.41×10^{-3}	3.6×10^{-3}
SB3	80k	80k	0.333	1.030	7.41×10^{-3}	3.6×10^{-3}
SB4	80k	160k	0.333	2.057	7.41×10^{-3}	3.6×10^{-3}